SAPIENZA
UNIVERSITÀ DI ROMA

TESI DI DOTTORATO

UNIVERSITÀ DEGLI STUDI DI ROMA *La Sapienza*

Dipartimento di Ingegneria Informatica, Automatica e Gestionale
A. Ruberti

Dottorato in Automatica, Bioingegneria e Ricerca Operativa

Da

Marwa Hassan

Nonlinear and sampled data control with application to power systems

Tesi presentata e difesa il 17/09/2018 all' universita degli studi di Roma la Sapienza

Evaluating commitee:

Prof. Luigi Fortuna	Università *Catania*	Reviewer
Prof. Almoataz Youssef Mohamed	Università *Cairo*	Reviewer
Prof. Costanzo Manes	Università *Aquila*	Examiner
Prof. Mauro Ursino	Università *Bologna*	Examiner
Prof. Raffaele Pesenti	Università *Ca' Foscari*	Examiner
Prof. Salvatore Monaco	Università *La Sapienza*	Advisor

Acknowledgments

First of all, I am grateful to the Almighty God for establishing me to complete this thesis.

I sincerely would like to thank the reviewers for taking time reviewing my work.

I would like to deeply thank my principle supervisor Professor Salvator Monaco for his valuable advice, excellent guidance and effective support. I would especially wish to express my endless gratitude to my mentor professor Noha who have been guided me since I have known her.

I also want to express my gratitude to all the contributors especially Professor Dorothee and Mattia Mattoni who helped me a lot through my research.

I would also like to acknowledge Sapienza university and Arab Academy for Science and Technology for funding my PhD project.

Most importantly, I would like to thank my Family members to whom this thesis is dedicated for your believe in me.

Short bio

Marwa A. Abd El Hamied Phd student at Sapienza University of Rome. She received B.Sc. and M.Sc. first degrees of honors in electrical and control engineering from the Arab Academy for Science and Technology and Maritime Transportation, Egypt in 2009 and 2012 respectively. Her currently research interest includes application of nonlinear control and sampled data design,surgical Robotics , Smart Grid , Renewable Energy,Electrical Machines , Power system Protection , Control Applications , Mathematical modeling , Artificial Intelligence and Hybrid system, PLC, Human resources and management system.In 2014 She received a scholarship from Sapienza university to conduct her Phd studies.

Contents

List of Figures

List of Main Symbols and Acronyms

Symbols

r	Relative degree
T_s	Sampling time
δ	Multi rate model Sampling time
R_s	Stator phase resistances
R_r	Rotor phase resistances
Ls	Stator per phase winding inductance
Lr	Rotor per phase winding inductance
M	Magnetizing inductances
i_{sd}	Stator direct axis current
i_{sq}	Stator quadratic axis current
i_{rd}	Rotor direct axis current
i_{rq}	Rotor quadratic axis current
V_{sd}	Stator voltage via direct frame
V_{sq}	The voltage of the stator in the quadratic frame
V_{rd}	Rotor voltage via direct frame
V_{rq}	Rotor voltage via quadratic frame
λ_{sd}	stator-flux linkage for direct axis frame
g	Gear box ratio
p	Number of pole per pair
J	Moment of inertia
c_{em}	Magnetic torque
c_{er}	Rotational Torque
$\lambda_o pt$	Optimal speed ratio
W_r^*	Optimal slip speed
W_s	synchronous speed
R	the radius of the blad
ρ	density of the air in $kg/m3$
β	Bitch angle

Acronyms

MR	Multi Rate
SR	Single Rate
CTD	Continuous Time Design
DTD	Discrete-time design
SDD	Sampled Data Design
NLIC	Non Linear Artificial Intelligent Controller

DIC Digital Intelligent Controller

SISO Single Input Single Output

LTM Linear Tangent Model

FOH First Order Hold

ZOH Zero Order Hold

GOH General Order Hold

MIMO Multi Input Multi Output

FFL Fully Feedback Linearizable

NIC Non Interacting Control

DDP Disturbance Decoupling Problem

AOT Asymptotic Output Tracking

FL Feedback Linearization

FLC Fuzzy Logic Controller

MPPT Maximum Power Point Tracking

DFIG Doubly Fed Induction Generator

PID Proportional Integral Derivative

PMSG Permanent Magnets Synchronous Generator

AI MPPT Artificial Immunity sensorless Maximum Power Point Tracking

AISE Artificial Immunity System Estimator

MRAS Model Reference Adaptive System

RSC Rotor Side Converter

TSR Tip Speed Ratio

AIS Artificial Immunity System

WT Wind Turbine

PV photovoltaic

PSF Power Signal Feedback

P and O Perturb and Observe

OTC	Optimum Torque Control
PPT	power point tracking
SVCs	Static Var Compensators
PSS	Power System Stabilizers
STATCOMs	Shunt Static Synchronous COMpensators

List of Publications

Publications in Proceedings

I Marwa A. Abd El-Hamid," Tracking and controlling maximum power point Utilizing artificial intelligent system", in the proceeding of the IEEE International Conference on Smart City, Chengdu, China, pp. 586-589,December 2015.

II Marwa A. Abd El-Hamid and Noha H. El-Amary,"Permanent Magnet Synchronous Generator Stability Analysis and Control,in the proceeding of Complex Adaptive System conference , Los Angeles , November 2016,PP 507-515.

III Mattia Mattioni, Marwa Hassan, Salvatore Monaco1 and Dorothee Normand-Cyrot,"On partially minimum phase systems and nonlinear sampled-data control", in the proceeding of the 56th IEEE Annual Conference on Decision and Control (CDC) Melbourne, Australia,pp. 6101-6106,December 2017.

IV Marwa Hassan and Noha H. El-Amary,"Asymptotic Output Tracking in Control of a Grid Connected Wind Turbine Based on Doubly Fed Induction Generator",accepted in EEEIC the 18th International Conference on Environment and Electrical Engineering, palermo, June 2018.

Submitted Chapters and Journal Articles

I Marwa Hassan , Noha H. El-Amary and Hanady H. Issa,Alsnosy Balbaa,Asymptotic Output Tracked Artifcial Immunity Controller for Eco-Maximum Power Point Tracking of Wind Turbine Driven by Doubly Fed Induction Generator, accepted in Energies journal.

II Mattia Mattioni, Marwa Hassan, Salvatore Monaco1 and Dorothee Normand-Cyrot,On partially minimum phase systems and disturbance decoupling stability submitted to nonlinear dynamics journal.

III Marwa Hassan and Hanady H. Issa,"Artificial Intelligent controller for Wind system driven by Permanent magnet Synchronous generator" submitted to Journal of Electrical Engineering and Technology.

Other publication

I Marwa A. Abd El-Hamid, Noha H. El-Amary, Mohamed M. Mansour, "MICRO GRID STUDIES DUE TO FAULT OCCURRENCE USING IMMUNITY TECHNIQUE ", proceeding of the 11th IASTED European Conference on Power and Energy Systems , Napoli, Italy , pp. 20-25, 2012.

II Noha H. El-Amary, Marwa A. Abd El-Hamid, Mohamed M. Mansour, "Immunity Technique in Determine Micro Grid Studies due to Fault Occurrence", Accepted in Advanced Science Letters Journal, 2012. (through the acceptance in 2012 International Conference on Advanced Electrical Engineering (ICAEE 2012), Cebu, Philippines, August 29th-30th, 2012.

III Marwa A. Abd El-Hamid," Controlling Robotic Arm Assisted in Knee Surgery Utilizing Artificial Immunity Technique", proceeding of the UKSIM2013 the IEEE international conference on modeling and simulation, Cambridge, England, April 2013.

IV Marwa A. Abd El-Hamid," Diesel Engine Working Cycle Utilizing Artificial Intelligent Systems", Accepted in Applied Mechanics and Materials Journal, 2014. (through the acceptance in 2013 International Conference on Power Science and Engineering (ICPSE 2013), Paris, France, December 20th-21th, 2013.

V Marwa A. Abd El-Hamid and Noha H. El-Amary : Voltage Instability Prediction Using Artificial Immunity-Technique. International Journal of Scientific and Engineering Research, Volume 4, Issue 11, November-2013.

VI Marwa A. Abd El-Hamid: Total Knee Replacement Surgery Model. International Journal of Computing and Digital Systems, Vol 2, No3, 123-128 (2013).

General Introduction

chapter*

The application of nonlinear-based control to power systems is more and more popular due to the development of nonlinear control methods and the effectiveness of the model to represent the real process. In fact, a vast number of researches have been introduced aiming to solve power systems most common problems such as stability and robustness. Part of these researches was focused on the study of modeling and controlling power system machines. Examples of some of the successful techniques investigated in this area of research can be found in ([26, 79, 96, 82, 13, 89, 20]). Another exciting topic in this field is the ability of designing a controller that ensures damping oscillation in power systems, thereby guaranteeing satisfactory performance following significant network disturbances. The traditional Power System Stabilizers (PSS), Static Var Compensators (SVCs), and Shunt Static Synchronous COMpensators (STATCOMs) controller often suffers from poor performance due to the variation of the state of the system as they tuned based on power system linearization model. A thesis conducted by Aykovnle shows that designing nonlinear control schemes for electrical power system stabilizer provide better results([8]).

Besides due to the power use of the digital devices which applied to the control of the modern electric power systems. It is recognized that digital control can offer a significant advantage in enhancing power system performances.

Three approaches are known to be developed in the digital control design: 1)Continuous Time Design (CTD) where the controller is designed using continuous time control tools and then implemented in discrete-time through sample and holder.The most common approach when dealing with static feedback on a nonlinear plant is to directly implement Zero Order Holder (ZOH)of a continuous control computed at sampling instant.This procedure is denoted as "emulation design".A modified continuous time plant or modified continuous time procedure ('redesign methods) can be used to compensate the effects of sampling and holding devices.First results in the nonlinear context in these lines arr in[[39, 69, 24, 31]]. The emulation design procedure usually consists of three steps: continuous-time design, controller discretization , and digital implementation. The design of a continuous time controller is performed in the first step without taking into account the sampling procedure.The effectiveness of the emulation and redesign techniques are usually depend on the extend on which the continuous time performance are maintained by the resulting sampled data control scheme.The most accurate results are developed in the area of robust control lyapanov's type techniques in the wide frame work of input to state stability[[93, 23, 54]].
2)Discrete-time design (DTD) The controller is directly designed on the exact or approximate equivalent sampled data model of the plant.This design faces major problem when it's applied into the nonlinear context, as the usual sampled data model do not admit a closed form representation.The problem is more complicated

if not standard holding devices are used;properties of the plant which are relevant for the controller design may be lost under sampling. To quote a few, among the most traditional drawbacks of sampled models, put in light in a linear context too, let us recall that : minimum phase property is lost under usual sampling with the appearance of critical sampling zeroes [[6]]; structural or control properties can be lost depending on the sampling procedure and/or the order of approximation performed in the computation.Even though there have been huge development in the discrete time control theory , but the problem will always come down to the choice of sampling procedure , the computation of the equivalent sampled data model and the accuracy of the approximated sampled data model [[81, 2, 95, 5]].
3) Sampled Data Design (SDD) The controller is still designed on the discrete-time model of the plant, but now strictly taking into account two major aspects:the discrete-time model is issued from sampling and the variables under control are continuous-time ones.These aspects reflect in setting suitable performances on the behaviours not only at the sampling instant[[**?**, 51, 50, 80]].Despite the fact there have been wide theoretical research effort in nonlinear control , stimulated to work out adequate digital solutions, the increasing performances of computers in terms of speed and precision,suggested, at the opposite, to make use of emulation with appropriate sampling frequency. One might suggest based on the previous sentence that there are no need for SDD.Major objection to such a point of view was discussed in[[68]].In conclusion SDD is a very promising control design with a lot of advantages such as:it's ability to solve continuous-time control problems which do not admit standard solutions.

Coming from Egypt , where there has been the energy crisis in the last decade due to the rapid growth of population in addition to the economic difficulties facing the government and the increase in global fuel prices. I have been motivated to study the development of control for power systems with specific focus in their involvement in renewable energy.Starting from my first research conducted in my master thesis based on learning and artificial algorithms ([61, 74, 33]) I have noticed that control design is based on thr the accuracy of the model one deduce.
Through the study of my Ph.D., I have addressed the efficiency of the artificial intelligent controller in power machines, in addition, I tried to put in light the differences between the modern (artificial) controller and nonlinear-based control designs through the application of both techniques to the case of permanent magnet synchronous generator([32, 34]). In conclusion, I can say that the best results are provided by the collaboration of both control techniques.
An investigation activity have been developed in the sampled data context. with possible practical application to power machines. The methodological results are based on the analysis and further design of the so called zero dynamics whose role is of paramount importance in stability and stabilization. As it also allow to cope with effectiveness of the control in terms of performance and stability margin.

To Roughly outline the differences between Non-Linear Intelligent Controller (NLIC) and the Digital Non-Linear Intelligent Controller (DNLIC) shown in Figures 1,2, I am going to recall one of my results obtained in this thesis while investigating

the Maximum Power Point Tracking techniques for wind system fed by doubly fed induction generator .

Maximum power point tracking (MPPT) or sometimes just power point tracking (PPT) is a technique used commonly with wind turbines and photovoltaic (PV) solar systems to maximize power extraction under all conditions.In the wind system its referred to as the optimal value of the tip speed ratio at which the generator must be operated such that maximum power is generated.The MPPT algorithms can be classified into four control techniques. The first method is known as the Tip Speed Ratio (TSR) where the wind speed parameter and the measurement of the speed are used to regulate the rotor speed and capture the maximum wind power . This method requires accurate knowledge of the measured values. The second method is the Power Signal Feedback (PSF) and is based on the wind turbine maximum power curve. The curves usually obtained via simulation or through off line experiment. For that reason it is difficult to implement this technique in practical applications . The third method is the Perturb and Observe (P and O) method. Mainly it is used in the solar energy where the measurement of the current and voltage is collected from the photovoltaic cell and process this information through micro-controller . This technique is suitable for wind turbines with small inertia, but not for medium and large inertia wind turbine systems, since the (P and O) method adds a delay to the system control . Finally the Optimum Torque Control (OTC) consists of the adjusting of the generator torque to the optimum value to different wind speed. This MPPT strategy needs a look-up table of optimum torque. In conclusion the conventional methods have several drawbacks.An alternative solution is to use the Artificial Intelligent systems.In fact I developed a design that based on AI MPPT(Artificial Immunity maximum power point tracking). The developed strategy was applied to a wind system driven by a Doubly Fed Induction Generator DFIG operating at the variable speed.Figure 3 depicts the comparison of the doubly fed induction generator rotor speed for classical PID controller that is built on the linear approximation, Fuzzy logic controller and finally (NLIC) controller. The NLIC is formed on the bases of nonlinear- based control model, and the Artificial Intelligent (Immunity technique) is used as for the purpose of pattern recognition. One can note that a slower dynamic variation of the rotor speed is achieved through the NLIC which ensures better performance. Further analysis was to implement such a design in practical power system applications which indicate the need to apply digital control. The results generated from the sampled data implementation shown in figure 4 suggest that the fluctuation in speed is reduced compared to the NLIC found in figure 3. The results is illustrated in details in chapter five.

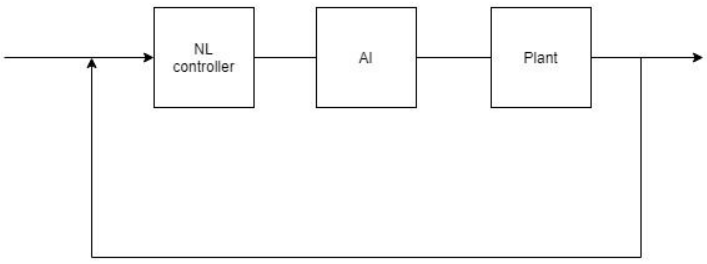

Figure 1: NLIC scheme

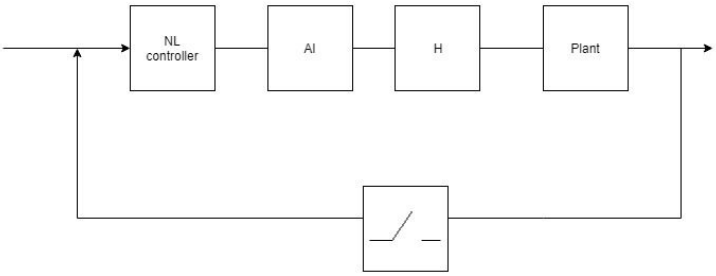

Figure 2: Emulation control scheme

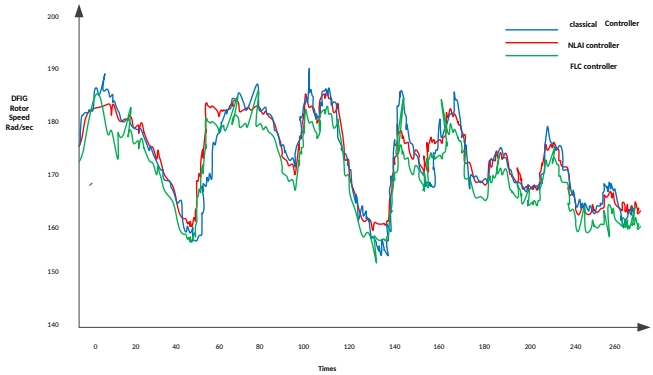

Figure 3: MPPT for doubly fed induction generator casting various type of control.

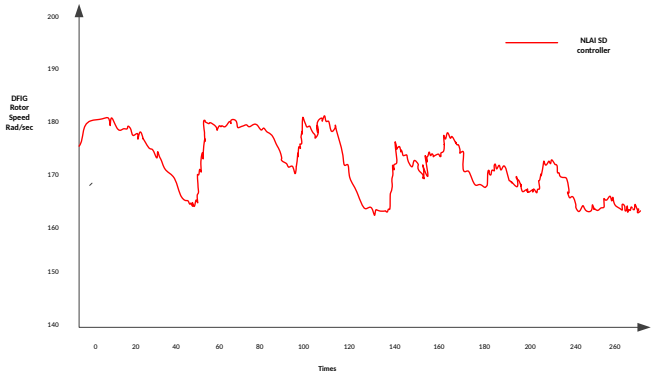

Contribution

The main contributions of this thesis are:

· Feddback lineariztion design for a class of nonlinear systems exhibiting a linear output with nonminimum phase property have been developed.
The idea bases on the concept of partially minimum phase systems. We showed that input-output feedback linearization with stability of the internal dynamics can be pursued via the use of a dummy output with respect to which the system is minimum-phase. The design strategy was introduced to multirate sampled-data context.

· Disturbance decoupling problem of a non minimum phase non linear Single Input Single Output (SISO) systems was introduced.We show that by using a simple idea that is based in factorizing the numerator of the non minimum phase transfer function of a LTI system a dummy output can be introduced with respect to which the zero dynamics subjected to one of the factors ,is stable.
Although there are several work that introduces a feedback control design that solves the Disturbance Decoupling Problem, but there are not actual solution that guarantee that the trajectories of the residual unobservable dynamics are bounded despite the effect of the disturbances. The proposed design consider a first step solution towards this problem.

· The Nonlinear control based techniques have been used to solve the Maximum Power Point problem for a Doubly Fed Induction Generator.Moreover we showed that using Artificial Intelligent system with Nonlinear based controller provide better solution.
Further more a case study for the DFIG when it's connected to grid showed that the use of Sampled-data design is better in performance than the direct implantation of the continuous-time (so called emulation design).For example the simulated tip speed ratio found in chapter five has smoother variation than the direct implementation design.This argument indicate that the sampled data design could provide promising results than the classical digital design.

Thesis Organization

Following this introduction, the contents of the thesis are presented into six chapters, that have been organised in two parts:

Part I

A self-contained treatment of the methods and techniques addressed in the nonlinear sampled data context, in particular around the concept of zero dynamics, which is

a fundamental concept as pointed out in chapter one.The results obtained in this context is found in chapter1,2,3,4,5]

In Chapter 2, we recall results on sampled-data models.In particular we focus on the effect of each model on the zeros of the system.Moreover, we show how we can manipulate the zeros of the system through the design of a stability defined feedback control law which perform partial dynamic inversion.

In Chapter 3, We set up a control design method for a class of nonlinear systems exhibiting a linear output.The proposed technique exploits the concept of partially minimum phase system. The methodology is illustrated when settling Input Output linearization with respect to which the system is minimum-phase.

In Chapter 4, we present a solution for the Disturbance Decoupling Problem with stability.This work is inspired by the very simple idea that by factorizing the numerator of a transfer function of a LTI system a dummy output can be introduced with respect to which the zero dynamics subjected to one of the factors , possibly stable.The design procedure for the sampled data system was investigated in the linear context and the solution was then extended to the nonlinear case.

In Chapter 5, We investigate the need for the nonlinear based control and the sampled data techniques in the power systems and the affect of incorporating with the artificial intelligent systems.Wind turbine driven by a doubly fed induction generator was chosen for the purpose of investigation.We track the Maximum Power Point through three different models.The first one is the Fuzzy logic controller where the actual need for the exact model is not necessary obtained while the second model was based on the linear approximation of the system followed by conventional PID controller, finally a nonlinear model and controller was developed.The Artificial Immunity was used as a source of pattern recognition.The results indicate that the best performance is provided based on the Non linear control model.For the purpose of study we compute the Nonlinear sampled data model and we obtained better performance than the previous methods.Further investigation will be developed in the future to see how can the sampled data control techniques be applied in power system application.

Part II

Part II is obtained by collecting a sample of the published work investigation the artificial intelligent controller beside the nonlinear control techniques.The papers is contained in chapter 6.

In Chapter 6,we include a sample of the published material developed in the power system machines through the study of my Phd thesis.The researches conducted in this part was mainly based on the Artificial Intelligent Systems in power system machines.We note that even though the use of some of the AI techniques such as Fuzzy Logic and Neural Network does not require the computation of the model of the application but it will still suffer from some drawbacks especially in terms of the implementation in practical applications.An alternative used approach is to use control techniques such as PID in the approximated linear model.This design is

very well known to be used but it does not take into account the non linearity of the model.In fact it seems that control design than is based on Nonlinear control provide better performances.

Collaboration

The results conducted in this thesis were a result of a Collaboration between several great researchers.Some original results in the sampled data control have been generated under the Collaboration with Professor DorothÃ©e Normand-Cyrot and Mattia Mattoni from Paris Sud university in France and the supervision of my Professor Salvator Monaco.

In the other side I have been collaborating with Associate Professor Noha H. El-Amary from Arab Academy.We have been working in developing artificial intelligent controller that based on nonlinear control model and it's application in renewable energy.

Part I

Sampled data control design with stability

Chapter 1

The concept and the role of zero dynamics

Contents

1.1 Introduction

The concept of zero dynamics was first introduced by Alberto Isidori thirty years ago. It's very well known that the zero dynamics plays in many circumstances a role similar to that of the zeroes of its extension to the nonlinear context of the linear system. Roughly speaking, one can say that the zero dynamics is a dynamical system that characterizes the internal behavior of a system once the initial condition and the input are chosen in such a way to constrain the output to be identically zero. In this thesis, we will investigate on the way such a concept can be used to deduce suitable nonlinear controller.

1.2 Zero dynamics from linear to nonlinear

In this section we give a brief illustration of the development history of zero dynamics from the linear to the nonlinear context. In the goal of evolution in the linear system theory sixtieth provided a better understanding of the role of the zeroes in the control design.It began with milestone contribution by Kalman, who introduced and developed the concept of controllability and observability and ended by the

development of sophisticated methods for the design. In a nutshell,the aim of these methods was to explore all possible theories that can be developed for a feedback design. Shortly after unavaliable so opening to a wide area of research the need to extend the concepts for the non linear systems became. The development of this investigation surfaced at the beginning of the seventies. A group of researches collaborate and established an equivalent corpus of theory and results for the case of the non linear systems. The first contribution was due to Hermann. He started the analysis of controllability and observability for non-linear control systems([37]).The work by Hermann was expanded in a series of major contribution by Haynes−Hermes([36]),Lobry([57]), Sussmann−Jurdjevic ([87, 88]), Brockett ([14]), Krener ([52]) and reached a culmination with the milestone paper of Hermann−Krener ([38]). The impact of this paper was enormous as it not only refined a number of earlier results, but it also introduced a framework that made possible to begin a systematic study of the feedback design problems for nonlinear systems.
The immediate follow of ([38]) was in fact the paper by isidori ([46])where the basic geometric tools for feedback design from linear to non linear systems were extended. One of the main aspects of the geometric theory either for linear or non linear system is the study of how observability properties can be influenced under feedback. This study was conceived in the context of disturbance decoupling. This paper also reaches to promising results in a number of domains. One of these results was the possibility of characterizing in geometric terms the notion of "zero" of the transfer function of a system. In fact, the geometric tools developed by ([46]) was the bases for several further works that appeared in the following years and help to introduce the zero dynamics concept.

Consider a class of Single Input- Single Output class of nonlinear system

$$\begin{aligned} \dot{x} =& f(x) + g(x)u, \quad x \in \mathbb{R}^n, u \in \mathbb{R}, y \in \mathbb{R} \\ y =& h(x). \end{aligned} \tag{1.1}$$

where $x = 0$ is an equilibrium point (i.e., $f(0) = 0$). The system is said to possess a well define relative degree $r \leq n$ at the origin;if, $L_g L_f^i h(x) = 0$ for $k < r - 1$ and $L_g L_f^{r-1} h(x) \neq 0$ in a neighbourhood of $x = 0$. As consequence one can locally define a mapping $\phi(x) : \mathbb{R}^n \to \mathbb{R}^n$ that will underline the essential feature of the system.

Definition 1.1 [Normal form] The locally defined coordinate transformation

$$z = \begin{pmatrix} \zeta \\ \eta \end{pmatrix} = \phi(x) = \begin{pmatrix} h(x) \\ \vdots \\ L_f^{r-1} h(x) \\ \phi_2(x) \end{pmatrix}. \tag{1.2}$$

where $\phi_2(x)$ is s.t. $L_g \phi_2(x) = 0$ locally puts the system into the normal form; i.e.,

it gets the form

$$\dot{\zeta} = \hat{A}\zeta + \hat{B}(b(\zeta,\eta) + a(\zeta,\eta)u) \tag{1.3a}$$
$$\dot{\eta} = q(\zeta,\eta) \tag{1.3b}$$
$$y = \zeta_1 \tag{1.3c}$$

with

$$\hat{A} = \begin{pmatrix} \mathbf{0} & I_{r-1} \\ \mathbf{0} & \mathbf{0} \end{pmatrix}, \quad \hat{B} = \begin{pmatrix} \mathbf{0} \\ 1 \end{pmatrix}, b(\zeta,\eta) = b(z) = L_f^r h(\phi^{-1}(\zeta))$$
$$a(\zeta,\eta) = a(z) = L_g L_f^{r-1} h(\phi^{-1}(\zeta)). \tag{1.4}$$

In order to understand the zero dynamic concept, we analyse the problem of zeroing the output on the normal form of the system.
Recalling from the normal form

$$y(t) = \zeta_1(t) \tag{1.5}$$

constraining the output $y(t), = 0$ to be zero for all t entails

$$\dot{\zeta}_1(t) = \dot{\zeta}_2(t) = \cdots = \dot{\zeta}_r(t) = 0 \tag{1.6}$$

that is $\zeta = 0$ for all times. Thus, we note that when the output is set identically to zero, its state is constrained to evolve in such away that also ζ is identically zero.In addition the input u must be the solution of

$$0 = b(0,\eta(t)) + a(0,\eta(t)u(t)) \tag{1.7}$$

The behaviour of η is governed by the differential equation

$$\dot{\eta} = q(0,\eta(t)) \tag{1.8}$$

The following fact is deduced from the previous analysis .If the output $y(t)$ has to be zero , then necessary the initial state of the system must be set to a value such that $\zeta(0) = 0$,whereas $\eta(0) = \eta^0$ can be chosen arbitrary.According to the value of η^0, the input is set as

$$u^*(t) = -\frac{b(0,\eta(t))}{a(0,\eta(t))} \tag{1.9}$$

where $\eta(t)$ denotes the solution of the differential equation

$$\dot{\eta}(t) = q(0,\eta(t)) \quad \text{with initial condition} \quad \eta(0) = \eta^0 \tag{1.10}$$

The zero dynamics described the "internal behaviour" of the system when the input and the initial condition have been chosen in such a way to constrain the output to remain identically zero.The residual behaviour is defined by (1.8).

Remark 1.1 *If the system is linear,*

$$\dot{x} = Ax + Bu$$
$$y = Cx$$

so it is the map $q(0,\eta)$;i.e, $q(0,\eta) = q_\eta$ and one get that $\rho(q)$ coincides with the zeroes of the transfer function associated to it.

Remark 1.2 *If the transfer function of the linear system has negative zeroes then the dynamics $\dot{\eta} = q(0,\eta)$ are asymptotically stable([42]).*

In conclusion one can say that from a general point of view the zero dynamics specifies the residual internal dynamics of a dynamical system when the input and the initial condition are chosen in such a way to force the output to be zero.With that in mind one can guarantee that zero dynamics cancellation is involved in each technique.
The zero dynamics plays a crucial role in stabilization problems where dynamical inversion is explicitly or implicit involved so being fundamental for preserving stability in closed loop.

In the linear case, this corresponds to designing a feedback that assigns part of the eigenvalues coincident with the zeros of the system so making the corresponding dynamics unobservable. In general Inversion methods are naturally involved in any control methods.In what follows we are going to investigate the influence of the zero dynamics in control design techniques and how it can limit it's performance.

1.2.1 Zero dynamics in input output feedback linearization

The main idea of feedback linearization is to transform a nonlinear system dynamics into a (fully or partly) linear one, so that linear design techniques can be applied. Roughly speaking, feedback linearization cancels the nonlinearities . The development of feedback linearization techniques for nonlinear systems can be tracked back to the 80s.As we have seen in the previous section, there exists a static feedback for a SI-SO system that linearize the system if the system normal form equation (1.8) possess a trivial zero dynamics.The zero dynamics is the counterpart we are making it unobservable under feedback.
The first attempt to extend the feedback design control law to the Multi Input-Multi Output system case was introduced in ([47]). The results were obtained under the assumption that the system poses the same number of inputs and outputs and satisfy the invert ability assumption proposed by Singh([84]) . Other classes of systems were investigated in ([27]) where the authors showed that a certain class of MIMO systems can be transformed by means of suitable dynamic extension , into a system posing a Multi Input Multi Output (MIMO) version of the normal form. As a consequence if $dim(\eta) = 0$ for the obtained normal form, the original system can be rendered linear, via dynamic state feedback and change of coordinates.The result was enhanced in ([55]), where it is shown that a linear behaviour can be achieved

to some extent, by pure static feedback. Note that the system whose zero dynamics are trivial are such that their state can be expressed as a function of its output and their higher derivatives. Note that it is always possible to design a dummy output in case there isn't a given specific output function.In order to design dummy output for MIMO system , the system must be invertible and possess a trivial zero dynamics. The dummy output in question has been called linearizing outputs([42]). Several examples are discussed in([42]).From the earliest investigation, the concept of zero dynamics has been extended to several even complex situation.Examples of non minimum phase systems that can be handeled by the same method have been discussed in([72]).Several techniques and applications referred to in([?, 90, 35, 3, 19]).

1.2.2 Zero dynamics in non interacting control

The problem of noninteracting control has been studied since the late sixties by several authors. The papers of Falb and Wolovich ([28]), Gilbert ([30]) and Wang ([92]) are cornerstones in the noninteracting control theory for linear systems. In ([70]),([71]) and, independently, in ([10])the problem of noninteracting control has been formulated and solved in the framework of linear geometry,using mathematical tools such as linear vector spaces and matrix theory. These tools have been successfully used to address the issue of internal stability: an exhaustive theory is contained in ([75]). The first efforts to extend to nonlinear systems the noninteracting control theory, available for linear systems, peeped in only at the beginning of the seventies with the paper of Porter ([77]), followed by few others ([83]).In general a nonlinear system is noninteractive if there exists a disjoint block partition of the input vector such that each component of the *ith* output block is influenced only by the components of the *ith* input block. In 1988 Alberto Isidori and his colleagues introduces one of the earliest results in nonlinear feedback design ([45]).The paper put the base for the condition needed to obtain internal stability when non interaction is achieved via static state feedback.This work was an extension of the earlier results of Gilbert.The paper shows that there exists a well define internal dynamics, a sub-dynamics of the zero dynamics of the system , which is fixed with respect to any decoupling regular static state feedback.Thus,non interacting with stability via regular static state feedback can only be obtained if the dynamics in question is asymptotically stable.In the case of linear system, this obstruction can be destroyed if the dynamic feedback is used, as shown in earlier by Wonham.Thus the question arises whether or not similar results can be obtained in nonlinear control. A counter example in ([45]) showed it is not possible.Later a deeper analysis for the necessary condition for non interacting control with stability via dynamic feedback was carried out ([91]).The results shows that there exists a sub dynamics of the fixed dynamics identified in ([45]) which can't be eliminated by any regular dynamic feedback which make the system non interactive.Deeper analysis was obtained in [([25])]. Finally one must recall the major contribution in this field introduced by Stefano Battilotti ([11])where he analyized and introduced various designs for the nonintaracting problem with stability.

1.2.3 Zero dynamics in the output regulation problem

The output regulation problem of nonlinear systems is one of the central issues in control theory. It has attracted considerable interest in the last decades after the fundamental contribution given by Alberto Isidori and Christopher Byrnes in 1990 ([44]). In general, the problem is concerned with having the regulated variables of a given controlled plant to asymptotically track (or reject) all desired trajectories (or disturbances) generated by some fixed autonomous system, called the exosystem. The problem is much more complicated in the presence of unstable zero dynamics. The key contribution introduced in this topic can be found in ([44]) where the authors state that the problem is solvable if and only if specific nonlinear partial differential equations (called regulator equations) are solvable; a feedback law achieving local asymptotic output regulation is constructed via the solution of the regulator equations.

A lot of researches has been developed in the nonlinear regulator problem following the results obtained by Isidori and his coworkers ([16, 78, 41]). They established a set of necessary and sufficient conditions for the solution of the problem of the asymptotic output regulation under the additional constraint that the regulation strategy is insensitive to small variations of uncertain plant parameters. Output regulation has also been the object of the research efforts of other groups, both for linear ([60])and nonlinear systems see ([21, 22, 59]). In particular, they conducted there work under the plant minimum phase assumption. Several examples could be found in ([97, 86]) In fact, the focus on the study of the nonminimum phase system was not started until the nineties.A sample of the work discusses the output regulation problem for nonminimum phase system can be found in ([53, 73, 76]).

1.2.4 Zero dynamics in high gain feedback

The development of high gain feedback design started to take place in the 80s. The base for the investigation for this technique was the fact that nonlinear systems whose zero dynamics are globally asymptotically stable can, under appropriate assumptions lend themselves to the implementation of stabilization strategies based on high gain output feedback. In this context ([12]), discussed the stabilizability properties . Roughly ,speaking the paper discussed the ability to design a feedback control law that preserves a given equilibrium and is such that in the associated closed loop system the equilibrium is asymptotically stable, with a domain of attraction. In fact, paper ([12]) claimed that if the system is globally minimum phase, then it is possible to semiglobally stabilize it utilizing feedback.The claim was incomplete because the law in question is sufficient to keep trajectories bounded and to steer them in an arbitrary small neighbor of origin. This is not sufficient for asymptotic stability unless the equilibrium $z = 0$ is also exponentially stable. A further investigation of paper([81]) was pursued in a subsequent paper([9]) for a system having relative degree bigger than one. This paper claim that certain derivative feedback is capable of semiglobally stabilizing a globally minimum phase

system.The claim was incomplete, as pointed out in ([15]). The complete solution was later provided by([58]). The results show that the stability results hold under the assumption that the dynamics of the inverse system are driven only by the output and not by its higher order derivatives.Additional work is illustrated in ([49, 4, 1, 85, 56])

1.2.5 Zero dynamics in optimization

[([43])] It is well-known that linear systems having zeros in the left-half plane are difficult to control, and obstructions exist to the fulfillment of certain control specifications. One of these is found in the analysis of the so-called cheap control problem, namely the problem of finding a stabilizing feedback control that minimizes the functional

$$J_\epsilon = .5 \int_0^\infty [y^T(t)y(t) + \epsilon u^T u(t)dt] \tag{1.11}$$

when $\epsilon > 0$ is small. As $\epsilon \to 0$, the optimal value J_ϵ^* tends to J_0^*, the ideal performance. It is well-known that, in a linear system, $J_0^* = 0$ if and only if the system is minimum phase and right invertible and, in case the system has zeros with positive real part, it is possible to express explicitly J_0^* in terms of the zeros in question. If the (linear) system is expressed in normal form as

$$\dot{z} = Fz + G\eta \tag{1.12}$$
$$\dot{\eta} = Hz + k\eta + bu \tag{1.13}$$
$$y = \eta \tag{1.14}$$

with $b \neq 0$, and the zero dynamics are antistable (that is all the eigenvalues of F have positive real part), it can be shown that J_0^* coincides with the minimal value of the energy

$$J_\epsilon = .5 \int_0^\infty \zeta^T(t)\zeta(t)dt \tag{1.15}$$

required to stabilize the (antistable) system$\dot{z} = Fz + G\eta$.In other words, the limit as $\epsilon \to 0$ of the optimal value of J_ϵ is equal to the least amount of energy required to stabilize the dynamics of the inverse system.

Those arguments extend to the case of nonlinear dynamic so underlying that the zero dynamics plays an important role in control design as it form some boundaries in the control problem which limit the performances of the nonlinear systems.

1.3 Zero dynamics in discrete time

The study of the nonlinear systems in discrete time has been the focus of research since the eighties.In this section we are going to recall briefly the definition of the

Zero dynamics in discrete time (see [63, 65, 17]

$$\Sigma_D : \begin{cases} x_{k+1} = f(x_k, u_k) \\ y_k = h(x_k) \end{cases} \tag{1.16}$$

where,
x: is the state evolving in open subset $M \in \mathbb{R}^n$ and vector field $f(.)$,g(.),$h(.)$ are analytic on M and assume that $u = 0$; i.e., $f_0(x_k) = f(x_k, 0)$

1.3.1 Discrete time Relative degree

The discrete time system is said to have relative degree r_d if

$$\frac{\partial h_0 f_0^k f(x_k, u_k)}{\partial u} = 0, \quad \text{for} \quad 0 \leqslant k \leq r_d \tag{1.17}$$

$$\frac{\partial h_0 f_0^{r_d - 1} f(x_k, u_k)}{\partial u} \neq 0 \tag{1.18}$$

Proof: The proof can be exploited by considering the discrete time output and it's derivatives

$$y_k = h(x_k) \tag{1.19}$$

$$y_{k+1} = h(f(x_k, u_k)), \quad \text{if } \frac{\partial h_0 f}{\partial u} = 0 \tag{1.20}$$

$$y_{k+2} = h_0 f_0(x_k), \quad \text{if } \frac{\partial h_0 f_0 f(x_k, u_k)}{\partial u} = 0 \tag{1.21}$$

. (1.22)

$$y_{k+r} = h_0 f_0^{r-1}(x_k), \quad \text{if } \frac{\partial h_0 f_0^{r-1} f(x_k, u_k)}{\partial u} \neq 0 \tag{1.23}$$

■

we can note from the definition of the relative degree the independency of the functions $h(x), \ldots, h.f_\circ^r$, consequently a coordinate transformation in the form of

$$Z = \phi(x) = \begin{pmatrix} \phi_1(x) \\ \phi_2(x) \end{pmatrix} = \begin{pmatrix} \zeta \\ \eta \end{pmatrix} \tag{1.24}$$

$$\zeta_{k+1} = \phi_1(x).f(\phi^{-1}(\zeta_k, \eta_k), u_k) = \begin{pmatrix} h(x_k) \\ \vdots \\ L_{f_k}^{r-1} h(x_k) \\ \phi(x_k) \end{pmatrix} \tag{1.25}$$

$$\eta_{k+1} = \phi_2(x).f(\phi^{-1}(\zeta_k, \eta_k), u_k) \tag{1.26}$$

puts the system in the normal form

$$\begin{cases} \dot{\zeta}_{1(k+1)} = \zeta_{2k} \\ \dot{\zeta}_{2(k+1)} = \zeta_{3k} \\ \dot{\zeta}_{(r-1)(k+1)} = \zeta_{rk} \\ \dot{\zeta}_{r(k+1)} = \Phi(\zeta_k, \eta_k, u_k) \\ \dot{\eta}_{k+1} = q(\zeta_k, \eta_k, u_k) \\ y(k) = \zeta_{1k} \end{cases} \tag{1.27}$$

Definition 1.2 The zero dynamic of the discrete time is defined from

$$Q = \frac{\eta_{k+1}}{\partial u(k)} = 0 \tag{1.28}$$

Remark 1.3 *The system is said to have asymptotic zero dynamics if and only if Q is nonsingular.*

1.4 Summary

The concept of nonlinear zero dynamics is now firmly placed at the foundation of control theory. From a general point of view, the zero dynamics can be specified as the internal dynamics under which the system evolves when the input is applied to force the output to be identically zero.In this chapter we have recalled some of the famous control techniques and we illustrated the impact of zero dynamics in limiting there performances.

Due to the enormous evolution in digital application the researches shift there interest in extending the zero dynamic concept under sampling.

Chapter 2

On the Sampled Data Equivalent Model

Contents

2.1 Overview

The sampling scheme represented in Figure 2.1 is composed of three basic elements: a continuous time a plant , a sampler and holder device. The main function of the basic elements can be stated as:

I The hold device used to generate the a continuous time input to the system, $u(t)$, from a sequence of values u_k, defined at specific time instants .

In what follows we recall the various types of holders.

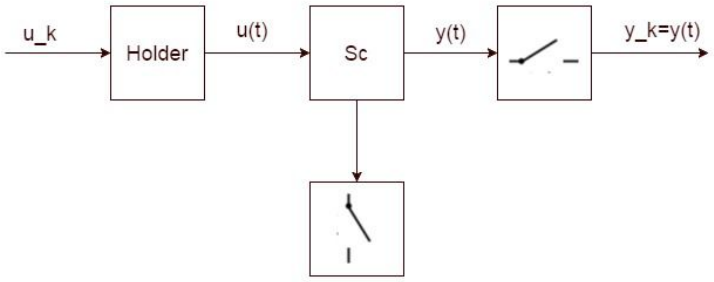

Figure 2.1: Sampling process

- **Zero Order Hold (ZOH)**, which simply keeps its output constant for T instant of time. The output from the input u_k is constant over each the time interval $[0, T[$ i.e:

$$u(t) = u_k \quad \text{for} \quad t \in [kT, (k+1)T[\tag{2.1}$$

- **First-Order Hold (FOH)**,which does a linear extrapolation using the current and the previous elements of the input sequence, i.e.:

$$u(t) = u_k + \frac{u_k - u_{k-1}}{T}, \quad t \in [kT, (k+1)T[\tag{2.2}$$

- **Generalised Hold Functions GHF or Periodic hold function**,This type of holder provides more degree of freedom as one can choose the feedback to fulfil any additional requirement for the system.

$$u_k = \alpha_i u_k \text{for} t \in [kT + \frac{(1-i)}{r}T, kT+]\frac{iT}{r}[\tag{2.3}$$

where r is the degree of the sampler

II The continuous-time system, defined by a set of differential equations evolving in continuous time.

III The sampling device, which gives the output and the state sequences of samples.The sample device for the output and the state can work at different sampling period which might be constant or time varying , periodic or not. It is assumed in our work that the samples are taken each sampling instant T instant of time and all the samples are measured.

In the following sections we recall the different types of sampled data models.

2.2 Sampled Data Equivalent Model to LTI system and the Zeros

Consider a SISO linear time-invariant model in the form :

$$\Sigma_L : \begin{cases} \dot{x} = Ax + Bu, \quad x, u, y \in \mathbb{R} \\ y = Cx. \end{cases} \tag{2.4}$$

The system has a well define relative degree r such that

$$CA^k B = 0, \forall \quad k = 1, \ldots, r-2$$
$$CA^{r-1}B \neq 0.$$

The representation for the system in the Laplace domain can be defined as

$$Y(s) = G(s)U(s) \tag{2.5}$$

where $U(s), Y(s)$ are the Laplace transformation of $u(t), y(t)$ respectively and the transfer function $G(s)$ can be represented as a quotient of polynomials:

$$G(s) = \frac{N(s)}{D(s)} \tag{2.6}$$

The roots of $N(s)$ and $D(s)$ determine the zeros and the poles of the system, respectively It is very well known that there exists multiple techniques to obtain the sample data model describing the evolution of 2.4 at any sampling instant $t = kT$ and with respect to variation of the control.The model can be derived directly from the transfer function or from the state space model.In the next section we are going to recall the various types of sampled data models.

2.2.0.1 The sampled-Single Rate model

Single Rate sampling procedure describe the scheme in which the continuous - time system input is generated using zero order hold working at the same frequency as the sampler device. In that case the evolution (2.4) of any $t = kT$ can be described through the so called SR equivalent model to keep the form of a discrete-time system parametrized by the sampling period T;i.e,

$$\Sigma L : \begin{cases} x_{k+1} = A^T x_k + B^T u_k \\ y_k = C x_k. \end{cases}$$

with, $A^T = e^{AT}$, $B^T = \int_0^T e^{A\tau} d\tau B$ and relative degree $r_d = 1$. The discrete-time transfer function representation of the sampled-data system can be obtained as

$$W(z) = \frac{T(z)}{F(z)} = C^T (zI - A^T)^{-1} B^T \tag{2.7}$$

where

$$T(z) = C^T \quad adj(zI - A^T) \quad B^T = det \begin{pmatrix} zI - A^T & -B^T \\ C & 0 \end{pmatrix} \tag{2.8}$$

$$F(z) = det(zI - A^T) \tag{2.9}$$

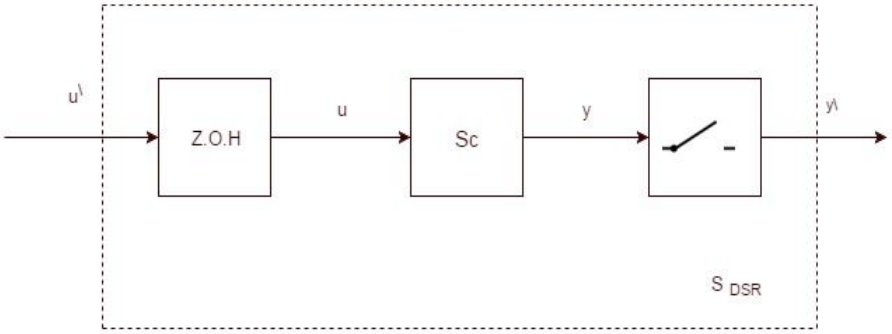

Figure 2.2: SR sampled data model scheme

2.7 is equivalent to the pulse transfer function obtained directly from the continuous-time transfer function, as stated in the following lemma

Lemma 2.1 *The sampled-data transfer function $W(z)$ can be obtained using the inverse Laplace transform of the continuous-time step response, computing its Z-transform, and dividing it by the Z-transform of a discrete-time step:*

$$W(z) = (1 - z^{-1})\mathbf{Z}\left\{\mathcal{L}^{-1}\left\{\frac{G(s)}{s}|_{t=kT}\right\}\right\} \tag{2.10}$$

$$= (1 - z^{-1})\frac{1}{2\pi j}\int_{\alpha-j\infty}^{\alpha+j\infty}\frac{e^{sT}}{z - e^{s\delta}}\frac{G(s)}{s}ds \tag{2.11}$$

where T is the sampling period.Furthermore, if the integration path in (2.8) is closed by a semicircle to the right, we obtain:

$$W(z) = (1 - z^{-1})\int_{l=-\infty}^{\infty}\frac{G((logz + 2\pi jl))\ T}{logz + 2\pi jl} \tag{2.12}$$

let us now consider the frequency domain and replace $z = e^{jw\delta}$.The previous equation rewrites as

$$G(e^{jWT}) = \frac{1}{T}\int_{l=-\infty}^{\infty}\frac{1 - e^{-Ts}}{T}(jw + j\frac{2\pi l}{T})G(jw + j\frac{2\pi l}{T}) \tag{2.13}$$

where $\frac{1-e^{-Ts}}{T}$ is the laplace transformation of H_{ZOH} This equation illustrates the well-known aliasing effect.

2.2.0.2 Eigenvalues and Zeroes of Single Rate model

The relation between the poles of the sample data model and the continuous time one can be understood from the analysis of $A^T = e^{AT}$, $B^T = \int_0^T e^{A\tau}d\tau B$.Sampling indices one new zero (the so called sampling zeros) which are generally unstable.This study has been extended to sampled data LTI system with continuous-time relative degree $r \leqslant n$ ([6]).It was shown that

1 The relative degree of the corresponding sampled-data equivalent model generally falls to $r_d = 1$.

2 $r-1$ induced by sampling coinciding as $T \to 0$.

As consequence , sampling induces s new $(r-1)$ dimensional zero-dynamics which is generally unstable as $r \geqslant 2$ [67] so not preserving, in general, the minimum-phase property of the original continuous-time plant.

2.2.1 First Order Hold FOH sampled-Single Rate model

The FOH is a type of holder in which the control signal of the piecewise linear type starting from two subsequent values of the discrete-time(u_k, u_{k+1} The sampled data

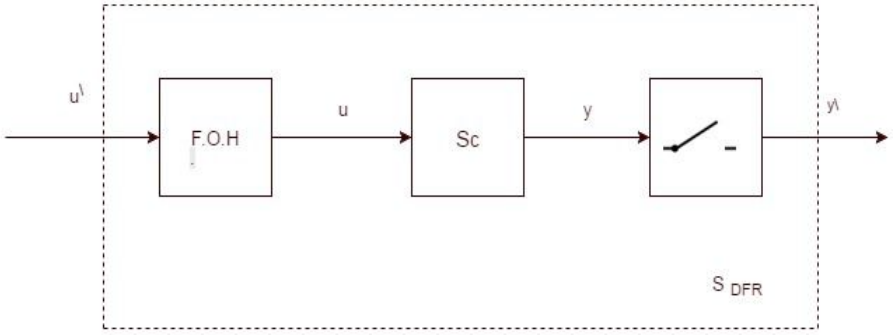

Figure 2.3: FOH sampled-Single Rate model scheme

model of the system (2.4) is described by

$$\begin{aligned} \begin{pmatrix} x_{k+1} \\ u_k \end{pmatrix} &= \begin{pmatrix} A^T & B^{T_1} \\ 0 & 0 \end{pmatrix} \quad \begin{pmatrix} x_k \\ u_{k-1} \end{pmatrix} + \begin{pmatrix} B^{T_2} \\ 1 \end{pmatrix} u_k \\ y_k &= [C \qquad 0] \begin{pmatrix} x_k \\ u_{k-1} \end{pmatrix} \end{aligned} \tag{2.14}$$

with $A^T = e^{AT}$, $B^{T_1} = \int_0^T (2 - \frac{\tau}{T}) e^{A\tau} d\tau B$, $B^{T_2} = \int_0^T (\frac{\tau}{T} - 1) e^{A\tau} d\tau B$.$T_1, T_2$ denote the sampling instant with respect to u_k, u_{k+1} respectively. As for the discrete-time transfer function it can be obtained from

$$W(z) = [C \quad 0](\begin{pmatrix} zI - A^T & -B^T \\ 0 & z \end{pmatrix})^{-1} \begin{pmatrix} B^{T_2} \\ 1 \end{pmatrix} \tag{2.15}$$

2.2.1.1 Eigenvalues and Zeros of FOH model

The relation between the eigenvalues of the sampled data model are similar to the one obtained via ZOH.As the poles can be described by both the eigenvalues of e^{AT} plus one pole at the origin.on the other hand, the zeroes the will be generically different from the ones obtained when using a ZOH.Moreover an additional sampling zeros will appear due to the sampling process.

2.2.2 Sampled Data-Multi Rate model

([29]) Multi Rate sampling relies upon the idea of "sampling" and " holding" the input signal with a frequency that is ($r$times) faster than he state and the output.The input $u(t)$ is assumed to be constant over subintervals of amplitude $\delta = \frac{T}{r}$and $u(t) = u_{ik}, \quad t \in [k\delta + \frac{(1-)}{r}\delta), k\delta + \frac{\delta}{r}$ In this setting, the evolution(2.4) at any

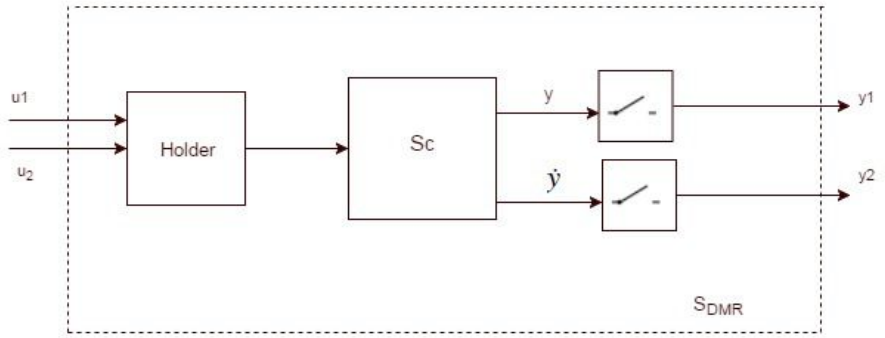

Figure 2.4: MR sampled data model scheme

sampling instant are described the so called MR equivalent model in the form of

$$x_{k+1} = A^{\delta}x_k + (A^{(r-1)\delta}B^{\delta}, \ldots, B^{\delta}) \begin{pmatrix} u_1 \\ \vdots \\ u_r \end{pmatrix} \tag{2.16}$$
$$y_k = Cx_k.$$

The MR sampled data equivalent model is a multi input system. This scheme offers further degree of freedom than the classical single rate one.Those further control variation can be exploited to fulfil extra control specification.

Throughout the current Thesis, we will see that multi rate sampled data model will play a very important role in guaranteeing stability.In particular we will focus on the idea of the feedback design of a multi rate sample data model and how we can benefit from it in case of the existence of unstable zeros in the continuous time model.

2.2.2.1 Eigenvalues and zeros of Multi Rate model

In case of Multi Rate sampling, one can easily deduce that the eigenvalues are preserved.As a matter of fact if $\lambda \in \sigma(A)$ in (2.4), then $e^{\lambda\delta} = e^{\lambda T} \in \sigma e^{AT}$.As far as the zeros are concerned, it was proven in [[67]] that the zeroes of the continuous-time system (2.4) are preserved under multi rate sampling when the multi rate order

is set as the relative degree and the extended output

$$\hat{y} = \begin{pmatrix} C \\ CA \\ \vdots \\ CA^{r-1} \end{pmatrix} x$$

is considered namely , the transmission zero of the square system

$$x_{k+1} = A^T x_k + A^{(r-1)\delta} B^\delta u_{1k} + \cdots + B^\delta u_{rk}$$
$$\hat{y} = \begin{pmatrix} C \\ CA \\ \vdots \\ CA^{r-1} \end{pmatrix} x$$

coincide with $e^{z\delta}$ where z:$(i = 1, \ldots, n-r)$ denotes the zeros of (2.4).

Accordingly,MR sampling preserves the relative degree and the zeros of the continuous-time plant.Moreover , MR prevents from the appearance of the sampling zeros.

2.2.3 Sampling via generalized hold function as a case of MR

Sampling via generalized hold function is a particular a case of MR.When setting $u_{ik} = \alpha_i u_k$ for $\alpha_i \in u_k \in \mathbb{R}$ and $u_k := u(k\delta)$ one recover the sampling procedure through GHF. In that case , the sampled-data equivalent model is described by the

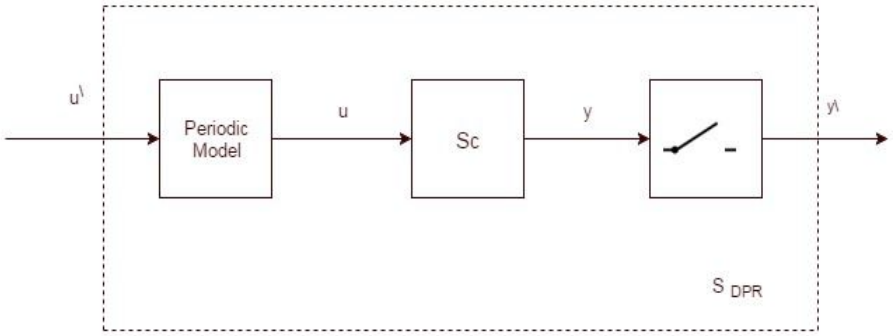

Figure 2.5: Periodic MR model scheme

system

$$x_{k+1} = A^\delta x_k + (\alpha_1 A^{(r-1)\frac{\delta}{r}} + \ldots + \alpha_r I) B^{\frac{\delta}{r}}) u_k \tag{2.17}$$
$$y_d(k) = C x_k. \tag{2.18}$$

Note that through applying the GHF the sampled-data equivalent model (2.16)is reduced to a a single input dynamics.

2.2.4 Eigenvalues and zeros of -Periodic MR model

In this case,it can be shown that α_i can be chosen to assign the sampling zeros of the equivalent model (5.5.6).Accordingly, by setting such parameters one can indiuce stable sampling zeroes. such a scheme is not preserving the relative degree ([48, 18])

2.2.5 Asymptotic sampling zeros

It's important to analyze the asymptotic behaviour of the zeros in sampled-data models, as the sampling period goes to zero.The development in the study of the zeros role in sample data system can be tracked back to the earlier results obtained by Astrom.He stated that for a class of linear system if the pole excess of a transfer function is equal to one the stability,respectively instability of the zeros is maintained under sampling,while for pole excess larger than two for small sampling period the pulse of the transfer function always has unstable zero.

The pulse transfer function corresponds to the nth order integrator $w(s) = s^{-n}$ at a sampling period T is expressed as

$$w(z) = \frac{T^n}{n!}\frac{B_n(z)}{(z-1)^n} \tag{2.19}$$

in

$$B_n(z) = b_1^n(z^{n-1}) + \cdots + b_n^n \tag{2.20}$$

$$b_k^n = \sum_{l=1}^{k}(-1)^{k-l}l^n\binom{n+1}{k-l} \tag{2.21}$$

Remark 2.1 *The polynomials defined in $B_n(z), b_k^n$ correspond, to the polynomials :*

1 *Their coefficients can be computed recursively:*

$$b_1^n = b_n^n = 1, \quad \forall n \geqslant 1 \tag{2.22}$$

$$b_k^n = kb_k^{n-1} + (n-k+1)b_{k-1}^{n-1}; \quad k = 2, \ldots, n-1 \tag{2.23}$$

2 *Their roots are always negative real numbers.*

3 *every root of the polynomial $B_{n+1}(z)$ lays between every two adjacent roots of $B_n(z)$, for $n \geqslant 2$.*

4 *The following recursive relation holds:*

$$B_{n+1}(z) = z(1-z)\frac{dB_n}{dz}(nz+1)B_n(z); \quad n \geqslant 1 \tag{2.24}$$

Remark 2.2 *sampled-data models for n-th order integrator play a very important role in obtaining asymptotic results. Indeed, as the sampling rate increases, a system of relative degree n, behaves as an n-th order integrator.*

Remark 2.3 *The relationship between the continuous-time poles and those of the discrete-time model can be easily determined. However, the relationship between the zeros in the continuous and discrete-time domains is much more involved. We consider the asymptotic case as the sampling rate increases. In conclusion one can say that for a continuous time transfer function in the form*

$$G(s) = \frac{N(s)}{D(s)} = \frac{k(s-z_1)\dots(s-z_m)}{(s-p_1)\dots(s-p_n)} \tag{2.25}$$

and Gq(z) the corresponding pulse transfer function. Assume that $m < n$*,i.e., G(s) strictly proper.Then as the sampling period* $T \to 0$*, the zeros* m *of Gq(z) go to* 1 *as* $e^{z_i\delta}$*, and the remaining* $(n-m-1)$ *zeros of* $G(z)$ *go to the zeros of the polynomial* $B_{n-m}(z)$ *defined in the previous argument i.e.*

$$G(Z) \xrightarrow{\det\approx 0} \frac{T^{n-m}(z-1)^m B_{n-m}(z)}{(n-m)!(z-1)^n} \tag{2.26}$$

2.2.5.1 Example.1

SR sampling Consider the system in the form

$$\begin{aligned} \dot{x}_1 &= x_2 \\ \dot{x}_2 &= u \\ y &= x_1 \end{aligned} \tag{2.27}$$

The system obtain relative degree $r = 2$ as $CAB \neq 0$.The transfer function corresponding to the the LTM is given by $\frac{1}{s^2}$and the sample data model is

$$\begin{pmatrix} x_1(k+1) \\ x_2(k+1) \end{pmatrix} = \begin{pmatrix} 1 & T \\ 0 & 1 \end{pmatrix} \quad \begin{pmatrix} x_{1k} \\ x_{2k} \end{pmatrix} + \begin{pmatrix} \frac{T^2}{2} \\ T \end{pmatrix} u(k) \tag{2.28}$$

$$y = x_{1k}. \tag{2.29}$$

The transfer function w.r.to the sampled-data model is given by

$$W_{SR}(z) = \frac{\frac{T^2}{2}(z+1)}{(z-1)^2} \tag{2.30}$$

as we can see from figure 2.6 an extra zero will appear which has no counterpart in continuous time.Moreover the relative degree of the sample data model drops to one ($C^T B^T = \frac{T^2}{2}$).

MR sampling Going back to the case of the double integrator we compute the the multi rate sampling data model at $\delta = \frac{T}{2}, T = 0.1$

$$\begin{aligned} \begin{pmatrix} x_1(k+1) \\ x_2(k+1) \end{pmatrix} &= \begin{pmatrix} 1 & 2T \\ 0 & 1 \end{pmatrix} \begin{pmatrix} x_{1k} \\ x_{2k} \end{pmatrix} + \begin{pmatrix} \frac{3}{2}T^2 & \frac{1}{2}T^2 \\ T & T \end{pmatrix} \begin{pmatrix} u_{1k} \\ u2k \end{pmatrix} \\ Y(x_k) &= \begin{pmatrix} Cx \\ CAx \end{pmatrix} = \begin{pmatrix} 1 & 0 \\ 0 & 1 \end{pmatrix}. \end{aligned} \tag{2.31}$$

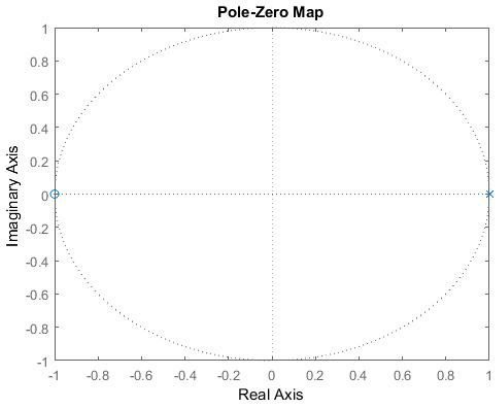

Figure 2.6: Pole Zero map of SR sample data model

The MR sampled data model obtain relative $r_d = 2$ which is the same as the continuous time system.In the other hand the MR sampled data model convert the system into MIMO system which indicate that the system will have two types of zeros the invariant zeros and the transmission zero.Through computing the zeros of the MR model

$$N(s) = \det \begin{pmatrix} ZI - A^{\delta} & -B^{\delta} \\ C^{\delta} & D^{\delta} \end{pmatrix} = \det \begin{pmatrix} z-2 & -2T & \frac{-3}{2}T^2 & \frac{-1}{2}T^2 \\ 0 & z-1 & -T & -T \\ 1 & 0 & 0 & 0 \\ 0 & 1 & 0 & 0 \end{pmatrix} = T^3 \quad (2.32)$$

It can be easily noted that the multi rate sampling technique prevent from the appearance of asymptotic sampling zeros as the transfer function of continuous time and the sampled data models have no zero's.

GHF sampling The GHF can be used to assign the sampling zeros or to achieve additional control requirement.For example we could design a feedback control law such that a zero is assigned at the origin.In such a case and through computation we obtain transfer function

$$W_{PR}(z) = \frac{(\frac{T^2}{2}z)}{(z-1)^2} \quad (2.33)$$

2.3 Nonlinear Systems

Models for continuous-time systems typically take the form of (nonlinear) differential equations. In this section we are going to discuss the affect of sampling on the nonlinear continuous time systems([29])

2.3.1 Equivalent sampled data models

Consider the nonlinear system

$$\Sigma_{NL} : \dot{x} = f(x) + g(x)u, \quad x, y \in \mathbb{R}^n, u \in \mathbb{R} \tag{2.34}$$

$$y = h(x). \tag{2.35}$$

Posing an equilibrium at $\dot{x} = 0$ and a well defined relative degree $r \leqslant n$;i.e, $L_g L_f^k h(x) = 0, k = 1, \ldots, r-2$ and $L_g L_f^{r-1} h(x) \neq 0$

2.3.1.1 under single rate sampling

Consider $u(t) \in \mathcal{U}_T$ and $y(t) = y(kT)$ for $t \in [kT, (k+1)T[$,with T being the sampling period. Then the dynamics of Σ_{NL} at the sampling instants is described by the single-rate sampled-data equivalent model

$$\Sigma_d : \begin{cases} x_{k+1} = & F^T(x_k, u_k) \\ y_k = & h(x_k) \end{cases} \tag{2.36}$$

with $x_k := x(kT)$, $y_k := y(kT)$, $u_k := u(kT)$.

Definition 2.1 The system Σ_d defines the exact sampled equivalent of system Σ_c if for initialization $x(0)$ and for constant control over time interval of amplitude T the state evolution of Σ_d and Σ_c are the same at sampling instant $t = kT$;i.e. Assume for some values $k \geqslant 1$ ones have$x(kT) = x_k$.

The sample dynamics can be computed by integrating the continuous dynamics.The following Taylor expansion holds true

$$x(k+1) = x_c((k+1)T) \tag{2.37}$$

$$:= x_c(kT) + T\frac{dx_c(t)}{dt}|_{t=kT} + \frac{T^2}{2}\frac{d^2x_c(t)}{dt^2}|_{t=kT} + \ldots| \tag{2.38}$$

$$:= (1 + TL_f(f + u_k g) + \cdots + \frac{T^p}{p!}L_f^p(f + u_K g) + \ldots)(x(kT). \tag{2.39}$$

For any constant input u_K and T small enough the right hand side represents the series expansion of the solution of equation (2.35). As we have seen from the previous definition Σ_d presents the exact sampled-model.Still,computing an exact and closed form of $F^T(.,.)$ is to so that approximation are generally computed in practice by the series expansion (2.38) at any fixed order of in T.Whenever (2.38) admits a finite number of terms in power of T, we shall say that Σ_d admits a finite sampled-data equivalent model or that it is finitely descritizable.

2.3.1.2 under Multi rate sampling of order r

The concept of Multi rate sampling was first extended into the nonlinear context by professor Monaco and professor Dorothee Normand-Cyrot ([67]).For the sake of

clarity, we assume a single input $u(t) \in \mathbb{R}$, and being constant over subinterval of amplitude$\delta = \frac{T}{r}$ and denote as u_{iK} the value of $u(t)$ over$[kT + (i-1)\delta, [kT + i\delta[$ for $i = 1, .., r$

$$u_i(k) = u(kT + \frac{i-1}{r}T) \quad \text{for} t \in [kT + (i-1)\delta, kT + \delta[\tag{2.40}$$

The discrete time state- space representation Σ_d^rdescribing the continuous-time system Σ_c at any sampling instant $t = kT$, for $k \geqslant 0$ given by

$$\Sigma_d^r : \begin{cases} \dot{x}_d(k+1) = F^\delta(x_k, u_{1k}, \ldots, u_{rk}) \\ y_k = h(x_k). \end{cases} \tag{2.41}$$

Definition 2.2 The system Σ_d^r is referred to as the exact multi rate sampled-data equivalent of order r to system Σ_c if with the same initialization and constant controls over time interval of amplitude $\delta = \frac{T}{r}$,$\Sigma_d^r$and Σ_c exhibits the same input state behaviour,at sampling instant $t = kT$.

The multi rate sampled dynamics F^δ admits the following lie exponential representation

$$F^\delta(x_k, u_{1k}, \ldots, u_{rk}) = e^{\delta L_{f(.)} + u_1 k L_{g(.)}} \circ \cdots \circ e^{\delta L_{f(.)} + u_r k L_{g(.)}}. \tag{2.42}$$

as in the SR case, computing $F^\delta(.,.)$ in (2.41) might not be possible in practical.However , the power series form induced by (2.42)provided a powerful tool for computational facilities. A series expansion and approximate representation of a multi rate sampled model can be found in([40]).Its well known that sampling might not preserve certain properties of the continuous- time system.In particular the loss of relative degree and effect on the zero dynamics under sampling are the source of several difficulties in the design problems. As we have illustrated before ,the notion of the zero dynamics plays an important role in the solution of several control problems, we will discuss the behaviour of zero dynamics under sampling in the following section.

2.3.2 Relative degree under sampling

By applying the discrete-time definition 1.2 of the relative degree , we get that sampled-data dynamics Σ_d has relative degree r if

1 for any $i = 1, \ldots, r-3$, $\frac{\partial}{\partial u_i} h_o (F_0^T)^k o F^T(., u)(x) = 0$
$0 \leqslant k \leqslant r-3 \quad \forall (x, u) \in M * \mathbb{R}^m$

2 $\frac{\partial}{\partial u_i} h_o (F_0^T)^{r-1} o F^T(., u)(x) \neq 0$

The following lemma is an immediate consequence of the definition of Σ_d

Lemma 2.2 *([66]) Given a SISO linear analytic continuous time system Σ_c with relative degree r the relative degree associated to the exact sample equivalent system Σ_d is equal to one almost every where.*

The proof of this lemma is directly deduced from the expansion according to $\delta(T \in [0, \delta_0[)$ of the output system Σ_d as

$$y(k+1) = h(x(k+1)) = h(x_k) + \sum_{j \geqslant 1} \frac{T^j}{j!} y_c^j(kT) \tag{2.43}$$

$$= h(x_k) + \sum_{i \geqslant 1}^{r-1} \frac{T^i}{i!} L_f^i h + \frac{T^r}{r!}(L_f + uL_g) L_f^{r-1} h \tag{2.44}$$

where $y_c^j(kT)$ represents the j^{th} output derivatives of $y_c(t)$, computed at time $t = kT$ under sampled data feedback.Accordingly ,one obtains $\frac{\partial y_(k+1)}{\partial u} = \frac{T^r}{r!} L_g L_f^{r-1}(h)(x_k) = TL_g L_f^{r-1} h + \cdots +$.Thus the exact sample model has relative degree one regardless the relative degree of the continuous-time.

2.3.3 Zero dynamics under sampling

Along the lines of the continuous-time case, sampling induces an additional zero dynamics (the so called sampled-data zero dynamics) of dimension $n - r - 1$.Those dynamics are in general unstable as the continuous-time relative degree is $r \geq 2$.Roughly speaking any nonlinear system with relative degree higher than two exhibits its unstable zero dynamics under sampling for T sufficiently small.Consequently any control technique based on an zero dynamics inversion may induces unstability of the control system.As a matter of fact, SR sampling induces nonminimum phase of the sampled-data equivalent model despite of the original continuous-time performance.This problem was successfully solved through the use of MR sampling technique.In such a case , it is shown that the MR sampled-data model (2.41)with output

$$\hat{y} = \begin{pmatrix} h(x) \\ L_f h(x) \\ \vdots \\ L_f^{r-1} h(x) \end{pmatrix}$$

has vector relative degree $\hat{r} = (2, \ldots, 1)(|\ \hat{r}\ | = r$ and preserves the same zero dynamics as in continuous-time.

2.4 Conclusion

Different types of sampling procedures have been recalled in this chapter together with corresponding sampled-data equivalent model.Then,particular attention has been devoted to the way those sampling scheme affect the original continuous-time properties with focus on the relative degree and zero dynamics.More, in details it has been shown how multi rate can be suitably employed to overcome the issues linked to the loss of a relative degree and the new sampling zeros dynamics which a generally unstable.

Chapter 3

Feedback linearization with stability

Contents

3.1 Introduction

The solution of several nonlinear control problems required the cancellation of some intrinsic dynamics of the plant under feedback.It results that the so-defined control will ensure stability in closed-loop if and only if the dynamics to cancel are stable.In the case of LTI systems, this corresponds to assign part of the eigenvalues coincident to the zeroes.This will include the an unobservable dynamics whose stability depends on the location of such zeroes in the complex plane.What if those dynamics are unstable?
Classical control strategies through inversion might solve the problem while making the closed loop system unstable.Still the linear case suggests that when those dynamics are unstable a solution can be obtained.

Based on this idea, we consider non minimum phase nonlinear single-input single-output (SISO) systems that are controllable in first approximation and settle the

problem in the context of Input-Output linearization. In that case, because the zero-dynamics are unstable, classical techniques cannot be implemented to solve the problem with stability.
In this chapter we introduce an approach that is based on the notion of *partially minimum phase* systems. The design we propose proceeds in two steps: considering the linear tangent model (LTM) of the original system, we first define a dummy output based on a suitable factorization of the numerator of its transfer function so that the corresponding linearized system is minimum-phase; then, we perform classical input-output linearization of the locally minimum-phase nonlinear system with the aforementioned dummy output. Finally, we show that when applying the resulting feedback to the original system, input-output linearization still yields with respect to the original output while guaranteeing stability of the internal dynamics.

Then we extend the results to the sampled-data context; namely, measures of the output (say the state) are available only at some time instants and the control is piecewise constant over the sampling period.

3.2 Problem settlement

We consider nonlinear input-affine dynamics with linear output;namely,

$$\Sigma_{NL}: \begin{cases} \dot{x} = & f(x) + g(x)u, \quad x \in \mathbb{R}^n, u \in \mathbb{R}, y \in \mathbb{R} \\ y = h(x) = C(x). \end{cases} \tag{3.1}$$

We assume that the system has a well define relative degree $r \leq n$ at the origin in a neighbourhood of $x = 0$ i.e., $f(0) = 0$.Moreover , we assume that (3.2)is nonminimum phase;i.e,the origin is unstable equilibrium of the zero dynamics associated to (3.2).Here we are considering the problem of defining a feedback that makes the input output behaviour linear while ensuring stability of the overall dynamics.The input output feedback linear property is recalled.This problem was originally posed and solved by Isidori and kerner.Recalling from chapter 1 the can be transformed into normal form via a diffeomorphism $\phi(x) = [\zeta^T, \eta^T]$ if the relative degree r is well defined.The ζ coordinates are defined by

$$\zeta = L_f^{i-1} h(x), \quad \forall 1 \leqslant i \leqslant r. \tag{3.2}$$

and $\eta = \Phi_{r+i}(x), \quad 1 \leqslant i \leqslant n - r$ where $L_g \Phi_i(x) = 0$.The normal form rewrites as

$$\begin{aligned} \dot{\zeta} &= \hat{A}\zeta + \hat{B}(b(\zeta, \eta) + a(\zeta, \eta)u) \\ \dot{\eta} &= q(\zeta, \eta) \\ y &= \zeta_1. \end{aligned} \tag{3.3}$$

with

$$\hat{A} = \begin{pmatrix} \mathbf{0} & I_{r-1} \\ \mathbf{0} & \mathbf{0} \end{pmatrix}, \quad \hat{B} = \begin{pmatrix} \mathbf{0} \\ 1 \end{pmatrix} \tag{3.4}$$

The static feedback control law,

$$u = \frac{1}{a(\zeta,\eta)}(-b(\zeta,\eta)+v) \tag{3.5}$$

changes the rth equation of (3.3) to : $\dot{\zeta}_r = v$. As a result the map between the transformed input v and the output y is exactly linear.Thus,a linear state feedback controller can be synthesized to stabilize the ζ subsystem.The control when expressed in the original coordinates have the following form

$$u = \frac{1}{L_g L_f^{r-1} h(x)}(-L_f^r h(x)+v). \tag{3.6}$$

$$\tag{3.7}$$

The external input v can be chosen in order to assign a specific set of eigenvalues or to fulfil extra control requirement ;i.e,

$$v = b_{r-1}L_f^{r-1}h(x) + \cdots + b_o h(x) \tag{3.8}$$

and (3.9)

$$u = L_g L_f^{r-1} h(x)^{-1}(-L_f^r h(x) + b_{r-1}L_f^{r-1}h(x) + \cdots + b_o h(x)). \tag{3.10}$$

The asymptotic stabilization resulting from the input output linearization will be discussed fibrefill.

3.2.1 local stability

The input output linearized system is said to be locally asymptotically stable if the zero dynamics

$$\dot{\eta} = q(0,\eta) \tag{3.11}$$

is local locally asymptotically stable.

3.2.2 Global Stability

The feedback linearized system is said to be globally asymptotically stable if the zero dynamics (3.11) is asymptotically stable.The argument for this proceed as follows.The state ζ variables can be forced to zero arbitrarily fast by appropriate selection of controller tuning parameter b_i.Once the ζ variable converge to zero , the closed loop trajectories described by the zero dynamics (3.11).Because the zero dynamics are globally asymptotically stable by assumption , the η state variables converge to zero and the closed loop system is globally asymptotically stable.The argument does not hold if the system relative degree is bigger than two $r \geqslant 2$ due to the so called " peaking phenomena".High gain linear feedback can cause the linear state variable η to become very large before they decay to zero.These "peaking" variables act as destabilizing inputs to the zero dynamics.Consequently

more restrictive condition is required to insure hat the linearized feedback system is globally asymptotically stable.

Now let us assume that the system holds relative degree n .Then the exact feedback linearization problem consists in establishing a coordinate transformation $z = \phi(x)$ and a feedback control law $u = \alpha(x) + \beta(x)v$ so that

$$\dot{x} = f(x) + g(x)u$$

is linear at least locally in closed loop

$$\dot{z} = Az + Bv \tag{3.12}$$

Theorem 3.1 *The exact feedback linearization problem is solvable for $x(0)$ if and only if*

1 $\Delta_{n-1}(x)$ *has rank* $\Delta_{n-1}(0) = n$.

2 $\Delta_{n-2}(x) := span\left\{g, \quad ad_f g, \quad \ldots, \quad ad_f^{n-2} g\right\}$ *is involutive in a neighbour of origin*

As well known, controllability of the linearity to be controllable with controllability matrix

$$\mathcal{R} = \begin{pmatrix} B & AB & \ldots & A^{n-1}B \end{pmatrix} \tag{3.13}$$

verifying

$$\rho\{\mathcal{R}\} = n. \tag{3.14}$$

As well known , controllability in the first approximation of Σ_{NL} is necessary to solve the input output linearization problem;namely, determining

$$A = \varphi_f(0), \quad B = g(0). \tag{3.15}$$

we need

$$\begin{aligned} \dot{x} &= Ax + Bu \\ y &= Cx \end{aligned} \tag{3.16}$$

If (A, B, C) is not in the canonical controllable form (3.16), one preliminarily applies to (3.2) the linear transformation

$$\xi = Tx, \quad T = \begin{pmatrix} \gamma^\top & (\gamma A)^\top & \ldots (\gamma A^{n-1})^\top \end{pmatrix}^\top$$

with $\gamma = \begin{pmatrix} \mathbf{0} & 1 \end{pmatrix} \begin{pmatrix} B & AB & \ldots A^{n-1}B \end{pmatrix}^{-1}$ so transforming the system into the required form.

In this setting, we looks for a continuous-time feedback that ensures input-output linearization of (3.2) while guaranteeing stability of the internal dynamics. This will be achieved via partial dynamics cancellation. Then, we will extend the strategy to the sampled-data context through multirate sampled-data feedback. Finally we will extend the results to the square MIMO systems.

3.3 Partial zero-dynamics cancellation

First,let us sketch the idea that we are going to develop to the LTI case.To this end, consider a controllable LTI system with relative degree and transfer function

$$W(s) = C(sI - A)^{-1}B = \frac{N(s)}{D(s)} \tag{3.17}$$

with $N(s) = b_0 + b_1 s + \cdots + b_m s^m$ and $D(s) = a_0 + a_1 s + \cdots + a_{n-1}s^{n-1} + s^n$ and relative degree $\hat{r} = n - m$.

Given any factorization of the numerator $N(s) = N_1(s)N_2(s)$ and fixed $D(s)$, the dummy output $y_i = C_i x$ with $C_i = (b_0^i \dots b_{m_i}^i \ \mathbf{0})$ defines a new system

$$\dot{x} = Ax + Bu \tag{3.18}$$

$$y_i = C_i x \tag{3.19}$$

with transfer function

$$W_i(s) = C(sI - A)^{-1}B = \frac{N_i(s)}{D(s)} \tag{3.20}$$

and $N_i(s) := b_0^i + b_1^i s + \cdots + b_{m_i}^i s^{m_i} (i = 1, 2)$ as numerator and relative degree $r_i = n - m_i \ (i = 1, 2)$.
Accordingly, the outputs y, y_1 and y_2 are related by

$$y(t) = N_1(s)y_2(t), \quad y(t) = N_2(s)y_1(t) \tag{3.21}$$

so getting for $j \neq i$ and $\dot{=}\frac{d}{dt}$

$$y(t) = b_0^j y_i + b_1^j \frac{d}{dt} y_i + \cdots + b_{m_j}^j \frac{d^{m_j}}{dt^{m_j}} y_i \tag{3.22}$$

The feedback

$$u_i = -F_i x + v, \quad F_i = \frac{C_i A^{r_i}}{C_i A^{r_i - 1} B}, \quad i = 1, 2 \tag{3.23}$$

transforms (3.16) into a system with closed-loop transfer function given by

$$W^{F_i}(s) = C(sI - A - BF_i)^{-1}B \tag{3.24}$$

$$= \frac{N_j(s)}{s_i^r} = \frac{b_0 + b_1^j s + .. + b_{m_j}^j s^{m_j}}{s^{r_i}}, \quad j \neq i. \tag{3.25}$$

Remark 3.1 *The feedback $u = -F_i x$ coincides with the one deduced from the Ackermann formula assigning the poles of the system to the roots of $p_i^*(s) = s^{r_i} N_i(s)$. As a consequence, it rewrites $u_i = -F_i x, \quad F_i = -\gamma p_i^*(A)$ and γ is the last row of the controllability matrix.*

Proof: Assume the LTM is completely controllable, where we use the state feedback control $u = -F_i x$. Applying the feedback modifies the system to

$$\dot{x} = (A - BF_i)x \tag{3.26}$$

Let us define $\bar{A} = A - BF_i$.The feedback cancels zero's with the characteristic equation $SI - A - BF_i = s^n + \alpha_1 s^{n-1} + \cdots + \alpha_n$.Since the Cayley-Hamilton theorem states that$\bar{A}$ satisfies its own characteristic equation, we have

$$P(\bar{A}) = \bar{A}^n + \alpha_1 \bar{A}^{n-1} + \alpha_n I = 0 \tag{3.27}$$

In order to simplify the derivation we consider the case where $n = 3$ i.e.

$$\begin{aligned} &I = 1 \\ &\bar{A} = (A - BF_i) \\ &\bar{A}^2 = (A - BF_i)^2 = A^2 - AF_iB - BF_i\bar{A} \\ &\bar{A}^3 = A^3 - A^2F_iB - ABF_i\bar{A} - BF_i\bar{A}^2 \end{aligned} \tag{3.28}$$

Multiplying the preceding equations in order by $\alpha_3, \alpha_2, \alpha_1, and \alpha_0$ (where $\alpha_0 = 1$),respectively, and adding the results, we obtain

$$\begin{aligned} &\alpha_3 I + \alpha_2 \bar{A} + \alpha_1 \bar{A}^2 + \bar{A}^3 = \alpha_3 I + \alpha_2 A + \alpha_1 A2 + A3 \\ &- \alpha_2 BF_i - \alpha_1 ABF_i - \alpha_1 BF_i\bar{A} - A^2BF_i - ABF_i\bar{A} - BF_i\bar{A}^2 \end{aligned} \tag{3.29}$$

Referring to Equation (3.18), we have

$$\alpha_3 I + \alpha_2 \bar{A} + \alpha_1 \bar{A}^2 + \bar{A}^3 = P(\bar{A}) = 0 \tag{3.30}$$

$$\alpha_3 I + \alpha_2 A + \alpha_1 A^2 + A^3 = P(A) \neq 0 \tag{3.31}$$

Substituting the last two equations into Equation (3.18), we have

$$P(\bar{A}) = P(A) - \alpha_2 BF_i - \alpha_1 BF_i\bar{A} - BF_i\bar{A}^2 - \alpha_1 ABF_i - ABF_i\bar{A} - A^2BF_i \tag{3.32}$$

Since$P(\bar{A}) = 0$, we obtain

$$P(A) = [B : AB : A^2B] \begin{pmatrix} F_i + \alpha_1 F_i\bar{A} + F_i\bar{A}^2 \\ \alpha_2 F_i + F_i\bar{A} \\ F_i \end{pmatrix} \tag{3.33}$$

Premultiplying both sides of Equation (3.25) by the inverse of the controllability matrix, we obtain

$$[B : AB : A^2B]^{-1} P(A) = \begin{pmatrix} F_i + \alpha_1 F_i\bar{A} + F_i\bar{A}^2 \\ \alpha_2 F_i + F_i\bar{A} \\ F_i \end{pmatrix} \tag{3.34}$$

Pre multiplying both sides of this last equation by $[0 \quad 0 \quad 1]$, we obtain

$$[0 \quad 0 \quad 1][B : AB : A^2B]^{-1}P(A) = [0 \quad 0 \quad 1]\begin{pmatrix} F_i + \alpha_1 F_i\bar{A} + F_i\bar{A}^2 \\ \alpha_2 F_i + F_i\bar{A} \\ F_i \end{pmatrix} = F_i \quad (3.35)$$

which can be rewritten as

$$F_i = [0 \quad 0 \quad 1][B : AB : A^2B]^{-1}P(A) \quad (3.36)$$

For an arbitrary positive integer n, we have $F_i = [0 \quad 0 \quad \dots \quad 1][B : AB : \cdots : A^{n-1}B]^{-1}P(A)$ ■

The feedback $u = -F_ix + v$ places m_i eigenvalues of the system coincident with the zeros of $N_i(s)$ and the remaining ones to 0 so that stabilization in closed-loop can be achieved via a further feedback v if and only if $N_i(s)$ is Hurwitz. The previous argument is the core idea of assigning the dynamics of the system via feedback through cancellation of the stable zeros only. Accordingly, if $N(s)$ is not Hurwitz (i.e. $N_j(s)$ has positive real part zeros) the closed-loop system will still have non stable zeros that will play an important role in filtering actions but that will not affect closed-loop stability.For better understanding of the zero cancellation concept simple example is illustrated

3.3.1 Example

Consider the linear controllable system

$$\begin{aligned} \dot{x}_1 &= x_2 \\ \dot{x}_2 &= x_3 \\ \dot{x}_3 &= u \\ y &= -2x_1 - x_2 + x_3 \end{aligned} \quad (3.37)$$

with

$$A = \begin{pmatrix} 0 & 1 & 0 \\ 0 & 0 & 1 \\ 0 & 0 & 0 \end{pmatrix}, \quad B = \begin{pmatrix} 0 \\ 0 \\ 1 \end{pmatrix}, \quad C = [-2 - 1 \quad 1] \quad (3.38)$$

The system has a well define relative degree $r = 1$ as $CB = 1 \neq 0$.The zeroes of the system is partially minimum phase as one of the zero is with positive real part($s_1 = 2$) with the other is located in the negative side($s = -1$).Referring to remark (3.2) ,there exists a feedback control law that partially cancels the zeros of the system.To see this , let us consider the transfer function of (3.37)

$$W(s) = \frac{(s+1)(s-2)}{s^3} \quad (3.39)$$

whose numerator can be factorized as

$$W(s) = \frac{N_1(s)N_2(s)}{s^3} \quad (3.40)$$

with $N_1(s) = s + 1, \quad N_2(s) = s - 2$.Accordingly, exploiting such a factorization one defines the dummy output $y_1 = (110)x = x_1 + x_2$ with respect to which the system is minimum phase,

The relative degree w.r.to the new output $r_1 = 2$ and we get a feedback in the form

$$u = \frac{v - CA^2x}{CAB} \text{with} \quad CA^2 = \frac{[0 \quad 0 \quad 1]}{1} \quad \text{and} CAB = 1 \tag{3.41}$$

Through applying the feedback in the original system eq 3.29 we cancels the stable zero as we can see from the transfer function below

$$\bar{W}_1(s) = \frac{s-2}{s^2 - s - 2} \tag{3.42}$$

The original output is now rewrites as

$$(d-2)y_1 = \dot{y}_1 - 2y_1.$$

Which in general can be expressed as $y(t) = p(d)y_1$ with $p(d) = \frac{d}{dt}$
Concluding, given any controllable linear system one can pursue stabilization in closed-loop via partial zeros cancellation: starting from a suitable factorization of the polynomial defining the zeros, this is achieved via the definition a dummy output with respect to which the system is minimum phase.

3.4 Continuous-time feedback linearization of partially minimum phase systems

In what follows, we show how the idea developed in the linear context can be settled in the framework of feedback linearization of nonlinear dynamics of the form (3.1) that are not minimum phase in first approximation.

Lemma 3.1 *Consider the nonlinear system (3.2) and suppose that its LTM at the origin is controllable in the form (3.16) and non minimum phase with relative degree r. Denote by $N(s) = b_0 + b_1 s + \dots b_{n-r}s^{n-r}$ the not Hurwitz polynomial identifying the zeros of the LTM of (3.2) at the origin. Consider the maximal factorization of $N(s) = N_1(s)N_2(s)$*

$$N_i(s) = b_0^i + b_1^i s + \dots b_{n-r_i}^i s^{n-r_i}, \quad i = 1, 2 \tag{3.43}$$

such that $N_2(s)$ is a Hurwitz polynomial of degree $n - r_2$. Then, the system

$$\dot{x} = f(x) + g(x)u, \quad y_2 = C_2 x. \tag{3.44}$$

$C_2 = \begin{pmatrix} b_0^2 & b_1^2 & \dots & b_{n-r_2}^2 & \mathbf{0} \end{pmatrix}$ *has relative degree r_2 and is locally minimum-phase.*

Proof: By computing the linear approximation at the origin of (3.44), one gets that the matrices (A, B, C_2) are in the form (3.2) so that the entries of C_2 are the coefficients of $N_2(s)$ that is the numerator of the corresponding transfer function. By construction, $N_2(s)$ is a Hurwitz polynomial of degree $n-r_2$. It follows that, in a nearby of the origin, the relative degree of (3.44) is r_2. Furthermore, since the linear approximation of the zero-dynamics of (3.44) coincides with the zero-dynamics of its LTM model at the origin, one gets that (3.44) is minimum-phase. ■

Lemma 3.2 *Consider the nonlinear system (3.44) and introduce the normal form associated to $h_2(x) = C_2 x$*

$$\begin{pmatrix}\zeta\\ \eta\end{pmatrix} = \phi(x) = \begin{pmatrix} h_2(x) & \dots & L_f^{r_2-1}h_2(x) & \phi_2^\top(x)\end{pmatrix}^\top \tag{3.45}$$

with $\phi_2(x)$ such that $L_g\phi_2(x) = 0$ so that

$$\dot\zeta = \hat A\zeta + \hat B(b(\zeta,\eta) + a(\zeta,\eta)u) \tag{3.46a}$$
$$\dot\eta = q(\zeta,\eta) \tag{3.46b}$$
$$y_2 = \begin{pmatrix}1 & \mathbf{0}\end{pmatrix}\zeta \tag{3.46c}$$

Then, the feedback

$$u = \frac{1}{a(\zeta,\eta)}(v - a(\zeta,\eta)) \tag{3.47}$$

solves the Input-Output Linearization problem with stable zero-dynamics. for the system (3.44)

Proof: The proof is straightforward from construction of y_2 in Lemma 3.1. ■

Remark 3.2 *We recall that, in the original coordinates, the feedback (3.47) rewrites as*

$$u = \gamma(x,v) := \frac{v - L_f^{r_2}h_2(x)}{L_gL_f^{r_2-1}h_2(x)}. \tag{3.48}$$

Theorem 3.2 *Consider the nonlinear system (3.2) and suppose that its LTM at the origin is controllable in the form (3.16) and non minimum phase with relative degree r. Define the dummy output $y_i = h_i(x) = C_i x$ $(i = 1, 2)$ as in Lemma 3.1 and the state transformation (3.45) that puts the system into the form*

$$\dot\zeta = \hat A\zeta + \hat B(b(\zeta,\eta) + a(\zeta,\eta)u) \tag{3.49a}$$
$$\dot\eta = q(\zeta,\eta) \tag{3.49b}$$
$$y = N_1(\mathrm{d})y_2. \tag{3.49c}$$

Then, the feedback (3.47) solves the input-output linearization problem with stability of the internal dynamics of (3.1).

Proof: From Lemmas 3.1 and 3.2, by expliciting $y = N_1(\mathrm{d})y_2$ and exploiting (3.45) one gets

$$y = b_0^1 y_2 + b_1^1 \dot{y}_2 + \cdots + b_{r_2-r}^1 y_2^{(r_2-r)} = \begin{pmatrix} C_1 & \mathbf{0} \end{pmatrix} \zeta$$

so that in closed-loop (3.34) rewrites as

$$\dot{\zeta} = \hat{A}\zeta + \hat{B}v \tag{3.50a}$$
$$\dot{\eta} = q(\zeta, \eta) \tag{3.50b}$$
$$y = \begin{pmatrix} C_1 & \mathbf{0} \end{pmatrix} \zeta \tag{3.50c}$$

that exhibits a linear input-output behavior. Moreover, by construction, $y_2 \equiv 0$ implies $y \equiv 0$ so that the restriction of the trajectories of (3.50) onto the manifold identified by $y \equiv 0$ is described by the dynamics $\dot{\eta} = q(0, \eta)$ that has a locally asymptotically stable equilibrium by construction. Accordingly, when setting $v = F\zeta$ so that $\sigma(\hat{A} + \hat{B}F) \subset \mathbb{C}^-$, the closed-loop system has an asymptotically stable equilibrium at the origin. ■

The previous result shows that even if a nonlinear system is non-minimum phase, a suitable partition of the output can be performed on its LTM at the origin so that feedback linearization of the input-output behavior can be pursued while preserving stability of the internal dynamics.

Remark 3.3 *It is a matter of computations to verify that the LTM model of the closed-loop system (3.50) has transfer function* $W(s) = \frac{N_1(s)}{s^{r_2}}$. *Accordingly, one can interpret the nonlinear feedback (3.47) as the counterpart of the linear feedback presented in Section 3.3; roughly speaking, when applying (3.47) to the original plant* (3.1)*, one is inverting only the stable component of the zero-dynamics associated to* y. *As a consequence, as* $y \to 0$, *the trajectories of the closed-loop system are constrained onto the stable manifold associated to the dummy output* $y_2 = C_2 x$ *where they evolve according to* $\dot{\eta} = q(0, \eta)$.

3.4.1 Output partition for nonlinear system

In this section we investigate the ability of rewriting any generic output function as an application of derivative polynomial To this end we assume the dynamics $\dot{f}(x) + g(x)u$ to be exactly linearizable in the sense that there is exists a dummy output $\hat{y} = \phi(x)$ such that the system is Fully feedback linearizable and with relative degree n. This problem can be solved through defining a smooth mapping $\phi(x)$ so that the system

$$\begin{aligned} &f(x) + g(x)u \\ &y = \phi(x). \end{aligned} \tag{3.51}$$

has a well define relative degree $r = n$ in a neighbour of equilibrium ; basically $L_g\phi(x) = \cdots = L_g L_f^{r-2}\phi(x) = 0, \quad L_g L_f^{r-1}\phi(x) \neq 0.$

the following theorem recalled

Theorem 3.3 *The exact feedback linearization problem is solvable for $x(0)$ if and only if*

1 $\Delta_{n-1}(x)$ *has rank* $\Delta_{n-1}(0) = n$.

2 $\Delta_{n-2}(x) := span\left\{g, \quad ad_f g, \quad \ldots, \quad ad_f^{n-2} g\right\}$ *is involutive in a neighbour of origin*

Now we study the problem of defining a suitable partition of the zero dynamics of (3.1) by extending the result presented in the previous section to complete nonlinear characterization.

Lemma 3.3 *Consider the continuous time dynamics*

$$f(x) + g(x)u \tag{3.52}$$

possess an equilibrium at the origin and be forward complete with smooth vector field f, g.Moreover let the system be FFL.Then any output function $h(x)$ with relative degree$\hat{r}$ can be written as an application of linear differential polynomial of φi.e.

$$y = p(d)\varphi(x) \tag{3.53}$$

Proof: consider the nonlinear system $f(x) + g(x)u, \quad y = h(x)$ and introduce the normal form associated to $\phi(x)$

$$z = \begin{pmatrix} \varphi(x) \\ L_f\varphi(x) \\ \vdots \\ L_f^{n-1}\varphi(x) \end{pmatrix} \tag{3.54}$$

so that

$$\begin{aligned} &\dot{z} = \bar{f}(z) + \bar{g}(z) \\ &y = h(x) = H(\varphi(x), {}_f\varphi(x), \ldots, L_f^{n-\hat{r}}\varphi(x)) = h \circ \varphi^{-1}(z) \\ &= H(z_1, \ldots, z_{n-\hat{r}+1}). \end{aligned} \tag{3.55}$$

We can note that the prove lies straightforward in the structure of $H(z)$ ■

Theorem 3.4 *Consider the nonlinear system (3.1) under the hypothesis of Lemma 3.1.Let $\varphi(x)$ be the output with respect to which*

$$\begin{aligned} &\dot{f}(x) + g(x)u \\ \hat{y} = \varphi(x). \end{aligned}$$

is fully feedback linearizable.Then any output mapping $y = h(x)$ with respect to which (3.1) has relative degree r is defined by a differential mapping in

$$(\varphi(.), L_f\varphi(.), \ldots, L_f^{n-r}\varphi(x)); i.e$$

$y = h(x) = H(\varphi(x), L_f\varphi(x), \ldots, L_f^{n-r}\varphi(x))$ through a smooth function$H(.)$ *Proof:* Since the system

$$\dot{x} = f(x) + g(x)u, \quad y = \varphi(x). \tag{3.56}$$

have a well define relative degree n , then a coordinate transformation can be applied such that

$$\zeta = \bar{\phi}(x) = \begin{pmatrix} h(x) \\ \vdots \\ L_f^{n-1}h(x) \end{pmatrix}. \tag{3.57}$$

locally puts the system into the normal form; i.e., it gets the form

$$\begin{aligned} \dot{\zeta}_1 &= z_2 \\ \dot{\zeta}_2 &= z_3 \\ &\vdots \\ \dot{\zeta}_{r-1} &= z_n \\ \dot{\zeta}_n &= a(z,\eta) + a(z)u \\ y &= \zeta_1. \end{aligned} \tag{3.58}$$

Now we apply the same coordinate transformation to let $h(\varphi(x)) = h(\varphi(\phi^{-1}(z))) = h(z_1)$.The system w.r.to the output $\hat{y}$ become

$$\begin{aligned} \dot{\zeta} &= \hat{A}z + \hat{B}(b(\zeta) + a(\zeta)u) \\ y_n &= \tilde{H}(\zeta) \end{aligned} \tag{3.59}$$

Now by exploiting the fact that the system (3.1) has a well define relative degree r one gets that

$$\tilde{\mathcal{V}}_i(\zeta) = 0 \quad \forall i = n - r + 2, \ldots, n \tag{3.60}$$

$$\tilde{f}(\zeta) = \hat{A}(\zeta) + \hat{B}(\zeta), \quad \tilde{g}(\zeta) = \hat{B}a(\zeta) \tag{3.61}$$

$$L_{\tilde{g}}(\zeta)\tilde{H}(\zeta) = \mathcal{V}_{z_{eta}}H(\zeta)a(\zeta) = 0 \tag{3.62}$$

$$\vdots \tag{3.63}$$

$$L_{\tilde{g}}(\zeta)L_{\tilde{f}^{r-2}}(\zeta)\tilde{H}(\zeta) = \mathcal{V}_{z_{n-r+2}}H(\zeta)a(\zeta) = 0 \tag{3.64}$$

$$L_{\tilde{g}}(\zeta)L_{\tilde{f}^{r-1}} + (\zeta)\tilde{H}(\zeta) = \mathcal{V}_{z_{n-r+1}}H(\zeta)a(\zeta) \neq 0 \tag{3.65}$$

so implying

$$\mathcal{V}_{z_i} = 0 \quad \forall i = n - r = 2, \ldots, n \tag{3.66}$$

and the $\tilde{H}(\zeta_1, \ldots, \zeta_{n-r+1}) = H(\varphi, L_f\varphi, \ldots, L_f^{n-r}\varphi$. ■

Remark 3.4 *It can be easily verified that the zero dynamics is implicitly defined as*

$$\tilde{H}(\zeta_1, \ldots, \zeta_{n-r+1}) = 0 \tag{3.67}$$

3.4.1.1 Example

Consider the nonlinear system

$$\begin{aligned}\dot{x} &= \begin{pmatrix} x_3(1+x_2) \\ x_1 \\ x_2(1+x_1) \end{pmatrix} + \begin{pmatrix} 0 \\ 1+x_2 \\ -x_3 \end{pmatrix} u \\ y &= x_3(1+x_2).\end{aligned} \tag{3.68}$$

With relative degree $r = 2$.Now we introduce a coordinate transformation

$$\phi = \begin{pmatrix} z \\ \eta \end{pmatrix} = \begin{pmatrix} x_3 + x_3 x_2 \\ x_3 x_1 + x_2(1+x_1)(1+x_2) \\ x_1 \end{pmatrix}. \tag{3.69}$$

locally puts the system into the normal form; i.e., it gets the form

$$\begin{aligned}\dot{z}_1 &= z_2 \\ \dot{z}_2 &= a(z,\eta) + b(z,\eta)u \\ \dot{\eta} &= q(z,\eta) = z_1 \\ y &= z_1.\end{aligned} \tag{3.70}$$

The system zero dynamics is provided by $\dot{\eta} = 0$.The following step is to compute $\varphi(x)$

$$\begin{aligned} ad_f g &= \begin{pmatrix} 0 & 0 & 0 \\ 0 & 1 & 0 \\ 0 & 0 & -1 \end{pmatrix} \begin{pmatrix} x_3(1+x_2) \\ x_1 \\ x_2(1+x_1) \end{pmatrix} - \begin{pmatrix} 0 & x_3 & 1+x_2 \\ 1 & 0 & 0 \\ x_2 & 1+x_1 & 0 \end{pmatrix} \begin{pmatrix} 0 \\ 1+x_2 \\ -x_3 \end{pmatrix} \\ &= \begin{pmatrix} 0 \\ x_1 \\ -(1+x_1)(1+2x_2) \end{pmatrix} \\ ad_f^2 g &= \begin{pmatrix} 0 & 0 & 0 \\ 1 & 0 & 0 \\ -1-2x_2 & -2-2x_1 & 0 \end{pmatrix} \begin{pmatrix} x_3(1+x_2) \\ x_1 \\ x_2(1+x_1) \end{pmatrix} - \begin{pmatrix} 0 & x_3 & 1+x_2 \\ 1 & 0 & 0 \\ x_2 & 1+x_1 & 0 \end{pmatrix} \begin{pmatrix} 0 \\ x_1 \\ -(1+x_1)(1+2x_2) \end{pmatrix} \\ &= \begin{pmatrix} -x_1 x_3 + (1+x_1)(1+x_2)(1+2x_2) \\ x_3(1+x_2) \\ -x_3(1+x_2)(1+2x_2) - 3x_1(1+x_1) \end{pmatrix} \end{aligned} \tag{3.71}$$

Now we check the necessary conditions

$$[g, ad_f g, ad_f^2 g] = \begin{pmatrix} 0 & 0 & 1 \\ 1 & 0 & 0 \\ 0 & -1 & 0 \end{pmatrix} \tag{3.72}$$

System has full rank$n = 3$.

$$[g, ad_f g] = \begin{pmatrix} 0 & 0 & 0 \\ 1 & 0 & 0 \\ -1-2x_2 & -2-2x_1 & 0 \end{pmatrix} \begin{pmatrix} 0 \\ 1+x_2 \\ -x_3 \end{pmatrix} - \begin{pmatrix} 0 & 0 & 0 \\ 1 & 0 & 0 \\ 0 & 0 & -1 \end{pmatrix} \begin{pmatrix} 0 \\ x_1 \\ -(1+x_1)(1+2x_2) \end{pmatrix}$$
$$= \begin{pmatrix} 0 \\ -x_1 \\ -3(1+x_1)(1+2x_2) \end{pmatrix} \tag{3.73}$$

The matrix$[g, ad_f g, [g, ad_f g]$has rank 2 which means that the vectors that for it are linearly dependant. That means that the third column is not a new vector but a linear combination from the first two columns. This means that the desired distribution is involutive.Now we conclude that the system is can be Fully feedback linearizable, such that$\frac{\partial \varphi(x)}{\partial x} \begin{pmatrix} 0 & 0 \\ 1+x_2 & x_1 \\ -x_3 & -(1+x_1)(1+2x_2) \end{pmatrix} = 0$.The solution is any function $h(x_1)$ *i.e.* $\varphi(x) = x_1$.The system relative degree w.r.to $\varphi(x)$ $r_{\varphi(x)} = 3$ as $L_g\varphi(x) = 0, L_g L_f \varphi(x) = 0, L_g L_f^2 \varphi(x) \neq 0$. Since the system obtain a well define relative degree , then a coordinate transformation can be applied such that

$$\zeta = \begin{pmatrix} x_1 \\ x_3(1+x_2) \\ x_3 x_1 + x_2(1+x_1)(1+x_2) \end{pmatrix}. \tag{3.74}$$

locally puts the system into the normal form; i.e., it gets the form

$$\begin{aligned} \dot{\zeta}_1 &= \zeta_2 \\ \dot{\zeta}_2 &= \zeta_3 \\ \dot{\zeta}_3 &= a(z) + b(z)u \\ y &= h \cdot \phi^{-1}(\zeta) = H(\varphi(x), {}_f\varphi(x)) = \zeta_2. \end{aligned} \tag{3.75}$$

The zero dynamics is described $H(\zeta_1, \zeta_2) = \zeta_2 = 0$ which coincide with zero dynamics of the original system.

3.5 Feedback linearization of partially minimum phase systems under sampling

We now address the problem of preserving input-output linearization of 3.2 with stability under sampling by suitably exploiting the result in Theorem 3.2. As recalled in the introduction, the problem cannot be solved via standard (also known as single-rate) sampling procedures. Consider the Multirate sampled data model and set $u(t) = u_k^i$ for $t \in [(k+i-1)T, (k+i)T[$ for $i = 1, \ldots, r$ where $y(t) = y_k$ for

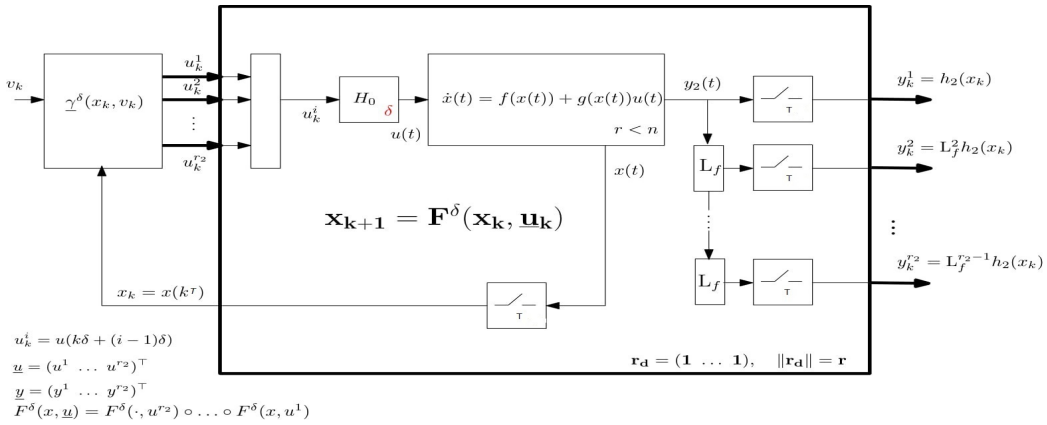

Figure 3.1: sampled data control scheme

$t \in [kT, (k+1)T[$ so that the multirate equivalent model of order r_2 of 3.2 gets the form

$$x_{k+1} = F_m^{\delta}(x_k, u_k^1, \dots, u_k^{r_2}) \tag{3.76}$$

where $\delta = \frac{T}{r_2}$ and

$$\begin{aligned} F_m^{\delta}(x_k, u_k^1, \dots, u_k^{r_2}) =& e^{\delta(L_f + u_k^1 L_g)} \dots e^{\delta(L_f + u_k^{r_2} L_g)} x\big|_{x_k} \\ =& F_m^{\delta}(\cdot, u_k^{r_2}) o \dots o F^{\delta}(x_k, u_k^1). \end{aligned}$$

In the sequel, we show how multirate feedback can be suitably employed with the arguments in Theorem 3.2 to achieve input-output linearization of 3.2 at the sampling

instant $t = kT$ ($k \geq 0$) with stability regardless the minimum-phase property. Accordingly, we first design a multirate feedback $\mathbf{u}_k = \gamma(\delta, x_k, \mathbf{v}_k)$ ($\mathbf{u} = \mathrm{col}(u^1, \ldots, u^{r_2})$ and $\mathbf{v} = \mathrm{col}(v^1, \ldots, v^{r_2})$ so to ensure input/output linearization of the $\mathbf{v}$-y_2 behavior of (3.44), at the sampling instants. This is achieved by considering the sampled-data dynamics (3.76) with augmented dummy output $Y_{2k} = H_2(x_k)$ composed of $y_2 = C_2 x$ and its first $r_2 - 1$ derivatives; namely, we consider

$$x_{k+1} = F_m^{\delta}(x_k, u_k^1, \ldots, u_k^{r_2}), \quad Y_{2k} = H_2(x_k) \tag{3.77}$$

with $\delta = \frac{T}{r_2}$ and output vector

$$H_2(x) = \begin{pmatrix} h_2(x) & L_f h_2(x) & \ldots & L_f^{r_2-1} h_2(x) \end{pmatrix}^\top$$

that has by construction a vector relative degree $r^T = (1, \ldots, 1)$. Now let us compute the feedback $\mathbf{u}_k = \gamma(\delta, x_k, \mathbf{v}_k)$ so that to reproduce, at the sampling instants $t = kT$, the trajectories of the dummy output of (3.44) and of its first $r_2 - 1$ derivatives in closed-loop under the continuous-time linearizing feedback (3.48). The existence of the sampled-data control is stated in the following result.

Lemma 3.4 *Consider the nonlinear system (3.44) under the hypotheses of Lemma 3.2 with multi-rate equivalent model of order r_2 provided by (3.77). Then, there exists a unique solution*

$$\mathbf{u}^T = \gamma(T, x, \mathbf{v}) = (\gamma^1(T, x, \mathbf{v}) \ \ldots \ \gamma^{r_2}(T, x, \mathbf{v}))^\top \tag{3.78}$$

to the input-output Matching (I-OM) equality

$$\begin{aligned} &H_2(F_m^T(x_k, \gamma^1(T, x_k, \mathbf{v_k}), \ldots, \gamma^{r_2}(T, x_k, \mathbf{v_k})) = \\ &e^{r_2 \delta (L_f + \gamma(\cdot, v) L_g)} H_2(x)\big|_{x_k} \end{aligned} \tag{3.79}$$

for any $x_k = x(kT)$ and $v(t) = v(kT) := v_k$, $\mathbf{v_k} = (v_k, \ldots, v_k)$. Such a solution is in the form of a series expansion in powers of δ around the continuous-time $\gamma(x, v)$; i.e., for $i = 1, \ldots, r_2$

$$\gamma^i(T, x, \mathbf{v}) = \gamma(x, \mathbf{v}) + \sum_{j \geq 1} \frac{T}{(j+1)!} \gamma_j^i(x, \mathbf{v}). \tag{3.80}$$

As a consequence, the feedback $\mathbf{u}_k^T = \gamma(T, x_k, \mathbf{v}_k)$ ensures Input-Output linearization of (3.77) with stability of the internal dynamics.

Proof: First, we rewrite (3.79) as a formal series equality in the unknown $\mathbf{u}^\delta$; i.e.,

$$\begin{pmatrix} T^{r_2} S_1^T(x, \mathbf{u}^T) & \ldots & T S_1^T(x, \mathbf{u}^T) \end{pmatrix}^\top \tag{3.81}$$

with, for $i = 1, \ldots, r_2$,

$$T^i S_i^T(x, \mathbf{u}^T) = e^{T(L_f + u^1 L_g)} \ldots e^{T(L_f + u^1 L_g)} L_f^{i-1} h_2(x) - e^{r_2 T(L_f + \gamma(\cdot,v) L_g)} L_f^{i-1} h_2(x).$$

Thus one looks for $\mathbf{u} = \gamma(T, x, v)$ satisfying

$$S^T(x, \mathbf{u}^T) = \begin{pmatrix} S_1^T(x, \mathbf{u}^T) & \ldots & S_1^T(x, \mathbf{u}^T) \end{pmatrix}^\top = \mathbf{0} \tag{3.82}$$

where each term rewrites as $S_i^T(x, \mathbf{u}^T) = \sum_{s \geq 0} T^s S_{ij}(x, \mathbf{u}^T)$ with

$$S_{i0}(x, \mathbf{u}^T) = \Big(T_j \mathbf{u}^T - r_2^{r_2 - i + 1} \gamma(x, v) \Big) L_g L_f^{r_2 - 1} h_2(x) \tag{3.83}$$

and $\frac{T_j}{j!} = (\frac{j^{r_2 - j + 1} - (j-1)^{r_2 - j + 1}}{j!} \; \frac{(j-1)^{r_2 - j + 1} - (j-2)^{r_2 - j + 1}}{j!} \; \ldots \; \frac{1}{j!})$. It results that $\mathbf{u}^T = \gamma(T, x, v) = (\gamma(x, v), \ldots, \gamma(x, v))^\top$ solves (3.82) as $T \to 0$. More precisely, as $T \to 0$, one gets the equation

$$S^{T \to 0}(x, \mathbf{u}^T) = \Big(T \mathbf{u}^T - D\gamma(x, v) \Big) L_g L_f^{r_2 - 1} h_2(x)$$

with $T = (T_1^\top, \ldots T_{r_2}^\top)^\top$ and $D = \mathrm{diag}(r_2^{r_2}, \ldots, r_2)$. Furthemore, the Jacobian of S^T with respect to $\mathbf{u}^T$ is

$$\nabla_{\mathbf{u}^T} S^\delta(x, (\gamma(x, v), \ldots, \gamma(x, v))^\top)\big|_{\bar{T} \to 0} = T \; L_g L_f^{r_2 - 1} h_2(x)$$

is full rank by definition of the continuous-time relative degree r_2 and because T is invertible so concluding the existence of $T \in]0, T^*[$ so that (3.79) admits a unique solution of the form (3.80) around the continuous-time solution $\gamma(x, v)$ (Implicit Function Theorem). Stability of the zero-dynamics is ensured by multi-rate sampling as proven in ([67]). ■

The feedback control is in the form of a series expansion in powers of T. Thus, iterative procedures can be carried out by substituting (3.80) into (3.79) and equating the terms with the same powers of T ([64]) where the explicit expression for the first terms are given). Unfortunately, only approximate solutions $\gamma^{[p]}(T, x, v)$ can be implemented in practice through truncations of the series (3.80)) at finite order p in δ; namely, setting $\gamma^{[p]}(T, x, v) = (\gamma^{1[p]}(\delta, x, v), \ldots, \gamma^{r_2[p]}(T, x, v)$, one gets for $i = 1, \ldots, r_2$

$$\gamma^{i[p]}(T, x, \mathbf{v}) = \gamma(x, \mathbf{v}) + \sum_{j=1}^{p} \frac{T}{(j+1)!} \gamma_j^i(x, \mathbf{v}). \tag{3.84}$$

When $p = 0$, one recovers the sample-and-hold solution $\gamma^{i[p]}(\delta, x_k, \mathbf{v_k}) = \gamma(x(KT), v(KT)$ or emulated control. Preservation of performances under approximate solutions has been discussed in ([62]) by showing that, although global properties are lost, input-to-state stability (ISS) and practical global asymptotic stability can be deduced in closed-loop even through the inter sampling instant. Similarly to the continuous-time case, the next result shows that applying the feedback (3.78) to (3.2) ensures input-output linearization of the input-output behavior at any sampling instant $t = kT$ $(k \geq 0)$ while preserving stability of the internal dynamics.

Theorem 3.5 *Consider the nonlinear system (3.2) under the hypotheses of Theorem 3.2 with multi-rate equivalent model of order r_2 provided by*

$$x_{k+1} = F_m^{\delta}(x_k, u_k^1, \ldots, u_k^{r_2}), \quad y_k = \begin{pmatrix} C_1 & \mathbf{0} \end{pmatrix} H_2(x_k) \tag{3.85}$$

and let the feedback (3.80) be the unique solution to the I-OM equality (3.79). Then the feedback $\mathbf{u}_k^T = \gamma(\delta, x_k, \mathbf{v}_k)$ ensures Input-Output linearization of (3.85) with stability of the internal dynamics.

Proof: We first note that y_k rewrites as a linear combination of Y_2. As a consequence, because the $\mathbf{v}$-Y_{2k} behavior is linear under (3.78), the $\mathbf{v}_k$-y_k is linear by construction. Moreover, we observe that $Y_2 \equiv 0$ implies $y_k \equiv 0$ by definition. Thus, by construction of (3.78), as $y_k \to 0$, the closed-loop trajectories of (4.57) are forced onto the zero-manifold defined by $Y_2 \equiv 0$ over which they are asymptotically stable. ■

Remark 3.5 *Denote by z_i^c the zeros of the non Hurwitz polynomial $N_1(s)$ in Lemma 3.1. When considering the LTM model of (3.85) in closed-loop under (3.78), one gets that, as $\bar{\delta} \to 0$, the closed-loop linearized system has exactly $r_2 - r$ zeros asymptotically approaching to the origin as $e^{\delta z_i^c}$ (namely, as $\delta \to 0$, $z_i^T \to e^{\delta z_i^c}$, $i = 1, \ldots, r_2$). Accordingly, by applying this result in the linear case, one gets that the feedback (3.78) is the one that assigns $n - r_2$ poles coincident with the stable zeros, without affecting the unstable ones.*

Remark 3.6 *Along the lines of the continuous-time case, when controlling (3.85) via the multirate feedback (3.78) one is constraining the trajectories of the closed-loop system onto the stable part of the zero-manifold identified by the non-minimum phase output.*

Remark 3.7 *A purely digital single-rate feedback might be computing over single rate sample data model*

$$\begin{aligned} x_{k+1} &= F^T(x_k, u_k) \\ y_k &= h(x_k) \end{aligned} \tag{3.86}$$

by settling Lemma 3.1 to this context. Assuming, for simplicity, that 3.1 is locally minimum-phase, one might define a partition of the original output $y_k = Cx_k$ based on the numerator $N^T(z)$ of transfer function of its LTM at the origin. Accordingly, one might deduce $y_2^{\delta} = C_2^{\delta} x_k$ with respect to which the original dynamics has no sampling zero dynamics and the $y = N(q) y_2^T$ where q denotes the shift operator and $N(q)$ is the polynomial defining the sampling zeros of the LTM. Though, an exact partition of the original output is hard to be found and only approximate solutions can be found based on the concept of limiting sampling zeros ([7]).

3.5.1 The TORA example

An academic working example is proposed on the basis of the TORA system

$$\begin{aligned}
\dot{x}_1 &= x_2 \\
\dot{x}_2 &= -x_1 + \varepsilon \sin x_3 \\
\dot{x}_3 &= x_4 \\
\dot{x}_4 &= \frac{\varepsilon \cos x_3 (x_1 - \varepsilon x_4^2 \sin x_3) + u}{1 - \varepsilon^2 \cos^2 x_3} \\
y &= \begin{pmatrix} \frac{2(\varepsilon^2-1)}{\varepsilon} & 0 & 1-\varepsilon^2 & 1-\varepsilon^2 \end{pmatrix} x
\end{aligned} \tag{3.87}$$

The system is fully feedback linearizable.i.e

$$[g, ad_f g, ad_f^2 g, ad_f^3 g]_{x=0} = \begin{pmatrix} 0 & 0 & 0 & \frac{\epsilon}{(1-\epsilon(2)} \\ 0 & 0 & \frac{\epsilon}{(1-\epsilon(2)} & 0 \\ 0 & -\frac{1}{1-\epsilon^2)} & 0 & \frac{-\epsilon^2+\epsilon^4}{(1-\epsilon^2)^3} \\ \frac{1}{1-\epsilon^2} & 0 & \frac{-\epsilon^2+\epsilon^4}{(1-\epsilon^2)^3} & 0 \end{pmatrix}$$

is full rank. Moreover the matrix$[g, ad_f g, [g, ad_f g], [g, ad_f^2 g]$ has rank less than$n$ for all x nearx_0 which indicate that the system is involutive. In this context, we consider the TORA dynamics with fictitious output

$$y = (\frac{2}{\epsilon}(\epsilon^2 - 1)\ 0\ 1 - \epsilon^2\ 1 - \epsilon^2)x$$

with respect to which the system is non-minimum phase and has relative degree $r = 1$. Thus, setting

$$T^{-1} = (\gamma^\top, A^\top \gamma^\top, \ldots, A^{n-1\top} \gamma^\top), \quad \gamma = (\mathbf{0}\ 1)\mathcal{R}^{-1}(A, B) \tag{3.88}$$

$$N_1(s) = s - 1 \tag{3.89}$$

we define the partition $N_1(s) = s-1$ and $N_2(s) = s^2+2s+1$ so that, in the original coordinates, we define the dummy

$$y_2 = (0\ \ -\frac{2}{\epsilon}(\epsilon^2 - 1), 1 - \epsilon^2, 0)x$$

with respect to which the system is minimum-phase in first approximation and has relative degree $r_2 = 2$. Accordingly, by applying Theorem 3.2, there exists a coordinate transformation

$$\phi_i(x) = \begin{pmatrix} h_2(x) \\ L_f h_2(x) \\ L_f^2 h_2(x) \\ \phi_2(x) \end{pmatrix} \tag{3.90}$$

that put the system into normal form

$$\begin{aligned}\dot{\zeta}_1 &= z_2\\ \dot{z}eta_2 &= b(z,\eta) + a(z,\eta)u\\ \dot{\zeta}_1 &= q_1(\zeta,\eta)\\ \dot{\zeta}_2 &= q_2(\zeta,\eta)\end{aligned} \tag{3.91}$$

The feedback (3.47) with

$$\begin{aligned}L_g L_f h_2(x) =& \frac{\epsilon^2-1}{\epsilon^2\cos^2(x_3)-1}\\ L_f^2 h_2(x) =& \frac{2x_2(\epsilon^2-1)}{\epsilon} - 2x_4\cos(x_3)(\epsilon^2-1) +\\ &+ \frac{\epsilon\cos(x3)(\epsilon^2-1)(x_1-\epsilon\sin(x3)(x_4^2+1))}{\epsilon^2\cos(x_3)^2-1}\end{aligned}$$

and $v = -k_1 h_2(x) - k_2 L_f h_2(x)$ achieves local asymptotic stabilization in closed-loop with $k_1, k_2 > 0$. To solve the problem under sampling, the multirate feedback $\gamma^{[1]}(\delta, x, \mathbf{v})$ in (3.84) is computed with first corrective terms

$$\gamma_1^1(x,v) = \frac{1}{3}\dot{\gamma}(x,\mathbf{v}), \quad \gamma_1^2(x,v) = \frac{5}{3}\dot{\gamma}(x,v)$$

and $\dot{\gamma}(x,v) = (L_f + \gamma(x,v)L_g)\gamma(x,v)$.

Figures (3.2),(3.3) and (3.4) depict simulations of the aforementioned situations under continuous-time feedback (3.47) and the sampled-data feedback (3.84) with first-order $p = 1$ corrective terms and for different values of the sampling period. The sample and hold (or emulated-based) solution is reported as well in a comparative sense. In particular, setting by $\eta = (\eta_1,\ \eta_2,\ \eta_3)^\top$, we denote the internal dynamics corresponding to the simulated situations. It is clear from Figure (3.2) that the continuous-time feedback computed via partial dynamic inversion yields feedback linearization while ensuring asymptotic stability in cosed-loop. Concerning sampled-data control, we note that, as T increases, the emulated based solution fails in stabilizing (and linearizing the input-output behavior) in closed-loop while the presented multi-rate strategy yields more than acceptable performances even in that case (see figure 3.4,3.5).

3.6 Conclusions

The notion of partially minimum-phase systems is used to get feedback input-output linearization while preserving stability. The proposed approach is introduced in continuous time and extended to the sampled-data context through multirate to overcome the well-known pathologies induced by the sampling zero dynamics. A working example shows the performances of the control strategies.

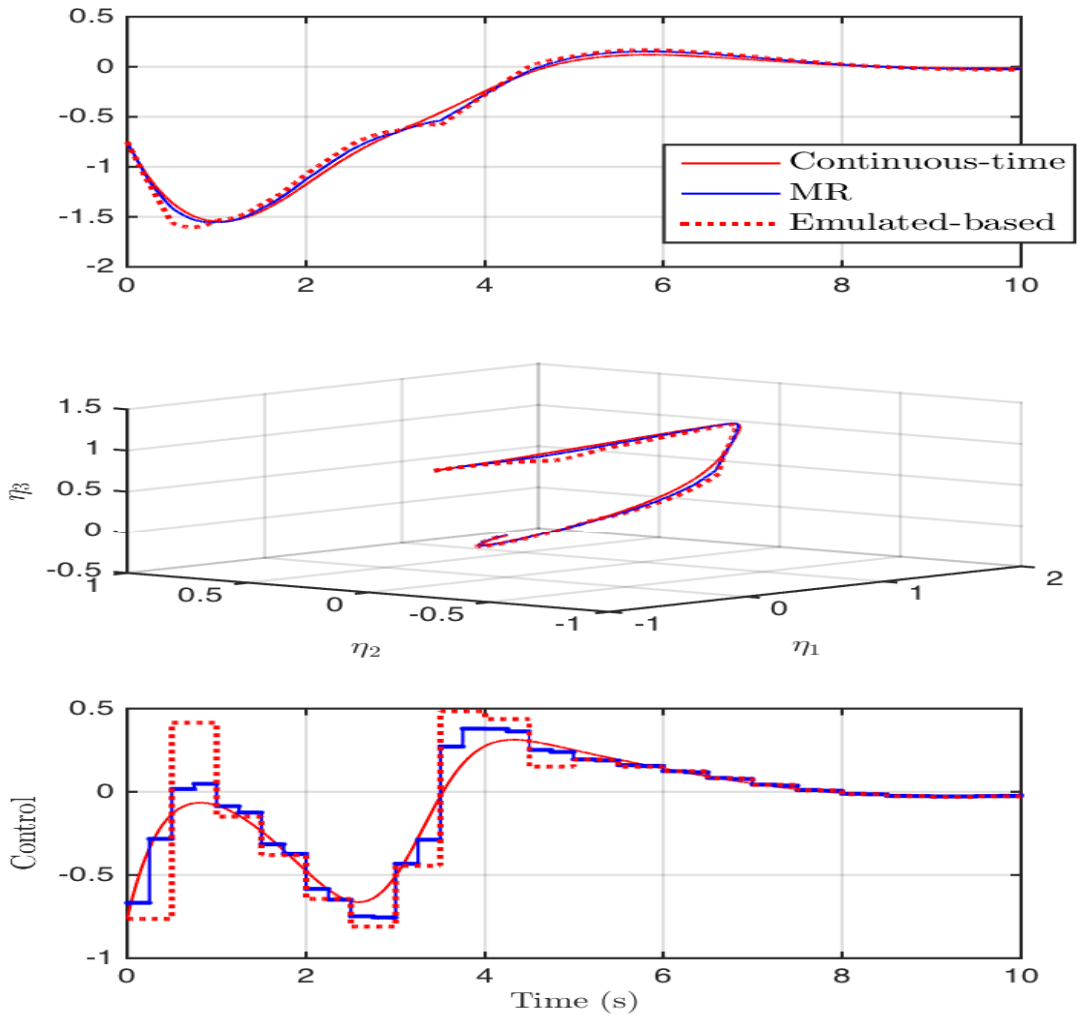

Figure 3.2: Partial feedback linearization of Tora example $T = .5$

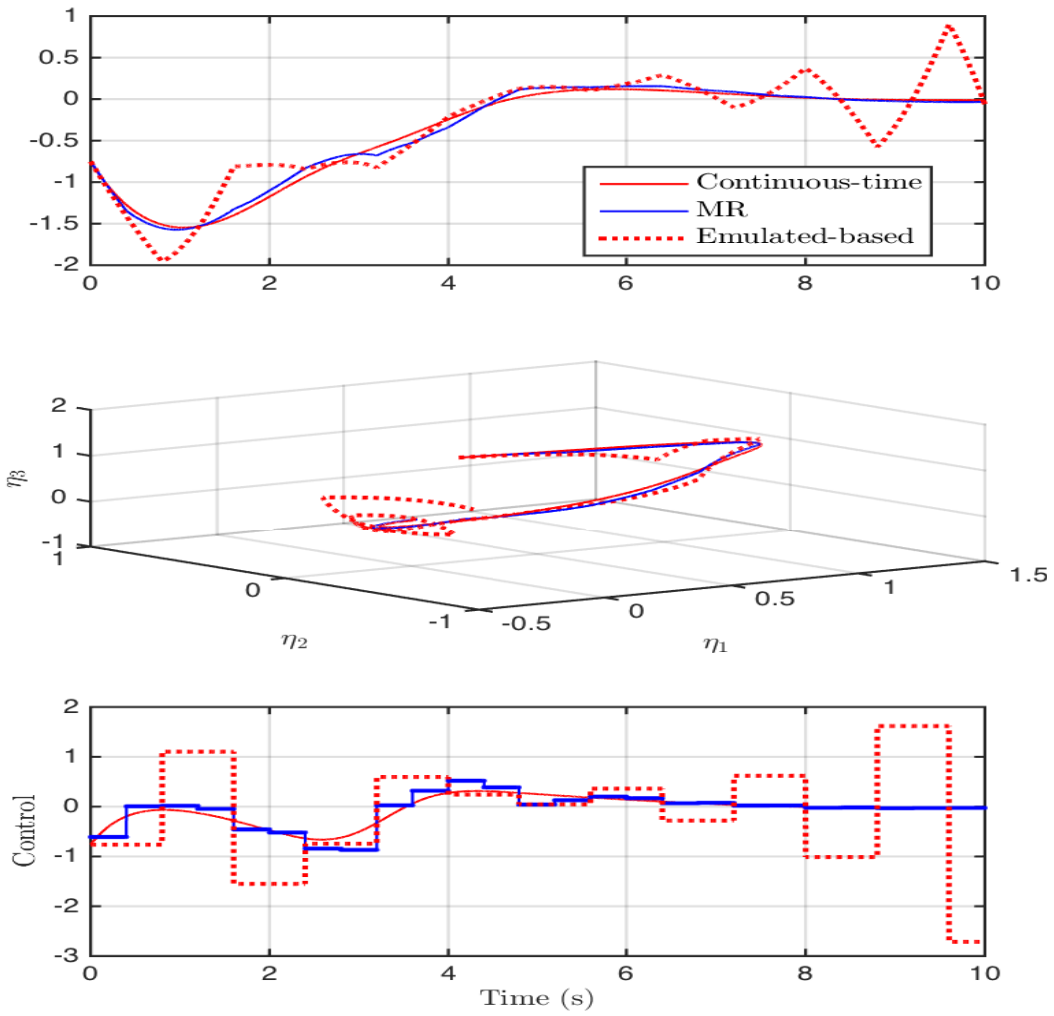

Figure 3.3: Partial feedback linearization of Tora example $T = .7$

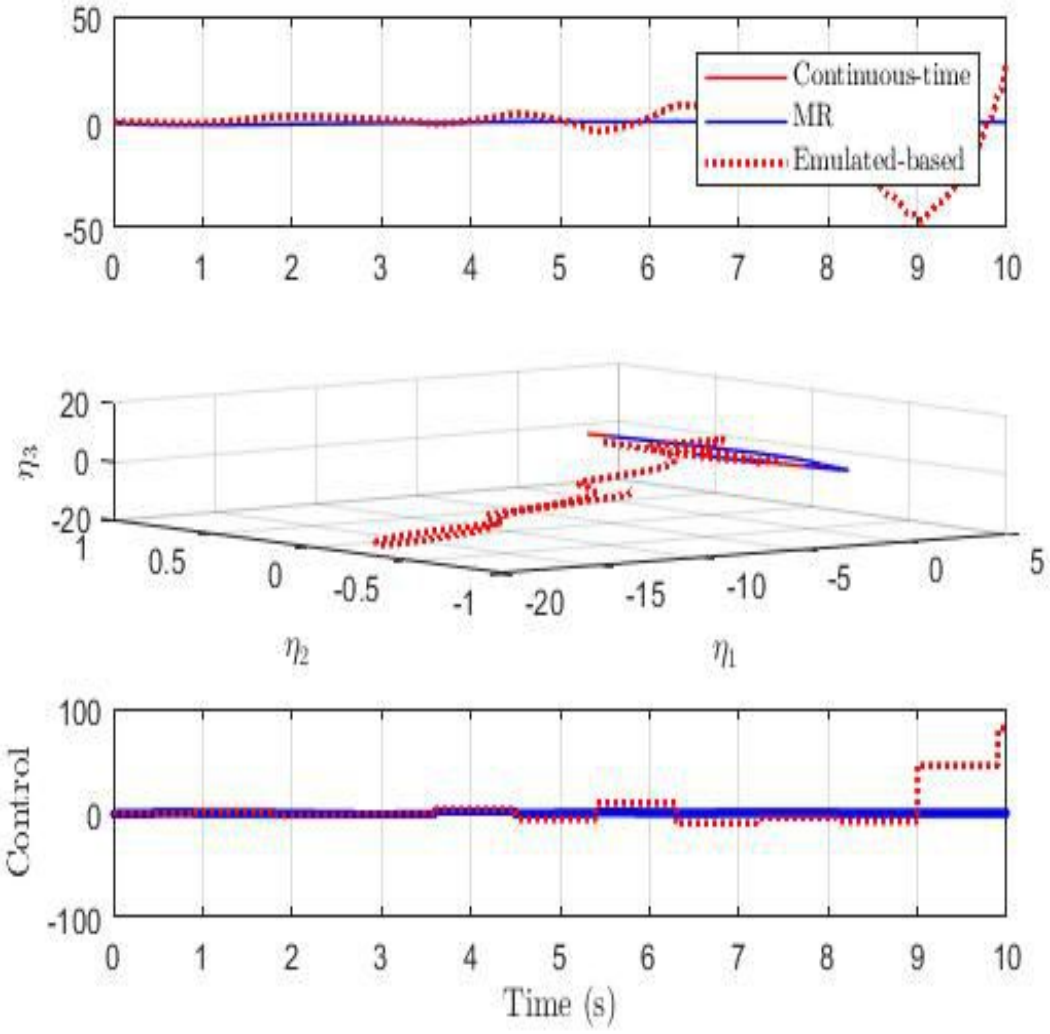

Figure 3.4: Partial feedback linearization of Tora example $T = .9$

Chapter 4

Disturbance Decoupling Problem with stability

Contents

4.1 Introduction

The problem of annihiuating the effect of disturbances from the output evolution of a dynamical system represent an evergreen area of research from both theoretical and practical point of view.Very important work results on this topic have been obtained by Wonham ([94]) and Isidori for both linear and nonlinear.
The proposed solutions shared the idea of constraining under feedback , the effect of disturbances onto a sub dynamical of the system which can be made unobservable.More precisely, the idea is to decouple the input-output evolution from the disturbance by limiting its effect onto the zero dynamics.
Condition for solving such a problem are well consolidated and are linked to the

concept of relative degree and dynamical inversion.Although a feedback solving the the problem might be defined, one still need to guarantee that the trajectories of the residual unobservable dynamics are bounded despite the effect of the disturbances.

Very few works have been addressing this second but essential problem so that only sufficient condition for solving the Disturbance Decoupling Problem while preserving stability of the overall system.Moreover,those conditions are to check after the feedback design with no insight toward the redefinition of a feedback that solves the with stability .At the same time preserving a good behaviour of the residual dynamic affected by the perturbations.In this chapter, a first step towards this goal is made

In chapter 3, we introduced, the very simple idea that by factorizing the numerator of the non minimum phase transfer function of a LTI system a dummy output can be introduced with respect to which the zero dynamics subjected to one of the factors ,is stable.Based on this idea we consider a class of non minimum phase non linear Single Input Single Output (SISO) systems that are controllable and are affected by an essentially bounded disturbances.Thus , we study the problem of defining a feedback preserving disturbances decoupling from the output evolutions .It will be shown that given a feedback linearizable nonlinear system with linear output necessary and sufficient conditions for solving(locally) the DDP can be easily deduced from LTM at the origin.

4.2 Motivation

In this section ,we show the arguments developed in chapter 3 can be exploited in the LTI case,To set necessary and sufficient condition to solve the DDP with stability. Consider the linear time-invariant system described by

$$\begin{aligned} \dot{x} &= Ax + Bu + Dw \\ y &= Cx \end{aligned} \tag{4.1}$$

where $x \in \mathbb{R}^n$ and $u, y, w \in \mathbb{R}$. The system have transfer function in the form

$$P(s) = \frac{N(s)}{D(s)} \tag{4.2}$$

where $N(s) = b_0 + b_1 s + \cdots + b_m s^m$, $D(s) = a_0 + a_1 s + \cdots + s^n$ and relative degree $r = n - m$.
Given any factorization of the numerator $N(s) = N^+(s)N^-(s)$ and fixed$D(s)$ rewrites the transfer function as

$$P(s) = N^+(s).\bar{W}(s), \quad \bar{W}(s) = \frac{N^-(s)}{D(s)} \tag{4.3}$$

The factor $N^-(s)$ defines a dummy output $\bar{y} = \bar{C}x$ with respect to which the relative degree is $\bar{r}$ and the system corresponding to

$$\dot{x} = Ax + Bu + Dw \tag{4.4}$$

$$y = \bar{C}x \tag{4.5}$$

is minimum phase.In this case the output rewrites as

$$y(t) = N^{+}(d)\bar{y}(t), \text{with} d = \frac{d}{dt}. \tag{4.6}$$

Remark 4.1 *The original output $y = Cx$ can be rewritten as a linear combination to the output $\bar{y}$ .The consequent $\bar{r} - r$ derivative via the coefficient of the non Hurwitz polynomial induced by*

$$N^{-}(s) = b_0 + b_1 s + \cdots + b_{\bar{r}-r} s^{\bar{r}-r}. \tag{4.7}$$

Proposition 4.1 *Let $N^{-}(s)$ and $N^{+}(s)$ be the factorization of the numerator $N(s)$ where $N^{-}(s), N^{+}(s)$ represent the stable and the unstable zeros respectively. Then the DDP is solvable with stability if and only if $\bar{r} \leqslant r_w$ where r_w denote the relative degree with respect to disturbances and is such that $CA^{i}D = 0, \quad \forall i = 0, ..., r_w - 2 and \quad CA^{r_w - 1}D \neq 0$. Equivalently, the DDP is solvable with stability if and only if*

$$ImD \subset V_s^* \subset kerC \tag{4.8}$$

$$with \tag{4.9}$$

$$V_s^* = ker \begin{pmatrix} \bar{C} \\ \cdots \\ \bar{C}A^{\bar{r}-1} \end{pmatrix} \tag{4.10}$$

and there exists feedback in the form

$$u^{*s} = -(\bar{C}A^{\bar{r}-1}B)^{-1}\bar{C}A^{\bar{r}}x \tag{4.11}$$

Remark 4.2 *It is clear that by decoupling the disturbance w from the dummy output $\bar{y}$,the original output $y(t)$ will remain decoupled.*

The subspace V_s^* defines the maximal subspace which can be made invariant and unobservable under feedback while preserving stability.It turns out that , the DDP admits a solution with stability if and only if the effect of perturbation can be constrained into V_s^*.

Remark 4.3 *V_s^* verifies the*

$$V_s^* \subset V^* = ker \begin{pmatrix} C \\ \cdots \\ CA^{r-1} \end{pmatrix} \subset kerC \tag{4.12}$$

where V^* is the largest subspace which can be made unobservable under feedback.Regardless its stability.
Accordingly, our condition complements the classical one by stating that the DDP is solvable if

- *$ImD \subset V^* \subset kerC$ (solvability)*
- *$ImD \subset V_s^*$ (stability).*

4.3 DDP with stability for LTI

Consider the LTI system

$$\begin{aligned} \dot{x} &= Ax + Bu + Pw \\ y &= Cx \end{aligned} \tag{4.13}$$

where P defines a family of disturbance action acting over.T he system obtain relative degree $r \leq n$ and being partially minimum phase.Based on the argument developed in the previous section.We will provide in this section the necessary and sufficient conditions for characterizing the action of disturbances which can be decoupled from the output under feedback with stability.In doing so, we shall show that the problem admits a solution if the disturbance can be contained onto the minimal dynamics of 4.13 which can be rendered unobservable under feedback while preserving stability of the closed loop ; in other words,the problem is solvable if and only if the action of disturbances to be decoupled is contained into the unobservable subspace generated by cancelling only the stable zeroes of 4.13.

Theorem 4.1 *Consider the system 4.13 being controllable and possessing relative degree $r \leq n$ and being partially minimum phase.Denote $N(s) = b_0 + b_1 s + \cdots + b_{n-r} s^{n-r}$ the not Hurwitz polynomial identifying the zeroes of 4.13.Consider the maximal factorization of $N(s) = N^+(s)N^-(s)$ with*

$$N_i(s) = b_0^i + b_1^i + \cdots + b_{n-r_i}^{n-r_i}, \quad i = 1, 2 \tag{4.14}$$

such that $N^-(s)$ is Hurwitz polynomial of degree $n-\bar{r}$ and introduce $\bar{C} = (\bar{b}_0 \dots \bar{b}_{m_2} \quad 0 \dots 0)$. Then DDP-S admits a solution for the system 4.13 for all P verifying

$$ImP \subseteq V_s \tag{4.15}$$

with $V_s \subseteq V^*$, V^* being the the maximal (A, B) invariant distribution and , for $\bar{r} = n - m_2$

$$V_s = Ker \begin{pmatrix} \bar{C} \\ \bar{C}A \\ \vdots \\ \bar{C}A^{\bar{r}-1} \end{pmatrix} \tag{4.16}$$

Proof: The proof is straight forward by showing that $V_s \subseteq V^* \subseteq KerC$.To this end, one exploit the deferential relation $y = N^+(d)\bar{y}$ by deducing

$$\begin{aligned} y &= Cx = N^+(d)\bar{C}x = b_0^+\bar{C}x + b_1^+\bar{C}Ax + \cdots + b_{\bar{r}-r}^+\bar{C}A^{\bar{r}-r}x \\ \dot{y} &= CAx = \dot{N^+}(d)\bar{C}x = b_0^+\bar{C}Ax + b_1^+\bar{C}A^2x + \cdots + b_{\bar{r}-r}^+\bar{C}A^{\bar{r}-r+1}x \\ &\vdots \\ y^{r-1} &= CA^{r-1}x = b_0^+\bar{C}A^{r-1}x + \cdots + b_{\bar{r}-r}^+\bar{C}A^{\bar{r}-1}x \end{aligned} \tag{4.17}$$

for $\bar{r} \leq r$ by construction. As consequence , one gets

$$\begin{pmatrix} C \\ CA \\ \vdots \\ CA^{r-1} \end{pmatrix} = \begin{pmatrix} b_0^+ & b_1^+ & \dots & b_{\bar{r}-r}^+ & 0 & \dots & 0 \\ 0 & b_0^+ & \dots & b_{\bar{r}-r-1}^+ & b_{\bar{r}-r}^+ & \dots & 0 \\ & & & & & & \\ 0 & 0 & \dots & * & * & \dots & b_{\bar{r}-r}^+ \end{pmatrix} \begin{pmatrix} \bar{C} \\ \bar{C}A \\ \vdots \\ \bar{C}A^{\bar{r}-1} \end{pmatrix} \tag{4.18}$$

so getting $V_s \equiv Ker\bar{C} \subseteq KerC \equiv V^*$. As a consequence, one gets that $V_s \subseteq KerC$ so getting that all the disturbances that can be made independent on the output are such that $ImP \subseteq V_s$ ■

Remark 4.4 *From the result above, it is clear that the problem is solvable if* $s \in \mathbb{C} s.t. N(s) = 0 \subset \mathbb{C}^+$ *that is whenever the system 4.13 is not partially minimum phase and only the trivial factorization holds with* $N^-(s) = 1$. *This pathology also embeds the case* $r = n - 1$ *corresponding to the presence of only one zero in 4.13 that is on the right hand side of the complex plane*

Remark 4.5 *The previous results shows that whenever 4.13 is partially minimum phase and DDP-S is solvable, the dimension of the range of the disturbances which can be decoupled under feedback while guaranteeing stability is denuclearising with respect to the standard DDP problem as* $dimV_s \leq dimV^*$. *This is due to the fact that one is con straining the disturbance to the act only on the solvable lower dimension component of the zero dynamics associated to 4.13 and evolving according to the zeroes defining the Hurwitz sub-polynomial* $N(s)$.

Remark 4.6 *The previous results might be reformulated by stating that DDP-S for 4.13 is solvable if and only if the classical DDP is solvable for the minimum phase system*

$$\begin{aligned} \dot{x} &= Ax + Bu + Pw \\ y &= \bar{C}x. \end{aligned} \tag{4.19}$$

deduced from 4.13 and having input- output behaviour transfer function $W^-(s) = \frac{N^-(s)}{D(s)}$

If DDP-S is solvable for 4.13 , then the disturbance output decoupling feedback is given by

Corollary 4.1

$$\bar{u} = \frac{v - \bar{C}A^{\bar{r}}x}{\bar{C}A^{\bar{r}-1}}Bx \tag{4.20}$$

Proof: First,introduce the coordinate transformation

$$\begin{pmatrix} \zeta \\ \eta \end{pmatrix} = \begin{pmatrix} \bar{C} \\ \bar{C}A \\ \vdots \\ \bar{C}A^{\bar{r}-1} \\ T_2 \end{pmatrix} x, \qquad zeta = col(\zeta_1, ..., \zeta_{\bar{r}}) \tag{4.21}$$

with T_2 such that $T_2B = 0$. By exploiting the deffirential relation

$$y = N^+(d)\bar{y} \tag{4.22}$$

with, in the new coordinates $\bar{y} = (\mathbf{10})\zeta$ and that $d\zeta_i = \dot{\zeta}_i = \zeta_{i+1}$ for all $i = 1, ..., \bar{r} - r$, the system 4.13 under the feedback 4.20 gets the form

$$\begin{aligned} \dot{\zeta} &= \hat{A}\zeta + \hat{B}v \\ \dot{\eta} &= \bar{Q}\eta + \bar{R}\zeta + \hat{P}w \\ y &= \hat{C}\zeta. \end{aligned} \tag{4.23}$$

with $\hat{C} = (b_0^- ....b_{\bar{r}-r}^- \not\vdash)$ clearly underlying that the the disturbance decoupling problem is solved .As for as the stability is concerned , it results that by constructing , $\sigma(\bar{Q}) \equiv s \in \mathbf{C} s.t. N^-(s) = 0 \in \mathbf{C}^-$ so implying that the unobservable dynamics 4.23 are asymptotically stable. ■

4.4 Disturbance decoupling with stability for nonlinear system

In what follows we show how the disturbance decoupling problem can be solved for a class of nonlinear systems.
Let us consider the SISO nonlinear system on the form:

$$\Sigma_{NL*} \begin{cases} \dot{z} = f(z) + g(z))u + p(z)w \\ y = Cz. \end{cases} \tag{4.24}$$

with $x \in \mathbb{R}^n$, $u, y, w \in \mathbb{R}$and $x = 0$ being the equilibrium point (i.e., $f(0) = 0$). The system has a well define relative degree $r \leq n$.The analysis of the problem is carried out under the following assumptions

1 the vector field $\tilde{p}(x)$ being such that $L_p L_f^j h(x) = 0$ in a neighbourhood of the origin.

2 The system is non minimum phase.

3 The system is Fully Feedback Linearizable when $p(x) = 0$

Remark 4.7 *Along the lines of chapter 3, we assume the LTM associated to 4.24 is in the controllable canonical form.If this is not the case , we introduce coordinate change that puts the linear part of the system into controllable form*

$$z = Mx, \quad , \quad B = \begin{pmatrix} \gamma^\top & (\gamma A)^\top & \dots (\gamma A^{n-1})^\top \end{pmatrix}^\top \tag{4.25}$$

where γ denotes the last row of the inverse of the controllability matrix $\mathcal{R}$ associated to the couple (A, B).

In the new coordinates, Σ_{NL} is transformed into

$$\Sigma_{NL}\begin{cases} \dot{x} = \tilde{f}(x) + \tilde{g}(x)u + \tilde{p(x)}w \\ y = h(x) = Cx. \end{cases} \tag{4.26}$$

where $\tilde{f}(z) = M\tilde{f}(M^{-1}z), \tilde{g}(z) = M\tilde{g}M^{-1}z), \tilde{p}(z) = Mp(M^{-1}z)$. The LTM at the origin of the nonlinear system Σ_{NL*} is given by

$$\Sigma_{L}\begin{cases} \dot{z} = A_c z + B_c u + D_c w \\ y = C_c z \end{cases} \tag{4.27}$$

The system has relative degree $\hat{r}$ coinciding, at least locally, with r and is partially minimum phase.

Lemma 4.1 *Consider the nonlinear system (4.24) and let its LTM at the origin (4.27) be non minimum phase with relative degree r.Denote by*$N(s) = b_0 + b_1 s + \dots b_{n-r}s^{n-r}$ *the not Hurwitz polynomial identifying the zeros of the LTM of (4.26) at the origin. Consider the maximal factorization of* $N(s) = N^+(s)N^-(s)$

$$N_j(s) = b_0^j + \dots + b_{n-r_j}s^{n-r_j}, j = 1, 2.$$

such that $N_2(s) = N^-(s)$*is a Hurwitz polynomial of degree* $n - \bar{r}$*. Then, the system* $\dot{x} = f(x) + g(x)u + p(x)w, \bar{y} = \bar{C}$*. where* $\bar{C}x = [b_0, \dots, b_{n-\bar{r}}]$ *has relative degree*$\bar{r} \geq r$ *and is locally minimum phase*

Lemma 4.2 *Consider the nonlinear dynamics*

$$\dot{x} = f(x) + g(x)u + p(x)w \tag{4.28}$$
$$\bar{y} = \bar{C}x \tag{4.29}$$

with relative degree $\bar{r} \leqslant n$ *and being locally minimum phase.*
Then, the DDP problem admits a solution with stability if $r_w \geq \bar{r}$ *with* r_w *such that*

$$L_p L_f^i \bar{h}(x) = 0, \quad i = 0, ..., r_w - 2 \tag{4.30}$$
$$L_p L_f^{r_w - 1}\bar{h}(x) \neq 0. \tag{4.31}$$

Accordingly , the feedback solving the problem is given by

$$u = \frac{1}{L_g L_f^{\bar{r}-1}\bar{h}(x)}(v - L_f^{\bar{r}})\bar{h}(x) \tag{4.32}$$

Proof: To see the result one set

$$\begin{pmatrix} \zeta \\ \eta \end{pmatrix} = \begin{pmatrix} \bar{h}(x) \\ L_f^{\bar{r}}\bar{h}(x) \\ vdots \\ L_f^{\bar{r}-1}\bar{h}(x) \\ \phi_2(x) \end{pmatrix} \tag{4.33}$$

with $L_g\phi_2(x) = 0$ so getting

$$\dot{\zeta} = \hat{A}\zeta + \hat{B}(a(\zeta,\eta) + b(\zeta,\eta)u) \tag{4.34}$$
$$\dot{\eta} = q(\zeta,\eta) + \varphi(\zeta,\eta)w \tag{4.35}$$
$$\bar{y} = \zeta_1 \tag{4.36}$$

where $y - w$ are decoupled.As far as stability of the zero dynamics is concerned, following line of chapter 3, one gets

$$\sigma(q) = s \in C \text{s.t.} N^-(s) = 0 \subset C^-, q = \frac{\partial q}{\partial \eta} \mid_{(q,0)} \tag{4.37}$$

■

Theorem 4.2 *Consider the nonlinear system (4.24) and suppose that its LTM at the origin 4.27 is controllable and non minimum phase with relative degree r. Define the dummy output $\bar{y} = \bar{C}x$ as in Lemma 4.1 and the state transformation* **??**.*If $r_w \geq r$ then DDP is solvable for (4.24)with stability. By applying the coordinate transformation 4.33 to 4.24 one gets*

$$\dot{\zeta} = \hat{A}\zeta + \hat{B}(b(\zeta,\eta) + a(\zeta,\eta)u) \tag{4.38}$$
$$\dot{\eta} = q(\zeta,\eta) + v(\zeta,\eta)w \tag{4.39}$$
$$y = C^+\zeta. \tag{4.40}$$

with $C^+ = [b_0^+, ..., b_{\bar{r}-r}^+ 0]$ being the cofficient of C^+. Thus , under (4.32) one obtains (4.34,4.35) with $y = C^+\zeta$ and thus the result

Remark 4.8 *Given nonlinear feedback linearizable input affine dynamics with linear output map as inΣ_{NL},under a static feedback $\bar{u}^*$ any perturbation satisfying*

$$\tilde{p} \subset ker\left\{\bar{C}x, \ldots, dL_{\tilde{f}}^{\bar{r}-1}\bar{C}x\right\} \tag{4.41}$$

can be decoupled.

Remark 4.9 *If the disturbance is measurable then decoupling of the output from the disturbance is possible if and only if*

$$p(x) \subset \Omega^{\perp} + span\{g(x)\} \quad \text{in a neighbour of the origin} \tag{4.42}$$
$$\Omega = span\left\{\bar{C}x, \ldots, dL_{\tilde{f}}^{\bar{r}-1}\bar{C}x\right\} \tag{4.43}$$

and $\Omega^{\perp}$ being the orthogonal distribution to Ω.

4.5 Disturbance Decoupling problem with stability under sampling

In this section we address the Disturbance decoupling problem for 4.24 with stability and under sampling.First the problem is investigated in the linear context.We shall see require $w(t) = w(k)$ as $t \in [kT, (k+1)T[$ and being measured.

4.5.1 The Linear Tangent Invarient under sampling

4.5.1.1 Single Rate Design

DDP with stability admits a solution under SR sampling if the continuous-time solution exists. Moreover the relative degree $r = 1$ and the original system is minimum phase itself.
In case it is partially minimum phase, Multi rate is always needed to preserve stability of the internal dynamics under the action of perturbation.To see this, one should notice that whenever a system is partially minimum phase one solves the problem through an auxiliary output with respect to the relative degree $\bar{r}$ is increased so getting $\bar{r} \geq 1$.Accordingly, we have shown in chapter 2 that multi rate sampling of order $\bar{r}$ is needed to preserve the requires properties under sampling because of the rise of the sampling zeroes.This prevent from the possibility of solving the DDP via Single Rate sampling.

4.5.1.2 Multi Rate Design

Consider the multi rate sampled- data equivalent model to (4.24)model as provided by

$$x_{k+1} = A^T x(k) + B_m^\delta \underline{u} + D^T w_k \tag{4.44}$$

with

$$A^T = e^{AT}, B_m^\delta = [A^{(\bar{r}-1)\delta} B^\delta, \quad \dots, \quad B^\delta] \tag{4.45}$$
$$D^T = \int_0^T e^{A\delta} d\delta D, quad B^\delta = \int_0^\delta e^{A\delta} d\delta B$$

In what follows ,we show how multirate feedback can be exploited and combined with the arguments of the 4.1 to solve DDP with stability under sampling.This is achieved by considering the sampled-data dynamics (4.44) with augmented dummy output $\bar{Y} = \Gamma(x)$ composed of $\bar{Y}_k = \bar{C}x$ and its first $\bar{r} - 1$ derivatives; namely, we consider

$$x_{k+1} = A^\delta x_k + B_m^\delta \underline{\mathbf{u_k}} + D^\delta w_k, \qquad \bar{Y_k} = \Gamma(x) \tag{4.46}$$

with $\delta = \frac{T}{\bar{r}}$ and output vector

$$\Gamma x = \begin{pmatrix} \bar{C} \\ \bar{C}A \\ \dots \\ \bar{C}A^{\bar{r}-1} \end{pmatrix} x$$

Remark 4.10 *It can be easily verified from the definition of the relative degree that the row vector $\bar{C}, \dots, \bar{C}A^{\bar{r}-1}$ are linearly independent and hence*

$$\rho(\Gamma) = \bar{r}$$

where ρ denotes the rank

Lemma 4.3 *Let (4.24)verify proposition 4.1 and consider the MR a sample data model in the form(4.44) to (4.24).Introduce* $\bar{y_k} = \Gamma x_k$ *as in (4.3) verifying*

$$Y_{k+1} = \Gamma A^{\delta} x_k + \Upsilon \underline{u_k} + \Gamma D^{\delta} w_k \tag{4.47}$$

where

$$\Upsilon = \begin{pmatrix} \bar{C}A^{(\bar{r}-1)\delta}B^{\delta} & \dots & \bar{C}B^{\delta} \\ & \vdots & \\ \bar{C}A^{\bar{r}-1}A^{(\bar{r}-1)\delta}B^{\delta} & \dots & \bar{C}A^{\bar{r}-1}B^{\delta} \end{pmatrix}$$

is the decoupling matrix.Then the matrix Υ *is invertible and there exists a feedback law that solves the DDP with stability and under sampling.Such a feedback takes the form*

$$\underline{u_k} = (\Upsilon)^{-1}(-\Gamma(A^{\delta}x_k + D^{\delta}w_k) + \underline{v_k}) \tag{4.48}$$

Theorem 4.3 *Consider the LTI in the form of (4.27) under the hypotheses of Theorem*4.1 *with multi-rate equivalent model of order* $\bar{r}$ *provided by*

$$x_{k+1} = A^{\delta}x(k) + \mathbb{M}^{\delta}\underline{\mathbf{u}} + D^{\delta}w_k, \quad \bar{Y_k} = \Gamma(x) \tag{4.49}$$

Then the feedback (4.48) solves the sample data disturbance decoupling problem with stability of the internal dynamics if and only if the decoupling matrix Υ *is nonsingular and there is exists a feedback control law that solves the problem in continuous time .*

Remark 4.11 *Simple computations show that the transmission zeros as* $T \to 0$ *coincide with the zeros of the continuous time system*

4.6 DDP under sampling for nonlinear systems

In this section we extend the previous result to the case of nonlinear systems which are partially minimum phase.As in the linear case it intuitive to deduce that the problem will admit a solution with stability under SR sampling if the original continuous-time system is minimum phase and with relative degree $r = 1$.In any other case Multi rate is necessary .
In what follows , we shall consider the dynamics (4.24)under the hypothesis of theorem 3.1 while considering the dummy output $\bar{y} = \bar{C}x$ with respect to which the relative degree is $\bar{r}$ for design purpose.

4.6.0.1 Multi Rate Sample Data Model of sampled data system under disturbances and DDP stability under sampling

Consider the Multi Rate Sampled-data model to the dynamics (4.24)as

$$\Sigma_D^{\delta} \begin{cases} x_{k+1} = F^{\delta}(x_k, w_k, u_{1k}, ..., u_{\bar{r}k}) \\ y = \bar{H}(x_k) \end{cases} \tag{4.50}$$

with $\delta = \frac{T}{\bar{r}}$ and

$$\bar{H}(x_k) = \begin{pmatrix} \bar{h} \\ L_f\bar{h} \\ \vdots \\ L_f^{\bar{r}-1}\bar{h} \end{pmatrix} \tag{4.51}$$

with $\bar{h}(x) = \bar{C}x$

Lemma 4.4 *The sampled dynamics $(F)^\delta$ admits the following exponential expansion*

$$(F)^\delta(x_k, w_k, u_{1k}, ..., u_{\bar{r}k}) = e^{\delta L_f(.)+\delta u_1 L_g(.)+\delta L_p(.)w} o \dots o e^{\delta L_f(.)+\delta u_{\bar{r}} L_g(.)+\delta L_p(.)w} x_k$$

with $\delta = \frac{T}{\bar{r}}$ and can be expanded according to power of delta or according to the power of the control tool.The dynamic (4.50)has relative degree $\bar{r} = (1....1)$ with $\bar{r}\delta = \bar{r}$.

Lemma 4.5 *Consider the nonlinear system (4.24) under the hypotheses of Lemma 4.2 with multi-rate equivalent model of order $\bar{r}$ provided by (4.50). Then, there exists a unique solution*

$$\mathbf{u}^T = \gamma(T, x, \mathbf{v}, w) = (\gamma^1(T, x, \mathbf{v}, w) \ \dots \ \gamma^{\bar{r}}(\delta, x, \mathbf{v}, w))^\top \tag{4.52}$$

to the equality

$$\begin{aligned} &\bar{H}(F^T(x_k, \gamma^1(T, x_k, \mathbf{v_k}, w_k), \dots, \gamma^{\bar{r}}(\delta, x_k, \mathbf{v_k}, w_k)) = \\ &e^{\bar{r}T(L_f+\gamma(\cdot,\cdot,v)L_g+L_p w)}\bar{H}(x)\big|_{x_k} \end{aligned} \tag{4.53}$$

for any $x_k = x(kT)$ and $v_k = v(kT) := v_k$, $\mathbf{v_k} = (v_k, \dots, v_k)$. Such a solution is in the form of a series expansion in powers of T around the continuous-time $\gamma(x, w, v)$; i.e., for $i = 1, \dots, \bar{r}$

$$\gamma^i(T, x, \mathbf{v}, w) = \gamma(x, \mathbf{v}, w) + \sum_{j\geq 1} \frac{T}{(j+1)!}\gamma_j^i(x, \mathbf{v}, \mathbf{w}). \tag{4.54}$$

As a consequence, the feedback $\mathbf{u}_k^T = \gamma(T, x_k, \mathbf{v}_k)$ solves the DDP with stability of the internal dynamics.

The feedback (4.54) solution to (4.53) is aimed at matching , at each sampling instant $t = kT$, the evolution of the output $\bar{y} = \bar{h}(x)$ and its $\bar{r} - 1$ derivative under the continuous-time feedback

$$\gamma(x, w, v) = \frac{1}{L_g L_f^{\bar{r}-1}\bar{h}}(v - L_f^{\bar{r}}\bar{h}). \tag{4.55}$$

$$\gamma(x, w, v) = \frac{1}{L_g L_f^{\bar{r}-1}\bar{h}}(v - L_f^{\bar{r}}\bar{h}). \tag{4.56}$$

By construction , such a feedback ensures convergence at any $t = kT$ of the dynamics onto the stable zero dynamics associated to $\bar{y} = h(x_2)$.

Theorem 4.4 *Consider the nonlinear system (4.24) under the hypotheses of Theorem 4.2 with multi-rate equivalent model of order $\bar{r}$ provided by*

$$x_{k+1} = F^{\delta}(x_k, u_{1k}, \ldots, u_{\bar{r}k}, w_k), \quad y_k = \begin{pmatrix} C_1 & \mathbf{0} \end{pmatrix} H_2(x_k) \tag{4.57}$$

and let the feedback (4.52) be the unique solution to the equality (3.79). Then the feedback $\mathbf{u}_k^T = \gamma(\delta, x_k, \mathbf{v}_k)$ ensures solves the DDP with stability.

4.6.1 Computation of Discrete time feedback design for the MR system

The purpose of this section is provide computational facilities to define the sampled data feedback. The feedback u^T comes in the form of a series expansion in power of δ.Accordingly, computing an exact and closed form is not possible in general. Still, one can exploit the power series form of (4.53) to deduce any term $\gamma_j^i(x, v, w)$ in (4.54). Through a constructive and iterative procedure by equating the terms with the same power of δ and solving at each step j, a linear equation in the unknown $\gamma_j^i(x, v, w) \quad i = 1, 2$.For the sake of simplicity assume relative degree $r = 1$ of the continuous time system (4.24) and the relative degree with respect to the dummy output $\bar{r} = 2$ and for a small time interval $\delta = \frac{T}{2}$. In this case the left hand side

rewrite as

$$e^{(L_f+u_1L_g+L_pw)}oe^{(L_f+u_1L_g+L_pw)}\bar{h}x = \bar{h} + \delta L_f\bar{h} + \frac{\delta^2}{2}L_f^2\bar{h} + \cdots + u_1(\delta L_g\bar{h} + \frac{\delta^2}{2}(L_fL_g\bar{h}$$

$$+ L_gL_f\bar{h})) + \frac{\delta^2}{2}L_pL_f\bar{h} \tag{4.58}$$

$$+ \delta L_f\bar{h} + \delta^2L_f^2\bar{h} + \frac{\delta^3}{2}L_f^3\bar{h} + \cdots + u_1(\delta^2L_fL_g\bar{h} + \frac{\delta^3}{2}(L_f^2L_g\bar{h} + L_fL_gL_f\bar{h})) + \frac{\delta^3}{2}L_pL_f^2\bar{h} \tag{4.59}$$

$$+ \frac{\delta^2}{2}L_f^2\bar{h} + \frac{\delta^3}{2}L_f^3\bar{h} + \frac{\delta^4}{4}L_f^4\bar{h} + \cdots + u_1(\frac{\delta^3}{2}L_f^2L_g\bar{h} + \frac{\delta^4}{4}(L_f^3L_g\bar{h} + L_f^2L_gL_f\bar{h})) + \frac{\delta^4}{4}L_pL_f^3\bar{h} \tag{4.60}$$

$$+ u_2\Big[\delta L_g\bar{h} + \delta^2L_gL_f\bar{h} + \frac{\delta^3}{2}L_gL_f^2\bar{h} + \cdots + u_1(\delta^2L_g\bar{h} + \frac{\delta^3}{2}(L_gL_fL_g\bar{h} + L_g^2L_f\bar{h})) + \frac{\delta^3}{2}L_gL_pL_f\bar{h}w \tag{4.61}$$

$$+ \frac{\delta^2}{2}L_fL_g\bar{h} + \frac{\delta^3}{2}L_fL_gL_f\bar{h} + \frac{\delta^4}{4}L_f^3L_g\bar{h} + \frac{\delta^4}{4}L_fL_gL_pL^f\bar{h}w \tag{4.62}$$

$$+ \frac{\delta^2}{2}L_gL_f\bar{h} + \frac{\delta^3}{2}L_gL_f^2\bar{h} + \frac{\delta^4}{4}L_gL_f^3\bar{h} + \cdots + \frac{\delta^4}{4}\ L_gL_pL_f\bar{h}w\Big] + w\Big[\frac{\delta^3}{2}L_pL_f^2\bar{h} + u_1(\delta^2L_pL_g\bar{h} \tag{4.63}$$

$$+ \frac{\delta^3}{2}(L_pL_fL_gh + L_pL_gL_f\bar{h}(x) + w(\frac{\delta^3}{2}L_p^2L_f\bar{h}) + \frac{\delta^2}{2}L_fL_p\bar{h} + \frac{\delta^3}{2}L_fL_pL_f\bar{h}$$

$$+ u_1(\frac{\delta^3}{2}{}_fL_pL_g\bar{h} + \frac{\delta^4}{4}(L_fL_pL_fL_g + L_fL_pL_fL_gL_f\Big] \tag{4.64}$$

$$= \bar{h} + 2\delta L_f\bar{h}) + \frac{\delta^2}{2}(4L_f^2\bar{h}) + u_1[\delta L_g\bar{h} + \frac{\delta^2}{2}(3L_fL_g\bar{h} + L_gL_f\bar{h}) + \frac{\delta^3}{3!}(6L_f^2L_g\bar{h} + 3L_fL_gL_f\bar{h})] + \tag{4.65}$$

$$u_2[\delta L_g\bar{h} + \frac{\delta^2}{2}(3L_gL_f\bar{h} + L_fL_g\bar{h}) + \frac{\delta^3}{3!}(6L_gL_f^2\bar{h} + 3L_fL_gL_f\bar{h})] + [\frac{\delta^2}{2}L_pL_f\bar{h} + \frac{\delta^3}{3!}(3l_pL_f^2h + 3L_fL_pL_f\bar{h}] \tag{4.66}$$

simultaneously we get

$$L_f\bar{h} = e^{(f+pw+u_2g)}.e^{(f+pw+u_1g)}L_fh(\bar{x})$$

with

$$e^{(f+u_1g)}L_fh(\bar{x}) = L_f\bar{h} + \delta L_f^2\bar{h} + \frac{\delta^2}{2}L_f^3\bar{h} + \cdots + u_1(\delta L_gL_f\bar{h} + \frac{\delta^2}{2}(L_fL_gL_f\bar{h} + L_gL_f^2\bar{h}) + \dots)$$

$$L_f\bar{h}(x_d(k+2\delta)) = L_f\bar{h} + \delta L_f^2\bar{h} + \frac{\delta^2}{2}L_f^3\bar{h} + \cdots + u_1(\delta L_gL_f\bar{h} + \frac{\delta^2}{2}(L_fL_gL_f\bar{h} + L_gL_f^2\bar{h})) + \frac{\delta^2}{2}L_pL_f^2\bar{h}w$$
$$+ \delta L_f^2\bar{h} + \delta^2 L_f^3\bar{h} + \frac{\delta^3}{2}L_f^4\bar{h} + \cdots + u_1(\delta^2 L_fL_gL_f\bar{h} + \frac{\delta^3}{2}(L_f^2L_gL_f\bar{h} + L_fL_gL_f^2\bar{h})) + \frac{\delta^3}{2}L_fL_pL_f^2\bar{h}w$$
$$+ \frac{\delta^2}{2}L_f^3\bar{h} + \frac{\delta^3}{2}L_f^4\bar{h} + \frac{\delta^4}{4}L_f^5\bar{h} + \cdots + u_1(\frac{\delta^3}{2}L_f^2L_gL_f\bar{h} + \frac{\delta^4}{4}(L_f^3L_gL_f\bar{h} + L_f^2L_gL_f^2\bar{h})) + \frac{\delta^4}{4}L_f^2L_pL_f^2\bar{h}w$$
$$+ u_2\Big[\delta L_gL_f\bar{h} + \delta^2 L_gL_f^2\bar{h} + \frac{\delta^3}{2}L_gL_f^3\bar{h} + \cdots + u_1(\delta^2 L_gL_f\bar{h} + \frac{\delta^3}{2}(L_gL_fL_gL_f\bar{h} + L_g^2L_f^2\bar{h})) + \frac{\delta^3}{2}L_gL_pL_f^2\bar{h}w$$
$$+ \frac{\delta^2}{2}L_fL_gL_f\bar{h} + \frac{\delta^3}{2}L_fL_gL_f^2\bar{h} + \frac{\delta^4}{4}L_f^3L_gL_f\bar{h} + +\frac{\delta^4}{4}L_fL_gL_pL_f^2\bar{h}w + \ldots$$
$$+ \frac{\delta^2}{2}L_gL_f^2\bar{h} + \frac{\delta^3}{2}L_gL_f^3\bar{h} + \frac{\delta^4}{4}L_gL_f^4\bar{h} + \frac{\delta^4}{4}L_gL_fL_pL_f^2\bar{h}w + \ldots\Big]$$
$$+ w\Big[u_1(\delta^2 L_pL_gL_f\bar{h} + \frac{\delta^3}{2}(L_pL_gL_f^2\bar{h} + L_pL_fL_gL_f\bar{h}) + \frac{\delta^2}{2}L_p^2L_f^2\bar{h}$$
$$+ (\frac{\delta^2}{2}L_fL_pL_f\bar{h} + \frac{\delta^3}{2}L_fL_pL_f^2\bar{h} + \frac{\delta^3}{2}L_fL_pL_gL_f + \ldots)u_1 + \ldots\Big]$$
$$= L_f\bar{h} + \delta(2L_f^2\bar{h}) + \frac{\delta^2}{2}(4L_f^3\bar{h}) + u_1[\delta L_gL_f\bar{h} + \frac{\delta^2}{2}(3L_fL_gL_f\bar{h} + L_gL_f^2\bar{h}) + \frac{\delta^3}{3!}(6L_f^2L_gL_f\bar{h} + 3L_fL_gL_f^2\bar{h})] +$$
$$u_2[\delta L_gL_f\bar{h} + \frac{\delta^2}{2}(3L_gL_f^2\bar{h} + L_fL_gL_f\bar{h}) + \frac{\delta^3}{3!}(6L_gL_f^3\bar{h} + 3L_fL_gL_f^2\bar{h})] + \frac{\delta^2}{2}L_pL_f\bar{h}w + \frac{\delta^3}{3!}(L_fL_pL_f\bar{h})w$$

and the output rewrites as

$$\bar{H} \approx= \begin{pmatrix}\bar{h}\\ L_f\bar{h}\end{pmatrix} + \delta\begin{pmatrix}2L_f\bar{h}\\ 2L_f^2\bar{h}\end{pmatrix} + \frac{\delta^2}{2}\begin{pmatrix}4L_f^2\bar{h}\\ 4L_f^3\bar{h}\end{pmatrix} + \Big[\delta\begin{pmatrix}L_g\bar{h} & L_g\bar{h}\\ L_gL_f\bar{h} & L_gL_f\bar{h}\end{pmatrix} + \tag{4.67}$$
$$\frac{\delta^2}{2}\begin{pmatrix}3L_fL_g\bar{h} + L_gL_f\bar{h} & 3L_gL_f\bar{h} + L_fL_g\bar{h}\\ 3L_fL_gL_f\bar{h} + L_gL_f^2\bar{h} & 3L_gL_f^2\bar{h} + L_fL_gL_f\bar{h}\end{pmatrix} + \frac{\delta^3}{3!}\begin{pmatrix}6L_f^2L_g\bar{h} + 3L_fL_gL_f\bar{h} & 6L_gL_f^2\bar{h} + 3L_fL_gL_f\bar{h}\\ 6L_f^2L_gL_f\bar{h} + 3L_fL_gL_f^2\bar{h} & 6L_gL_f^3\bar{h} + 3L_fL_gL_f^2\bar{h}\end{pmatrix} \tag{4.68}$$

with

$$\gamma = \begin{pmatrix}\bar{h}(x)\\ \vdots\\ L_f^{\bar{r}-1}\bar{h}(x)\end{pmatrix}$$

Denoting $B_m(\delta, \delta^2, \delta^3)$ the approximate decoupling matrix

$$B_m(\delta,\delta^2,\delta^3) = \delta\begin{pmatrix}L_g\bar{h} & L_g\bar{h}\\ L_gL_f\bar{h} & L_gL_f\bar{h}\end{pmatrix} + \frac{\delta^2}{2}\begin{pmatrix}3L_fL_g\bar{h} + L_gL_f\bar{h} & 3L_gL_f\bar{h} + L_fL_g\bar{h}\\ 3L_fL_gL_f\bar{h} + L_gL_f^2\bar{h} & 3L_gL_f^2\bar{h} + L_fL_gL_f\bar{h}\end{pmatrix} +$$
$$\frac{\delta^3}{3!}\begin{pmatrix}6L_f^2L_g\bar{h} + 3L_fL_gL_f\bar{h} & 6L_gL_f^2\bar{h} + 3L_fL_gL_f\bar{h}\\ 6L_f^2L_gL_f\bar{h} + 3L_fL_gL_f^2\bar{h} & 6L_gL_f^3\bar{h} + 3L_fL_gL_f^2\bar{h}\end{pmatrix}$$

Remark 4.12 *The existence of the solution of the previous equation derives from the implicit function theorem if and only if the decoupling matrix is invertible.*

$$\Psi = \begin{pmatrix}\Psi_1 & \Psi_2\\ \Psi_3 & \Psi_4\end{pmatrix}$$

where

$$\Psi_1 = \delta L_g\bar{h} + \frac{3\delta^2}{2}L_fL_g\bar{h} + \frac{\delta^2}{2}L_gL_f\bar{h} + \delta^3L_f^2L_g\bar{h} + \frac{\delta^3}{2}L_fL_gL_f\bar{h}$$
$$\Psi_2 = \delta L_g\bar{h} + 3\frac{\delta^2}{2}L_gL_f\bar{h} + \frac{\delta^2}{2}L_fL_g\bar{h} + \delta^3L_gL_f^2\bar{h} + \frac{\delta^3}{2}L_fL_gL_f\bar{h}$$
$$\Psi_3 = \delta L_gL_f\bar{h} + \frac{\delta^2}{2}(3L_fL_gL_f\bar{h} + L_gL_f^2\bar{h}) + \frac{\delta^3}{3!}(6L_f^2L_gL_f\bar{h} + 3L_fL_gL_f^2\bar{h})$$
$$\Psi_4 = \delta L_gL_f\bar{h} + \frac{\delta^2}{2}(3L_gL_f^2\bar{h} + L_fL_gL_f\bar{h}) + \frac{\delta^3}{3!}(6L_gL_f^3\bar{h} + 3L_fL_gL_f^2\bar{h})$$

is nonsingular

As for the left hand RHS of (4.53) is concerned one gets

$$\bar{H} + 2\delta(L_f + u_cL_g + wL_p)\bar{H} + \frac{(2\delta)^2}{2}(L_f + u_cL_g + wL_p)^2\bar{H} \tag{4.69}$$
$$= \bar{H} + 2\delta(L_f + u_cL_g + L_pw)\bar{H} + \frac{(2\delta)^2}{2}(L_f^2 + u_c(L_fL_g + L_gL_f) \tag{4.70}$$
$$+ \dot{u}_cL_g + u_c^2L_g^2 + w(L_fL_p + L_pL_f) + w^2L_p^2 + u_cw(L_pL_f + L_fL_p)\bar{H} \tag{4.71}$$

with

$$\bar{H} = \begin{pmatrix} \bar{h} \\ L_f\bar{h} \end{pmatrix} \tag{4.72}$$

Iteration can be made similarly to the left hand side.Now let us assume that the starting from the SISO system in the form of (4.24) and under the hypothesis of lemma 4.1 there is exists a continuous time feedback control law

$$u_c = \frac{1}{L_gL_f\bar{h}(x)}(-L_f^2h(x) - L_pwh(x) + v) = \alpha(x) + \beta(x) \tag{4.73}$$

which leads to

$$\ddot{\bar{y}} = v \tag{4.74}$$

The case of $v_{k+\frac{1}{2}} = v_k$ is chosen in order to simplify the computations .The MR sampled data model (4.50) is specified as

$$\begin{aligned} x_{k+1} &= F^\delta(x_k, u_{1k}, u_{2k}, w_k) \\ y_{1k} &= \bar{h}(x) = \bar{C}x \\ y_{2k} &= L_f\bar{h}(x) = L_f\bar{C}x. \end{aligned} \tag{4.75}$$

with

$$F^\delta(x_k, u_{1k}, u_{2k}, w_k) = e^{\delta(L_f + L_pw + u_1L_g)} \circ e^{\delta(L_f + L_pw + u_2L_g)}(x_k) \tag{4.76}$$

The multi rate sampled data feedback is given by$\gamma(T,x,v,w)$

$$\gamma(T,x,v,w) = (\gamma^1(T,x,v,w), \gamma^1(T,x,v,w) \tag{4.77}$$

with (4.78)

$$\gamma^j(T,x_k,v_k,w_k) = \gamma_0^j(x_k,v_k,w_k) + \Sigma_{i\geqslant 1} T^i \gamma_i^j(x_k,v_k,w_k). \tag{4.79}$$

substituting (4.79) into (4.53) and exploiting the parametrization by T one get

$$\bar{h}o\tilde{F}^{\delta}(x_k,u_{1k},u_{2k},w_k) = \bar{h}(x_k) + TL_f\bar{h}(x_k) + \frac{1}{2}\delta^2(L_f^2 + uL_gL_f + wL_pL_f)\bar{h}(x) + \dots \tag{4.80}$$

Note that under the assumption that the problem is solvable in continuous-time and the relative degree with respect to the dummy output $r_w = 2$ i.e. $L_p\bar{h} = L_pL_f\bar{h} = 0$. By substituting and equating equation we get

$$\gamma_0^1(x_k,v_k,w_k) = \gamma_{d0}^2(x_k,v_k,w_k) = u_c(x_k,v_k) \tag{4.81}$$

$$\gamma_0^1(x_k,v_k,w_k) = \frac{1}{6}\dot{u}_c \tag{4.82}$$

$$\gamma_0^2(x_k,v_k,w_k) = \frac{5}{6}\ddot{u}_c \tag{4.83}$$

that is

$$\gamma^1(x_k,v_k,w_k) = u_c(x_k,v_k,w_k) + \frac{1}{6}T\dot{u}_c + \dots \tag{4.84}$$

$$\gamma^2(x_k,v_k,w_k) = u_c(x_k,v_k) + \frac{5}{6}T\dot{u}_c + \dots \tag{4.85}$$

4.7 Example

Recalling the TORA example described in chapter 3

$$\begin{aligned}
\dot{x}_1 &= x_2 \\
\dot{x}_2 &= -x_1 + \varepsilon \sin x_3 \\
\dot{x}_3 &= x_4 \\
\dot{x}_4 &= \frac{\varepsilon \cos x_3 (x_1 - \varepsilon x_4^2 \sin x_3) + u}{1 - \varepsilon^2 \cos^2 x_3} \\
y &= \begin{pmatrix} \frac{2(\varepsilon^2-1)}{\varepsilon} & 0 & 1-\varepsilon^2 & 1-\varepsilon^2 \end{pmatrix} x
\end{aligned} \tag{4.86}$$

In this context consider a disturbance

$$p(x) = \begin{pmatrix} \frac{2}{\epsilon}(\epsilon^2 - 1) \\ 0 \\ 0 \\ (\epsilon^2 - 1) \end{pmatrix}$$

considering the auxiliary output

$$y_2 = (-1 \qquad 10 \qquad 0)Tx = (0 - \frac{2}{\epsilon}(\epsilon^2 - 1) \qquad (1 - \epsilon^2)0)x \tag{4.87}$$

where T is provided by

$$T = (\epsilon^2 - 1)\begin{pmatrix} -\frac{1}{\epsilon} & 0 & 0 & 0 \\ 0 & -\frac{1}{\epsilon} & 0 & 0 \\ \frac{1}{\epsilon} & 0 & -1 & 0 \\ 0 & \frac{1}{\epsilon} & 0 & -1 \end{pmatrix} \tag{4.88}$$

It is a matter of computation to verify that with respect to the new output 4.87 the system has relative degree $r_2 = 2$ and is minimum phase with transfer function of the corresponding LTM at the origin was provided by

$$w_2(s) = \frac{(s+1)^2}{s(1-\epsilon^2)s^2 + 1)} \tag{4.89}$$

Moreover, DDP with stability is solvable as the relative degree condition $r_w < r_2 > r$ is met so that the feedback being computed as

$$L_g L_f h_2(x) = \frac{\epsilon^2 - 1}{\epsilon^2 cos^2(x_3) - 1} \tag{4.90}$$

$$L_f^2 h_2(x) = \frac{2x_2(\epsilon^2 - 1)}{\epsilon} - 2x_4 cos(x_3)(\epsilon^2 - 1) + \frac{\epsilon cos(x_3)(\epsilon^2 - 1)(x_1 - \epsilon sin(x_3)(x_4^2 + 1))}{\epsilon^2 cos(x_3)^2 - 1} \tag{4.91}$$

fulfills the requirement.Moreover, setting $v = -k_1 h_2(x) - k_2 L_f h_2(x)$ one gets $y(t) \to 0$ as $t \to \infty$ whenever $k_1, k_2 > 0$ To solve the problem under sampling under sampling, the multirate feedback $\gamma^1(\delta, x, w, v)$ was computed for $p = 1$ with

$$\gamma_1^1(x, w, v) = \frac{1}{3}\dot{\gamma}(x, w, v), \gamma_1^2(x, w, v) = \frac{5}{3}\dot{\gamma}(x, w, v)$$

Figure 4.1 to 4.2 depict simulations of the aforementioned situations under continuous time feedback and the sample data feedback with one correcting term i.e $p = 1$ and different values of the sampling period an different simulating scenarios

It is clear from figure 4.1 to 4.2 that in case of the continuous time scenario that the pro boded feedback computed via partial dynamic inversion succeeded in isolating the effect of the disturbance from the output for the original system as the output goes to zero with an acceptable behaviour of the zero dynamics which is still converging to origin despot the perturbation.

As far as the sampled-data system is concerned,simulation underline that although an approximated feedback is implemented in a notable improvement of the performance is achieved with respect to the mere emulation case which is failing to stabilize the input output evolution T grows enough.

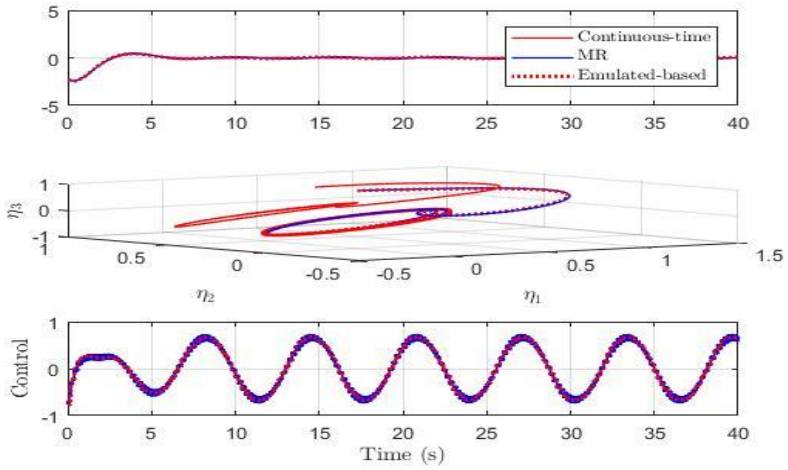

Figure 4.1: $\delta = 0.2$.

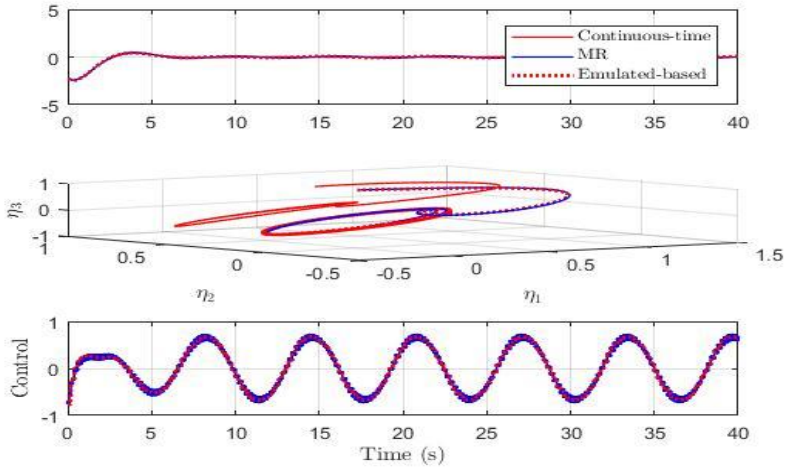

Figure 4.2: $\delta = 0.7$ s

4.8 Conclusion

In this chapter , we introduce new conditions for characterizing all the disturbances that can be locally decoupled from the output evolution of nonlinear systems have been deduced by also requiring the preservation of the internal stability. The introduced approach is based on a local factorization of the polynomial defining the zeros of the corresponding linear tangent model at the origin and , thus on partially dynamic cancellation.Future works are towards the extension of these argument to

the multi input- multi output case and to a global characterization of the results possibly combined with input -output stability and related results.

Chapter 5

Nonlinear and under sampling control for a wind system fed by a Doubly Fed Induction Generator

Contents

5.1 Introduction

In this chapter we investigate the effectiveness of nonlinear control-based model and the sampled-data design through power system application.In particular we study the model of a wind turbine system fed by a doubly fed induction generator and we track Maximum Power Point. (MPPT) extracts maximum power from the wind turbine from cut-in to rated wind velocity . Till date, many algorithms for MPPT have been reported, each with its own features.Through the development of this Two cases studied we aim to introduce a solution to this problem.
In the first case we focus on the study of the different models and control design . Three models have been used :the first one is the linearized state-space model

followed by a classical PID controller while the second one is the fuzzy logic controller.Finally a nonlinear model based controller is used.Moreover we have used the Artificial Immunity controller as a learning algorithm to collaborate with the nonlinear model.Through the chapter we will see that the best performance in terms of wind speed variation i.e, (steeling time, transient response, maximum over shoot) generated from the nonlinear based model supported by the artificial intelligent.Roughly, speaking the idea that the future of artificial intelligence lies in the sphere of nonlinear dynamics and chaos that is absolutely critical to understanding and modeling cognition processes.
In the other hand when the system is connected to grid there appear the need to use digital control.The development of Phasor measurement Unit and the availability of modern communication beside the fact that transferring power in DC is much more cheaper than AC all encourage the need to study solution to this problem in digital control.Figure 5.1,5.2 illustrate the operation of wind turbine when its connected to grid.As we have state in the introduction there are three designs can be applied in this concept.From our point of view direct implementation of the continuous- time model (the emulation design) does not always provide better results especially if one consider the transient behaviour.As for the Discrete- time design we will still faces difficulties in defining the exact model.A case study for the DFIG is developed through setting power factor into one so that we have only the direct axis frame.In this case the system is transformed from MIMO square system into SISO one.The sampled-data design has been used and a comparison have been made with respect to both emulation design and the sample data.We will see that the sampled-data provide better results in tracking the MPP.

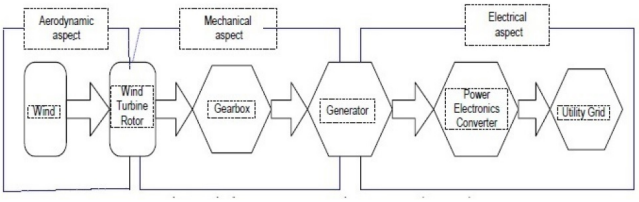

Figure 5.1: Wind system operation.

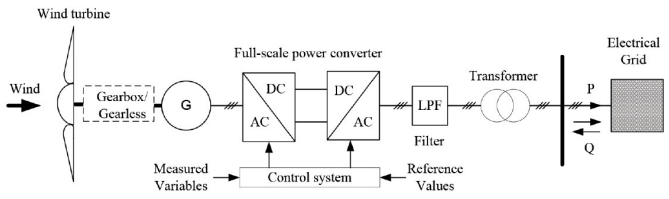

Figure 5.2: Three phase synchronous generator.

The artificial intelligent controller that is build on the bases of nonlinear based control design for a doubly fed induction generator DFIG.The controller consists of two clusters.The first part is developed based on a novel Artificial Immunity sensorless Maximum Power Point Tracking (AI MPPT) technique.To build the AI MPPT, an Artificial Immunity System Estimator (AISE) based on artificial immunity technique and a MRAS (model reference adaptive system) are used to estimate the Doubly Fed Induction Generator (DFIG) rotor speed. Then the AI MPPT is applied to provide the reference electromagnetic torque. Subsequently, the wind power is approximated from the data of the estimated generator speed and the reference electromagnetic torque.Finally, the wind speed is determined by the mechanical power.The second cluster is designed using a nonlinear Asymptotic output tracking technique.The purpose of this control is to track the reference signal of the rotor direct and quadratic current respectively.Thus, assigning specific zeros through feedback ensure the reproduction of an output that converges asymptotically to a required reference rotor current.The reference signal is generated from the previous controller that is based on the artificial immunity technique.The introduced approach method has been applied to a wind turbine generator driving a 3.7 KW.The MAT LAB program is used to simulate and test the performance of the proposed control methods.The results are featured to show the effectiveness of the proposed technique.

5.2 modeling

This section address the modeling of Doubly Fed Induction Generator (DFIG) and wind turbine model respectively.

5.2.1 Doubly Fed Induction Generator model

In order to simplify the Doubly Fed Induction Generator (DFIG) model ,the following assumption is assumed

1 The flow distribution is sinusoidal.

2 The air-gap is constant.

3 The influences of the heating and the skin effect are not taken into account.

4 The saturation of the magnetic circuit is negligible.

The DFIG modelling with respect to a rotor flux orianted reference frame will be expressed as:

5.2.1.1 Stator Equations

$$V_{sd} = R_s i_{sd} + \frac{d}{dt}\lambda_{sd} - \lambda_{sq} W_s \tag{5.1}$$

$$V_{sq} = R_s i_{sq} + \frac{d}{dt}\lambda_{sq} + \lambda_{sd} W_s \tag{5.2}$$

$$\lambda_{sd} = L_s i_{sd} + M i_{rd} \tag{5.3}$$

$$\lambda_{sq} = L_s i_{sq} + M i_{rq} \tag{5.4}$$

5.2.1.2 Rotor Equations

$$V_{rd} = R_r i_{rd} + \frac{d}{dt}\lambda_{rd} - \lambda_{rq} W_r \tag{5.5}$$

$$V_{rq} = R_r i_{rq} + \frac{d}{dt}\lambda_{rq} + \lambda_{rd} W_r \tag{5.6}$$

$$\lambda_{rd} = L_r i_{rd} + M i_{sd} \tag{5.7}$$

$$\lambda_{rq} = L_r i_{rq} + M i_{sq} \tag{5.8}$$

$$\tag{5.9}$$

Where, R_s and R_r are, respectively, the stator and rotor phase resistances, Ls, Lr, MStator and rotor per phase winding and magnetizing inductances and $W_s, W_r$are the stator and rotor speed of the synchronous reference frame.The direct and quadratic stator and rotor currents are respectively represented asi_{sd}, i_{sq}, i_{rd} and i_{rq}.The voltage of the stator side for both direct and quadratic defined as V_{sd}, V_{sq} while the voltage of the rotor direct and quadratic represented as V_{rd}, V_{rd}.The stator-flux linkage for direct and quadratic frame are given by$\lambda_{sd}, \lambda_{sd}$.The $\lambda_{rd}, \lambda_{rq}$ referred to the rotor flux for both the direct and quadratic respectively.Finally g is the ratio of the gear box.
The dynamics of the mechanical part of the wind turbine are represented by

$$J\frac{dW}{dt} = c_m - c_e - c_f W \tag{5.10}$$

$$c_e = p\frac{M}{L_s}(\lambda_{sq} i_{rd} - \lambda_{sd} i_{rq}) \tag{5.11}$$

where J is the moment of inertia while c_e, c_m represent the electromagnetic torque,mechanical torque respectively and c_f is the friction coefficient. The system now will be modeled with respect to the rotor side direct and quadratic (d,q)

synchronous reference frame.The input in such case are i_{rd}andi_{rq}.
First the system expression w.r.to d axis frame

$$v_{rd} = R_r i_{rd} + \frac{d}{dt}(L_r i_{rd} + M i_{sd}) - (L_r i_{rq} + M i_{sq}) W_r \tag{5.12}$$

$$= R_r i_{rd} + L_r \dot{i}_{rd}(1 - \frac{M^2}{L_s L_r}) - L_r W_r (1 - \frac{M^2}{L_s L_r}) i_{rq} \tag{5.13}$$

$$= R_r i_{rd} + L_r \Lambda \dot{i}_{rd} - L_r \Lambda W_r i_{rq} \tag{5.14}$$

$$\dot{i_{rd}} = \frac{1}{L_r \Lambda} v_{rd} - \frac{R_r}{L_r \Lambda} i_{rd} + w_r i_{rq} \tag{5.15}$$

$$\dot{i_{rd}} = \frac{1}{L_r \Lambda} v_{rd} - \frac{1}{\mathcal{T} \Lambda} i_{rd} + w_r i_{rq} \tag{5.16}$$

with $\Lambda = (1 - \frac{M^2}{L_s L_r})$,$\mathcal{T} = \frac{R_r}{L_r}$.

Now consider q axis frame

$$V_{rq} = R_r i_{rq} + \frac{d}{dt}\lambda_{rq} + \lambda_{rd} W_r \tag{5.17}$$

$$= R_r i_{rq} + L_r \Lambda \dot{i}_{rq} - L_r \Lambda W_r i_{rd} \tag{5.18}$$

$$\dot{i}_{rq} = \frac{1}{L_r \Lambda} v_{rq} - \frac{1}{\mathcal{T} \Lambda} i_{rq} - w_r i_{rd} \tag{5.19}$$

Finally we obtain the speed from the torque equation as: $\dot{W} = -\frac{C_f}{J} W - p\frac{M}{L_s}(\lambda_{sq} i_{rd} - \lambda_{sd} i_{rq})$.

5.2.2 Wind turbine model

For a given wind speed v_w, the mechanical power $P_m$generated by the turbine is expressed as

$$p_m = \frac{1}{2} \rho A c_p(\lambda, \beta) v_m^3 \tag{5.20}$$

where ρ is the density of the air in $kg/m3$; $A\pi R^2$ is the area swept by blade in $m2$, and R the radius of the blade in m. The aerodynamic model of a wind turbine can be determined by the $C_p(\lambda, \beta)$curves. C_p is the power coefficient, which is a function of both tip-speed-ratio λ and the blade pitch angleβ. The tip-speed ratio can be determine from$\lambda = \frac{\omega_r R}{v_m}$where$\omega_r$ represents the rotational speed of the wind turbine in rad/sec.The optimal DFIG speed to achieve a maximum wind power tracking is given by:

$$\omega_r^* = \frac{\lambda_o pt \hat{v_w}}{R} \tag{5.21}$$

The$\hat{v_w}$ is the estimated wind speed and $\lambda_o pt$ is the optimal tip-speed ratio. The power coefficient is non-dimensional term and is modeled by the following equation

$$c_p = 0.398 \sin(\frac{\pi(\lambda - 3)}{15 - .3\beta} - .0039(\lambda - 2)\beta \tag{5.22}$$

If the wind speed is below its rated value, the WTG operates in the variable speed mode, and C_p is kept at its maximum value.In this operating mode, the pitch control is deactivated. If the wind speed is above the rated value, the pitch control is activated in order to reduce the generated mechanical power.

5.3 DFIG Control strategy

The proposed technique will only consider the control of the Rotor Side Converter of the Doubly-Fed Induction Generator.The overall scheme of the RSC are shown in Figure1.The control of the generator rotor speedω_m^* and the reactive power Q_s is independently achieved by means of current regulations.As one can see from Figure1 there are two control loops.The outer loop control is realized using the Artificial Immunity System (AIS)technique(detailed illustration is provided in section 4).The outer loop control the rotor speed and the stator reactive power used to generate the reference signal of direct and quadratic current component. As for the inner loop it controls the direct and quadratic rotor axis current .The nonlinear control design will be applied in the inner loop.The control will be realized in the rotor reference frame so the d axis regulate the reactive power and the q axis regulate the active power.In general, the system will produce an output that, regardless of the initial state of the system will converge asymptotically to the rotor reference current signal.The nonlinear input output decoupling with tracking is illustrated below. In order to achieve a power decoupling control, the vector control strategy was adopted, with stator field orientation. Reactive power Qs and generator speed are respectively proportional to rotor currents i_{dr} and i_{qr}.

5.3.1 Decoupling and Asymptotic tracking by static feedback for the DFIG

The nonlinear model of the DFIG may be expressed as

$$\Sigma_C : \begin{cases} \dot{x} = f(x) + g_1(x)u_1 + g_2(x)u_2, \quad x \in \mathbb{R}^n, u \in \mathbb{R}^n \\ y = \begin{pmatrix} h_1(x) \\ h_2(x) \end{pmatrix} = \begin{pmatrix} i_{rd} \\ i_{rq} \end{pmatrix} \end{cases} \tag{5.23}$$

where, $x = [x_1 \quad x_2 \quad x_3]^T = [i_{rd} \quad i_{rq} \quad W_r]^T$,$u = [u_1 \quad u_2]^T = [v_{rd} \quad v_{rq}]^T$.The function$f(x), g(x)$ are smooth vector fields and the output function $h(x)$ is a smooth scalar function.

$$f(x) = \begin{pmatrix} -\frac{1}{\mathcal{T}\Lambda}x_1 + x_2x_3 \\ -\frac{1}{\mathcal{T}\Lambda}x_2 - x_2x_3 \\ -\frac{C_f}{J}x_3 - \frac{pM}{L_s}(\lambda_{sq}x_1 - \lambda_{sd}x_2) \end{pmatrix} \tag{5.24}$$

$$g_1(x) = \begin{pmatrix} \frac{1}{\mathcal{T}\Lambda} \\ 0 \\ 0 \end{pmatrix}, \quad g_2(x) = \begin{pmatrix} 0 \\ \frac{1}{\mathcal{T}\Lambda} \\ 0 \end{pmatrix}. \tag{5.25}$$

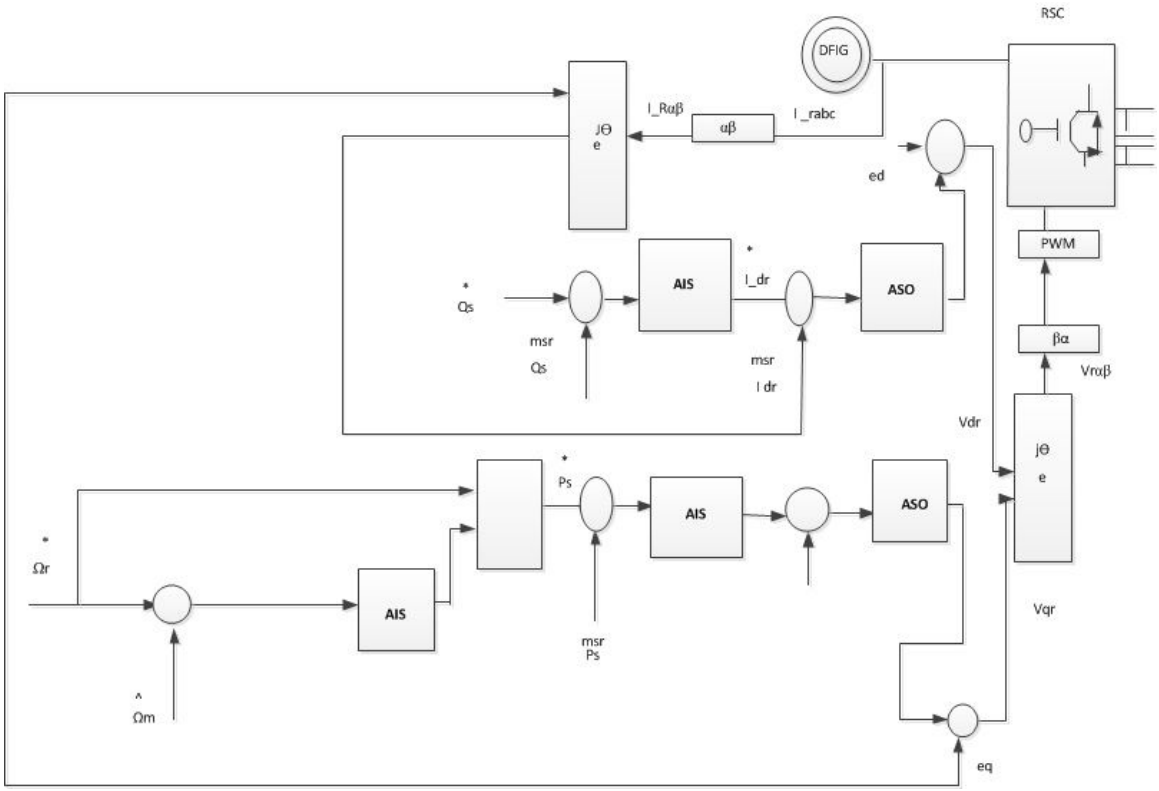

Figure 5.3: Block diagram of the overall RSC control scheme

Remark 5.1 *According to the previous results obtained by isidori, A multi variable nonlinear system in the form of (5.23) has a relative degreer*$_1, \ldots, r_m$ *at point* x^0 *if* $L_{g_j} L_f^k h_i(x) = 0$ *for all*$1 \leqslant j \leqslant m$, *for all* $1 \leqslant i \leqslant m$,*for all* $k \leqslant r_i - 1$, *and for all neighbour of*x^0.

The system has a defined relative degree $r = 2$.The relative degree with respect to the first and the second input are $r_1 = 1, r_2 = 1$ respectively. Now we compute the lie derivative of the output function

$$L_{g_1} h_1(x) = \frac{1}{\mathcal{T}\Lambda}, \quad L_{g_2} h_2(x) = 0 \tag{5.26}$$

$$L_{g_1} h_2(x) = 0, \quad L_{g_2} h_2(x) = \frac{1}{\mathcal{T}\Lambda} \tag{5.27}$$

Since the relative degree $r_1 = 1, r_2 = 1$ the decoupling matrix takes the form

$$M = \begin{pmatrix} L_{g_1} L_f^{r_1 - 1} h_1(x) & L_{g_2} L_f^{r_2 - 1} h_1(x) \\ L_{g_1} L_f^{r_2 - 1} h_2(x) & L_{g_2} L_f^{r_2 - 1} h_2(x) \end{pmatrix} = \begin{pmatrix} \frac{1}{\mathcal{T}\Lambda} & 0 \\ 0 & \frac{1}{\mathcal{T}\Lambda} \end{pmatrix} \tag{5.28}$$

Recalling from the non interacting control theory if the decoupling matrix is nonsingular then there is exists a static feedback control law in the form of

$$u = \alpha(x) + \beta(x) w \tag{5.29}$$

that solve the problem with

$$\alpha(x) = -M^{-1}(x) \begin{pmatrix} L_f^{r_1} h_1(x) \\ L_f^{r_2} h_2(x) \end{pmatrix} = \begin{pmatrix} x_1 - \mathcal{T}\Lambda x_2 x_3 \\ x_2 + \mathcal{T}\Lambda x_2 x_3 \end{pmatrix} \tag{5.30}$$

and

$$\beta(x) = M^{-1}(x) = \frac{1}{(\mathcal{T}\Lambda)} I \tag{5.31}$$

where I is the identity matrix. The imposition of the feedback yields a system characterized by

$$\dot{z}_{j,1} = z_{j,2}, \ldots, \dot{z}_{j,r_j-1} = z_{j,r_j} \tag{5.32}$$
$$\dot{z}_{j,r_j} = w_i \tag{5.33}$$
$$\dot{\eta} = q(z,\eta) + p(z,\eta)w \tag{5.34}$$
$$y_j = z_{j,1} \quad \forall j = 1,2 \tag{5.35}$$

Remark 5.2 *The zero dynamics of the system is described by*

$$\dot{\eta} = q(0,\eta) - p(0,\eta)M^{-1}(0,\eta)\alpha(x) = \frac{C_f}{J} x_2 \tag{5.36}$$

which can verify that the system is exponentially globally stable

Choosing the external control in the form

$$w = \begin{pmatrix} w_1 \\ w_2 \end{pmatrix} = \begin{pmatrix} -k_{1,1} z_{11} \\ -k_{2,1} z_{21} \end{pmatrix} \tag{5.37}$$

one obtain the dynamics

$$\dot{z}_{j,i} = z_{j,i+1}, \quad \forall i = 1, \ldots, r_{j-1} \tag{5.38}$$
$$\dot{z}_{j,r_j} = -kj,1 z_{j,1} + \cdots - kj, r_j z_{j,r_j}, \quad \forall j = 1,2 \tag{5.39}$$

where the coefficient $kj,1$ define Hurwitz polynomial.This property ensure the asymptotic output tracking of the required output behaviour.

5.4 AI MPPT algorithm

This section is dedicated to illustrate the novel of Artificial Immunity technique maximum tracking technique

5.4.1 Wind speed estimation

The traditional way of calculating the wind speed can be carried out using the data of wind turbine power,tip speed ratio and the pitch angle .A lookup table can be used to implement the inverse function.Nevertheless this method requires much memory space beside the calculation of the real-time nonlinear function roots may result in a complex and time consuming calculation.A solution for this problem is to use an Artificial Intelligent techniques, in particular Artificial Immunity (AI)technique is known to be very powerful tool due to its robustness and reliability.The wind estimation will be obtained through artificial immunity technique First the turbine mechanical power is calculated from the estimated DFIG speed given by Artificial Immunity System Estimator AISE .The reference electromagnetic torque of the DFIG is determine from the rotor speed controller (Figure5.3)and by taking into account power losses in the gearbox

$$W_m^* = gW_r^* \tag{5.40}$$

where W_m^* is the reference rotational speed of DFIG in rad/sec, g is the ratio of gearbox and W_r^* is the optimal speed of the turbine.

$$\hat{P_m} = T_{em}^{ref}\hat{W_m} + P_{loss,GB} \tag{5.41}$$

The $\hat{P_m}$is the estimated mechanical power, T_{em}^{ref} represent reference electromagnetic torque, while $\hat{W_m}, P_{loss,GB}$ represents the estimated DFIG rotor's speed and the power losses in the gearbox respectively.The wind speed estimated from the mechanical power provide the optimal DFIG rotor speed.

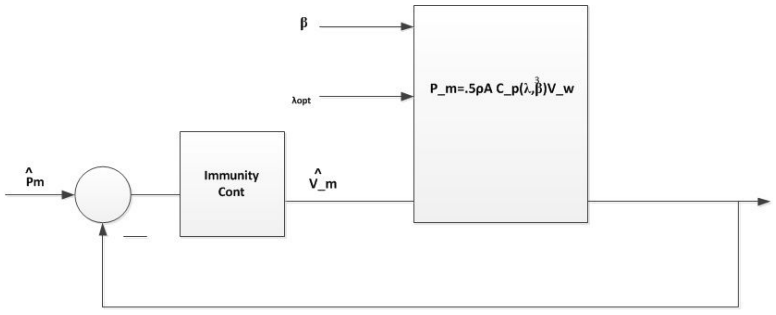

Figure 5.4: Artificial Immunity technique based wind speed estimation

5.4.2 DFIG rotor speed estimation

The proposed AISE observer consists of using an adaptive model and a reference model (MARS) in the closed loop scheme with an Artificial Immunity System (AIS). The AIS is used in order to reduce the error between the two models and provide the appropriate estimated rotor speed.The concept of colona selection was used to build the AI technique.The Colona System Pattern explains the immune response when an

antigenic pattern is recognized by a given antibody. In the clonal selection algorithm, the antigen (Ag) represents the problem to be solved (estimated speed), while the antibodies (Abs) are the candidate solutions of the problem. The antibody-antigen affinity indicates as well the matching between the solution and the problem. The algorithm performs the selection of antibodies based on affinity either by matching against an antigen pattern or by evaluating the pattern via an objective function.The data used to train the system is based on the fuzzy technique applied in .The overall AISE is shown in Figure5.4, 5.5 while the Artificial technique concept is shown in Figure5.6.The Colona System Pattern explains the immune response when an antigenic pattern is recognized by a given antibody. In the clonal selection algorithm, the antigen (Ag) represents the problem to be optimized and its constraints, while the antibodies (Abs) are the candidate solutions of the problem. The antibody-antigen affinity indicates as well the matching between the solution and the problem. The algorithm performs the selection of antibodies based on matching against an antigen pattern.The reference model is refereed in the previous section To achieve a power decoupling control, the vector control strategy is adopted, with a stator field orientation on the d-axis (λ_d is set to zero).As a consequence the q axis rotor current can now be rewritten as function of the stator current.

$$i_{rq} = \frac{L_s}{M} i_{sq} \tag{5.42}$$

The estimated rotor voltage used to build the adaptive model is defined as

$$\hat{v_{rq}} = -\frac{R_r L_s}{M} i_{sq} + (M - \frac{L_s L_r}{M}) \frac{di_{sq}}{dt} + \hat{W}_r((\frac{L_r}{M}\lambda_{sd}) + (M - \frac{L_s L_r}{M} i_{sd})) \tag{5.43}$$

In this paper MRAS observer,Artificial Immunity system are used to estimate the rotational speed of the DFIG $\hat{w_r}$ After estimating the rotor electrical angular velocity, the rotational speed of DFIG is estimated using the electrical frequency us throughout PLL (phase-locked loop).

5.4.3 Proposed sensorless MPPT algorithm

A sensorless MPPT solution based on the Artificial Immunity technique is introduced.The estimation of the overall power losses in the wind turbine generator and the estimated wind speed (shown in Figure 5.7) are used to provide the optimal value of power coefficient.The structure of AI MPPT is show in fig(5.8).The data used to train the system was provided from artificial fuzzy technique.The idea in simple term is that the system collect the input data and deal with it as an antigen.The data is then compared to the different scenarios , when a match is detected then the value of MPPT is determined. The main advantage of this sensor less AI MPPT is that it reduces the size of PWM back-to-back converter while tracks the maximum power point which reduces the overall system costs.Firstly, for the adopted MPPT algorithm, the optimal value of the power coefficient by taking into account the power losses is expressed as

$$c_p^{opt} = \frac{p_{losses} + p_{rated}}{2\rho A \hat{v_m}^3} \tag{5.44}$$

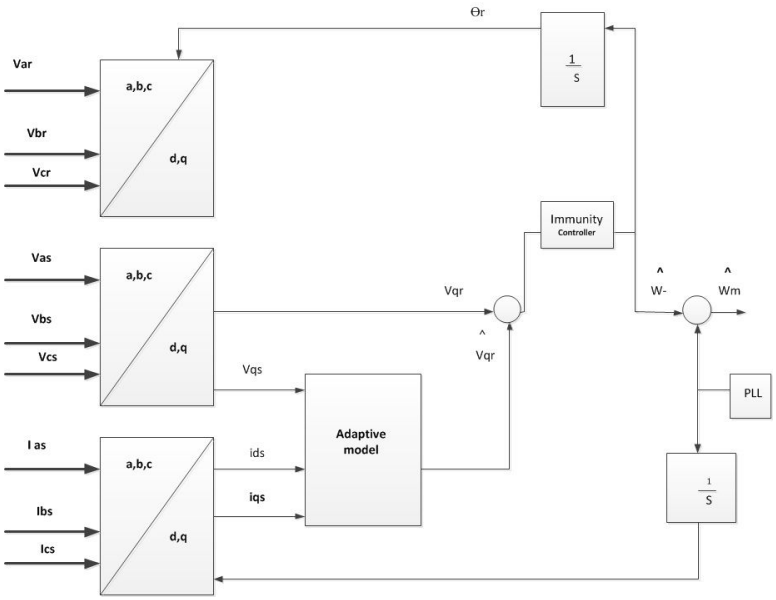

Figure 5.5: Artificial Immunity technique based wind speed estimation

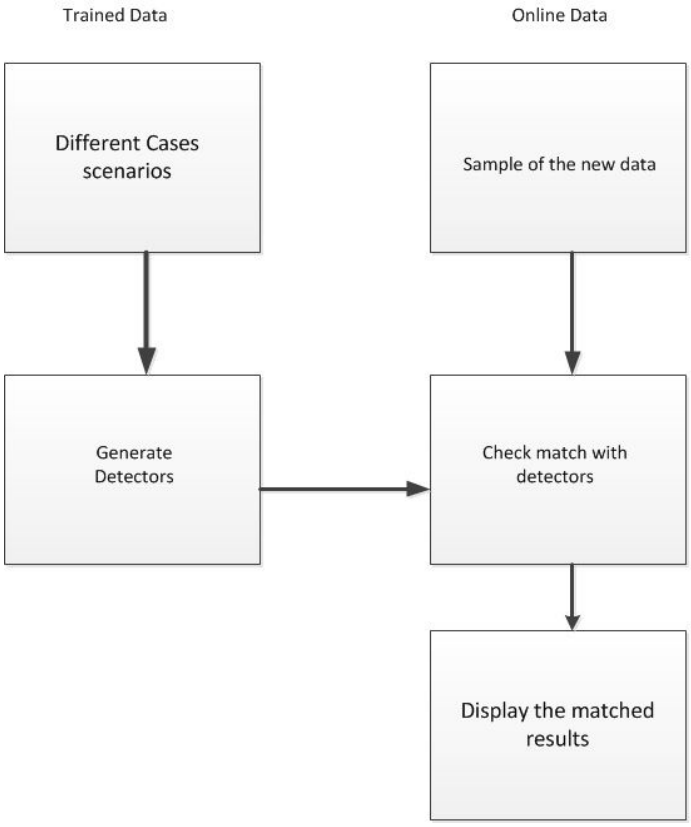

Figure 5.6: Detailed model of artificial immunity technique based wind speed estimation

where c_p^{opt}represents the optimal power coefficient to extract the maximum wind power,$\hat{v_m}$ is the estimated wind speed,p_{rated} is the the rated output power of DFIG.p_{losses} represents the estimated power losses.The AI MPPT algorithm calculate the value of the optimal ratio λ_{opt} which provide the optimal value of the power coefficient according to the estimated wind speed.The mathematical representation of the Cp curves is given $c_p = 0.398\sin(\frac{\pi(\lambda-3)}{15-.3\beta} - .0039(\lambda-2)\beta$ while the optimal generator reference speed W_r^* for maximum wind power tracking is determine from $W_r^* = \frac{\lambda_o pt\hat{v_w}}{R}$.The AI MPPT controller has been programmed in c code using an embedded MAT LAB function in MATLAB SIMULINK software there for a hardware implementation can be achieved using micro controller.

Figure 5.7: Calculation of optimal power coefficient

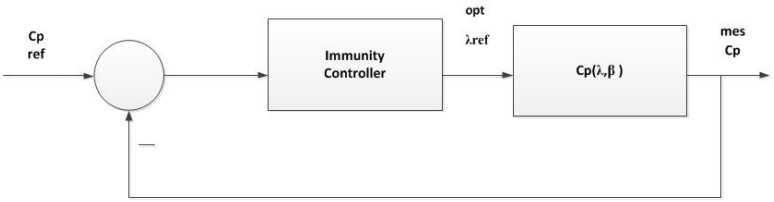

Figure 5.8: Structure of the AI MPPT

5.5 simulation and Results

This section is dedicated to the evaluate the performance of the proposed technique. The introduced approach method has been applied to a wind turbine generator driving a 3.7 kW. The MAT LAB program was used to emulate the wind variation and to compare the proposed AI MPPT with the conventional and fuzzy logic methods. It was also used to test the performance of the nonlinear technique. The parameter used to evaluate the performance and the effectiveness of the proposed technique

are shown in Table 1. The measured and the estimated wind speed are shown in Figure 5.9. The performance of the AISE is shown in Figure 5.10. It can be noticed that the tracking error less than 3%. The DFIG rotor speed estimation is illustrated in Figure (5.11,5.12), where the direct and quadratic rotor current and voltage of DFIG are shown respectively. To evaluate the ability of nonlinear technique to track the direct and quadratic rotor currents reference signal generated from the AIS controller (Figure 5.11) .It can be noticed from Figure 5.12 that the proposed control technique succeeded in reproducing a current signal that coincides with the required reference signal in both cases. Figure 5.13 illustrates the wind speed behavior at different time (i.e usually called wind speed profile). In order to analyse the effectivness of the proposed controller, a classical PID control is applied and simulated via MAT LAB using the same parameters. Figure 5.14 depicts the Maximum Power Point Tracking curves conducted from classical PID controller and new AI MPPT. The results indicate a slower dynamic variation of the rotor speed in the AI MPPT algorithm compared to the conventional one. The system behaviours which are illustrated in Figures 5.9 -5.16, are detected versus time (in seconds).

Moreover the performance of the proposed technique was compared to the Fuzzy logic controller . The fuzzy log model was also build on MATLAB . The results shown in Figure 5.15 proves that the AI MPPT provide better performance than both the Fuzzy Logic Controller and the conventional one. With the introduced AI MPPT strategy, the slip which is proportional to the size of power converters is reduced. Then, the power converters can be downsized without reducing the output power which leads to the reduction in both the cost and maintenance of the overall system by reducing the size of the back-to-back converters. Figure 5.16 shows the comparison of the optimal tip speed ratio of both MPPT strategies. The execution time generated from all techniques are illustrated in Table 2. Even though the execution time of fuzzy controller and conventional methods are less than the AIS. On the other hand the results generated from AIS in terms of tracking MPPT proved to be smoother and more reliable. Finally, since the executed time is considered sufficient, the c code used to build these models could be used in micro-controller applied in hardware implementation.

Table.1 The DFIG data sheet

The DFIG data of a typical 3.7 Kw generator	
Frame / power	3.7 Kw
Efficiency at rated speed	appr. 97...97.5
Voltage	690 V
Locked rotor voltage	approx. 1000 V
Operation speed range	1000...2000 rpm
Power factor	p.f. 0.90 cap ...1.0
Rotor Resistance	1 K Ω
Rotor Inductance	.2 mH
Stator Resistance	0.5 K Ω
Stator Inductance	.001 mH
Mutual inductance	Msr= 0.078 H
Number of poles	4
Inertia moment	j=0.3125 Nms2

Figure 5.9: Wind speed estimation.

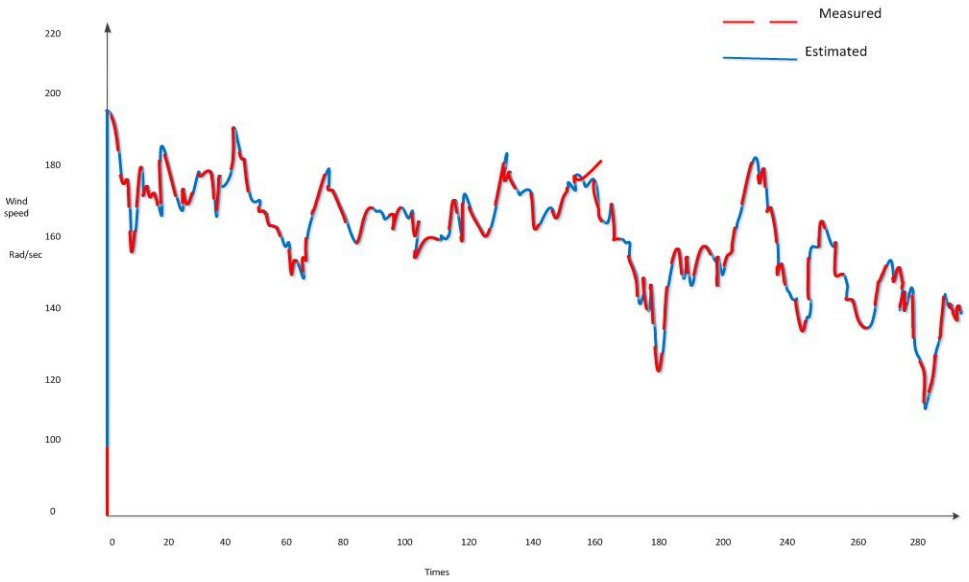

Figure 5.10: DFIG rotor speed estimation performance using AISE

Table.2 MAT LAB execution time for different techniques

Execution Time	
Fuzzy MPPT controller	14.11 second
Conventional Method	10.333 second
AIS MPPT	11.66 second
AISE	13.22 second
ASO	2.72 second
Total AI time	appr 23 second

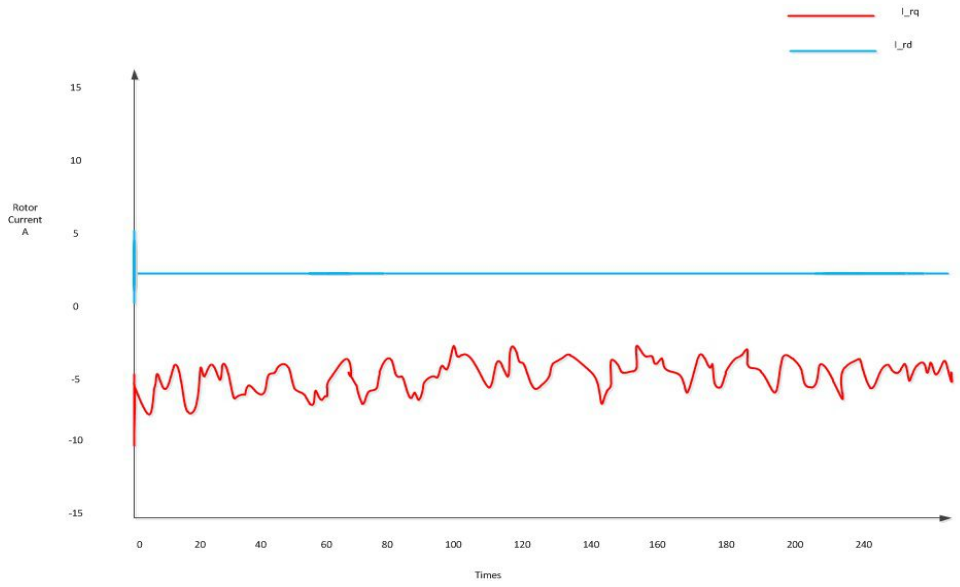

Figure 5.11: DFIG rotor current

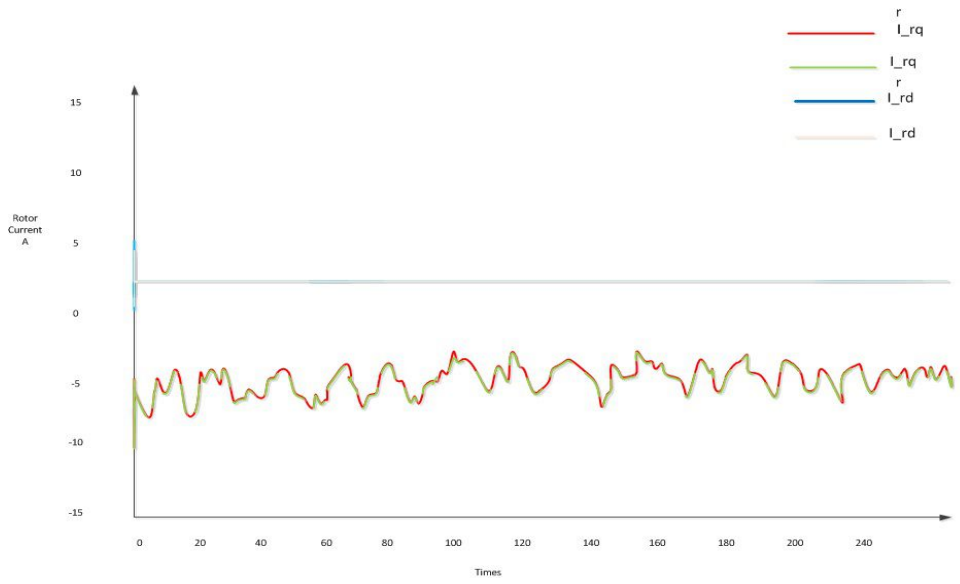

Figure 5.12: ASO traking rotor current

5.5.1 Second Case

In this section we study the effect of the doubly fed induction generator when it's connected to the grid

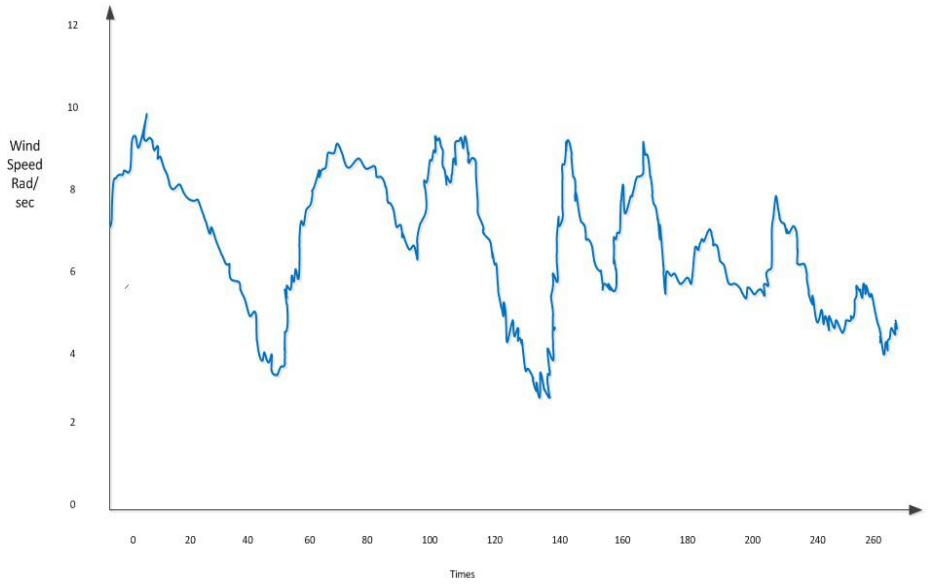

Figure 5.13: Wind speed profile.

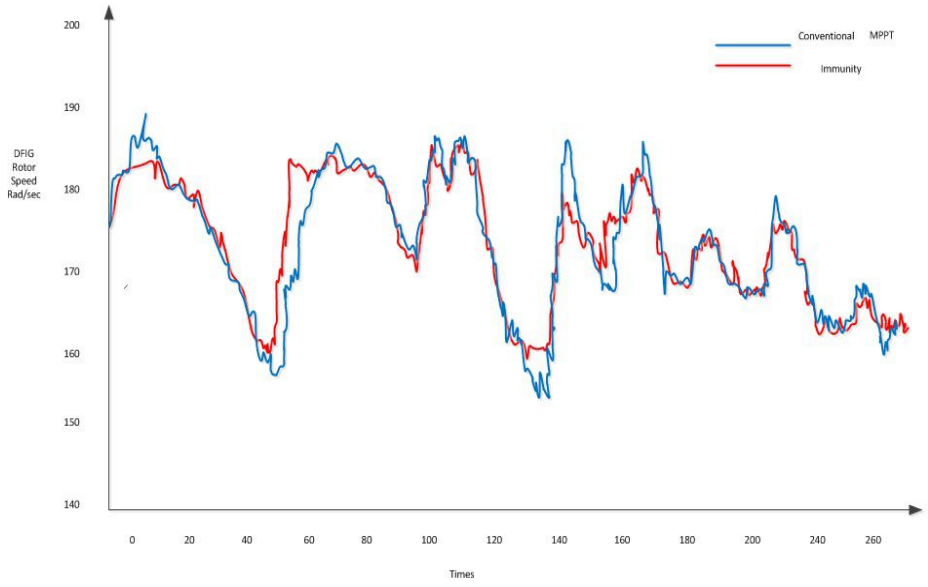

Figure 5.14: Comparison of DFIG rotor speed for classical and our design MPPT strategies.

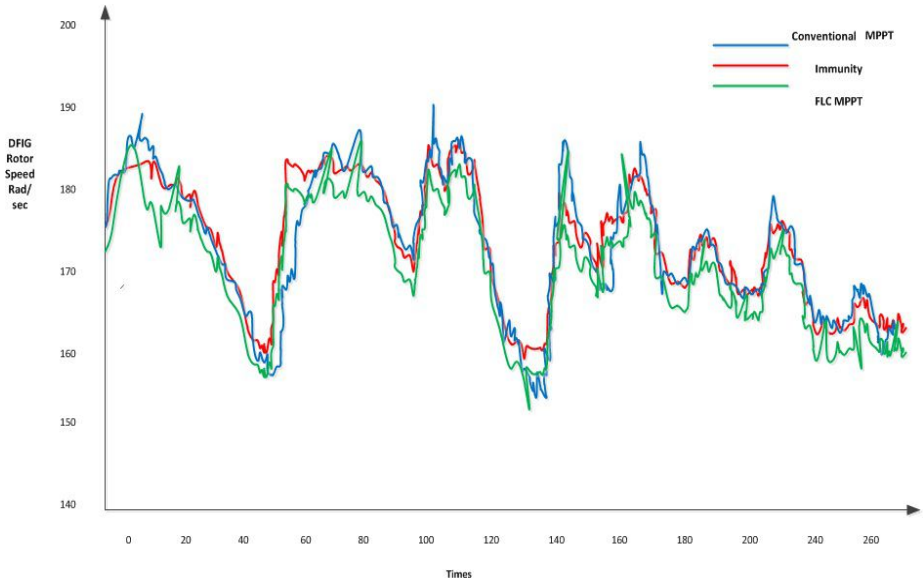

Figure 5.15: Comparison of DFIG rotor speed for different types of MPPT strategies.

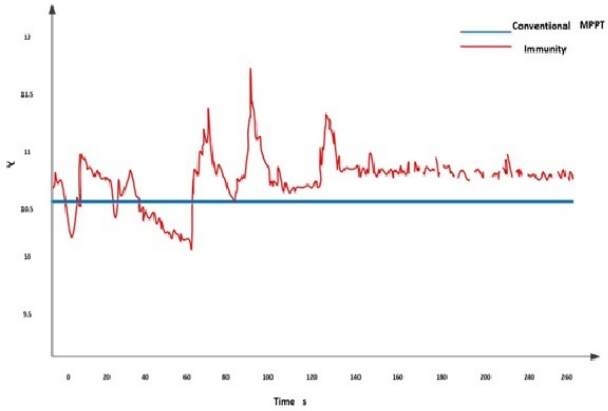

Figure 5.16: Comparison of TSR for different types of MPPT strategies.

5.5.2 Grid Side Converter command model

$$v_{fd} = R_f i_{fd} + L_f \frac{d}{dt} i_{fd} - W_r L_f i_{fq} - V_{Gd} \tag{5.45}$$

$$v_{fq} = R_f i_{fq} + L_f \frac{d}{dt} i_{fq} + W_r L_f i_{fd} - V_{Gq} \tag{5.46}$$

$$\dot{i}_{fd} = \frac{1}{L_f}(-R_f i_{fd} + v_{fd} + W_r L_f i_{fq} + V_{Gd}) \tag{5.47}$$

$$\dot{i}_{fq} = \frac{1}{L_f}(-R_f i_{fq} + v_{fq} - W_r L_f i_{fd} + V_{Gq}) \tag{5.48}$$

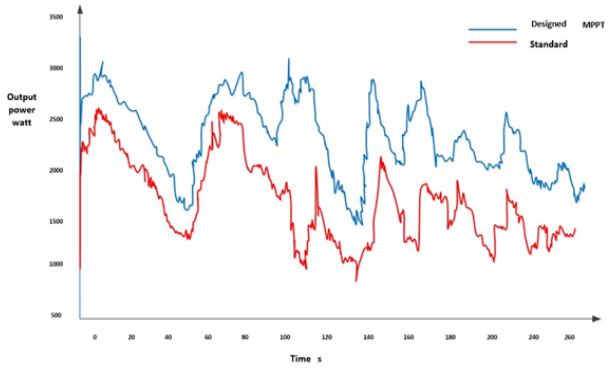

Figure 5.17: The difference between DFIG output power in both standard and MPPT cases.

with V_{Gd}, V_{Gq} indicated the input voltage of AC-DC converter in the direct and quadrature frame.The electric network components of voltage and current on the AC side for both the direct and quadrature frame are given by v_{fd}, v_{fq}, i_{fd} and i_{fq} respectively, while the L_f referred to the inductance of the system. The active and reactive power are expressed as:

$$P = V_{Gd} i_{fd} + V_{Gq} i_{fq} \tag{5.49}$$

$$Q = V_{Gq} i_{fq} - V_{Gd} i_{fd}. \tag{5.50}$$

Remark 5.3 *Through setting the power factor to be* 1 *and neglecting the filter losses one can get the following expression* $V_{Gd} = V_{fd} = V_G, \quad V_{Gq} = V_{fq} = 0$, *leading the active and reactive power to be* $P_f = V_G i_{fd} and Q_f = -V_G i_{fq}$.

5.5.3 Non linear grid side converter model

Referring to 5.3 we know that through setting the power factor to unity we get $V_{Gd} = V_{fd} = V_G, \quad V_{Gq} = V_{fq} = 0$.In such a case the system is converted into single input-single output system in the form:

$$f(x) = \begin{pmatrix} -\frac{R_f}{L_f} x_1 + x_3 x_2 \\ -\frac{R_f}{L_f} x_2 - x_3 x_1 \\ -\frac{f_r}{J} x_3 - \frac{p}{J} \phi_{rd} x_2 \end{pmatrix}, \quad g(x) = \begin{pmatrix} \frac{2}{L_f} \\ 0 \\ 0 \end{pmatrix} \tag{5.51}$$

$$y = x_1. \tag{5.52}$$

where, x:state vector$=[i_{fd} \quad i_{fq} \quad W_r]^T$,$U = [u_1 \quad u_2]^T$.

5.5.4 Non linear modelling and Control of the direct axis control

In this part the focus will apply the asymptotic output tracking technique in the direct axis reference filtered current.The system has a well define relative degree $r = 1$. Consequently one can apply a coordinate transformation in the form $\Gamma(x) = \begin{pmatrix} x_1 \\ x_3 \\ x_2 \end{pmatrix}$.
The state space description in the new coordinates

$$\begin{cases} \dot{z}_1 = a(z,\eta) + b(z,\eta) \\ \dot{\eta}_1 = \frac{f_r}{J}\eta_1 - \frac{p}{J}\phi_{rd}\eta_2 \\ \dot{\eta}_2 = -\frac{R_f}{L_f}\eta_1 - \eta_2 z_1. \end{cases} \tag{5.53}$$

Remark 5.4 *The system has a stable zero dynamics. In fact by calculating the jacobian matrix Q which describes the linear approximation at $\eta = 0$ of the zero dynamics of the original nonlinear system*

$$Q = \begin{pmatrix} \frac{f_r}{J} & -\frac{p}{J}\phi_{rd} \\ -\frac{R_f}{L_f}b & 0 \end{pmatrix} \tag{5.54}$$

we can see that the matrix is nonsingular.Hence the zero dynamics is asymptotically stable.The stability of the zero dynamics will depend on the parameters of the DFIG.

The stator of the DFIG was directly connected to the grid while its rotor was connected to it via a cascade (Rectifier, Inverter and Filter).In order to evaluate the grid side model the power factor was set to one , thus only the direct rotor current will be produced.The voltage on the output of the inverter will suffer from disturbance signals formed by the original of frequency $f = 50$Hz and other signals.A passive R-L filter was used to eliminate harmonics.The input in the form $u = \frac{1}{a(z,\eta)}(-b(z,\eta) + c_0 z_1))$ ensures the reproduction of an output i_{rd} that will track the required reference signal.Figure depict 5.20 that the system nonlinear controller has reproduced an output that will converge asymptotically to the required reference signals and minimizes the effect of disturbance.

5.5.5 Feedback design under sampling

We now address the problem of preserving under system behaviour under sampling.In fact, considering $u(t) \in U_T$ and $y(t) = y(kT)$ for $t \in [kT, (k+1)T[$(T the sampling period).Now we compute the single-rate sampled data equivalent model of (5.51)

$$x_{k+1} = F^T(x_k, u_k) \tag{5.55}$$

$$y_k = h(x_k) \tag{5.56}$$

with $xk := x(kT), yk := y(kT), uk := u(kT), h(x) = i_{rd}$ and $F^T(xk, uk) = eT(Lf + ukLg)x_K$.In this case we compute a digital control law

$$u_d = u(kT) + Tw_{1k} \tag{5.57}$$

which solve the problem

5.5.6 Results of simulation

The wind speed and the DFIG are shown in figures (5.18,5.19) while the rotor current are shown in figure(5.20).Figures (5.21,5.22) depict simulations of the aforementioned situations.It can be shown that sampled-data design provided better results i.e, the variation is smoother and the transient time is less than the emulated one).In addition the results of the the tip speed 5.5.6 has been reduced by more than 2% compared with the emulation design which indicate that the size of power converters is reduced.Then, the power converters can be downsized without reducing the output power.

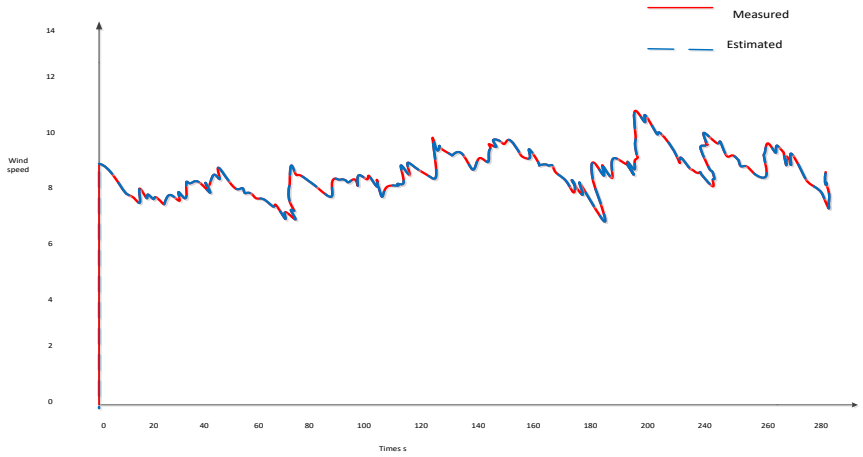

Figure 5.18: Wind speed estimation.

5.6 Conclusion

In this chapter we studied a wind speed estimation based on sensorless maximum power extracting for a variable speed Wind Turbine Generator system .Two case studies were developed.The first case study the wind turbine stands alone while the second case study the system when the rotor side is connected to grid.The main focus was to study the effect of modeling in the system.
The advanced control consists of two parts: the first part based on the Artificial Immunity Maximum Power Point Technique AI MPPT while the second part is based on the Input Output decoupling with asymptotic tracking technique. A significant advantage of the proposed intelligent controller is that it generates the same electrical power as the classical MPPT method, as it reduces the size of the power converter. The nonlinear control technique ensures the reproduction of the rotor direct and quadratic current that converge to the reference signal generated from the Artificial Immunity controller.The wind speed estimation is executed through

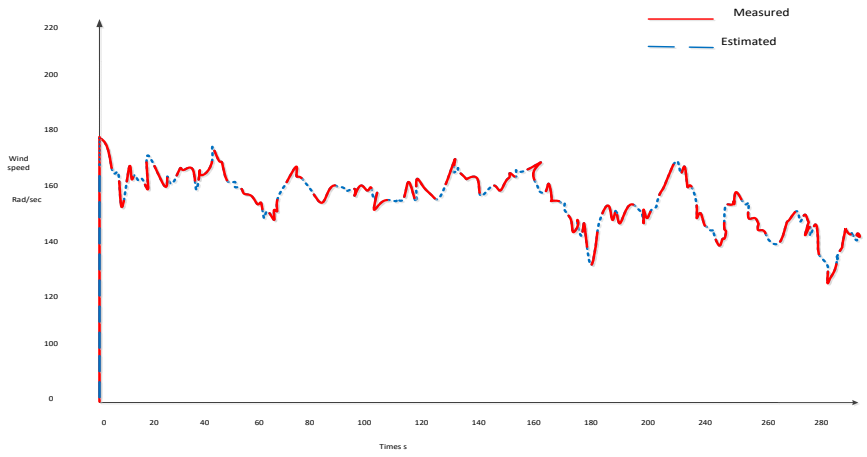

Figure 5.19: DFIG rotor speed estimation performance using AISE

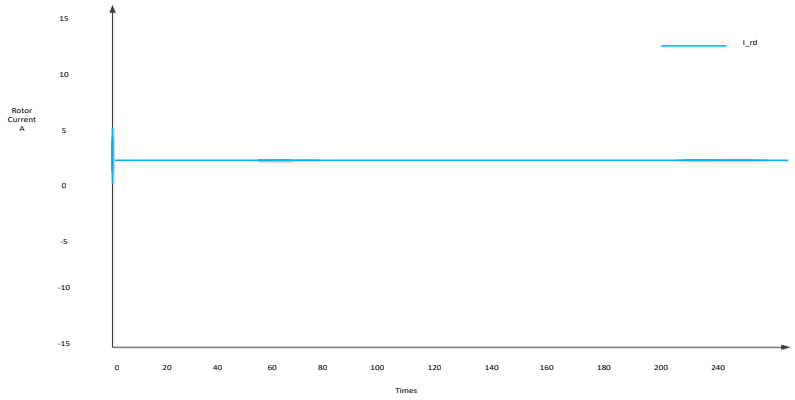

Figure 5.20: DFIG rotor current

two operations: First, the mechanical power is estimated via the DFIG rotor speed adaptive model and the electromagnetic reference, then the Artificial Immunity controller uses the estimated mechanical power values of the generated wind speed. The MatLab program is used to simulate and test the proposed technique. The simulation results of AI MPPT show that this approach has better performance compared to the classical method and the fuzzy logic technique that uses both output power and estimation of the overall power losses. The results of the nonlinear controller succeeded in reproducing an output signal that coincides with the required refer-

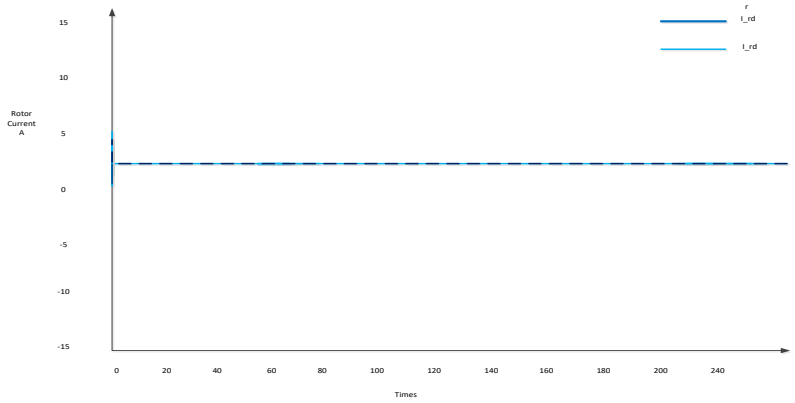

Figure 5.21: Nonlinar control applied to rotor current

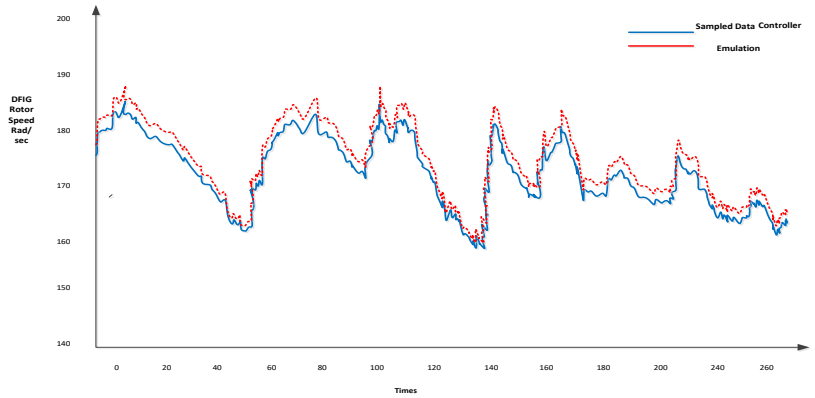

Figure 5.22: DFIG rotor speed for MPPT

ence signal. It was also shown that the system has a compelling performance under disturbance such as the wind variation. The AI controller has been programmed in c code using embedded MATLAB function in MATLAB (Simulink) software; therefore, the hardware implementation can be applied using the micro-controller. The DSPIC33FJ64MC706A-I pic could be used to build the nonlinear controller and AI MPPT.

The second case was developed on the base of wind system connected to grid. The sampled -data control techniques discussed in this thesis have been used as a

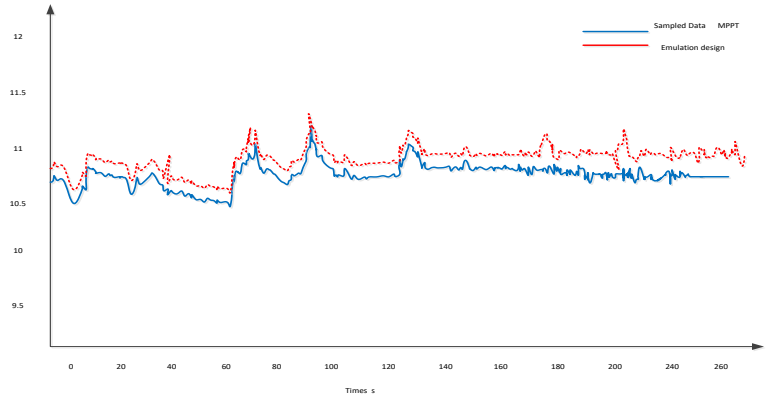

Figure 5.23: Tip Speed Ratio for MPPT .

suggested solution to the MPPT problem.The obtained results indicate better results than the direct implementation of continuous time design.Further investigation could be carried out in the future .

Part II
AI and Nonlinear design

Chapter 6

Other works

2015 IEEE International Conference on Smart City/SocialCom/SustainCom together with DataCom 2015 and SC2 2015

Traking and Controlling Maximum Power Point Utilizing Artificial Intelligent System

Marwa Ahmed Abd El Hamied
University of Rome La Sapienza
Roma, Italy
Marwa.hassan@uniroma1.it

***Abstract*—In this paper In this paper, a new technique based on Artificial Immunity System (AIS) technique has been developed to track Maximum Power Point (MPP). AIS system is implemented in a photovoltaic system that is subjected to variable temperature and insulation condition. The proposed novel is simulated using Mat Lab program. The results of simulation have been compared to those who are generated from Observation Controller. The proposed model shows promising results as it provide better accuracy comparing to classical model.**

Keywords—component; Artificial Immunity Technique; solar energy; perturbation and Observation; Power based methods.

I. INTRODUCTION

Due to several factors such as: instability in oil and gas prices. Also with the call of defenders of the environment to reduce pollution that cause global warming effect. The search for clean and reliable energy source becomes more essential. Solar energy history spans from the 7th Century to today. Even though multi mega watt Photovoltaic (PV) system start to be planted all over the world, the efficiency of energy conversion still consider insufficient. The output of (PV) cells various according to multiple conditions [1]. As shown from figure.1 the maximum efficiency can be obtained only at P max.

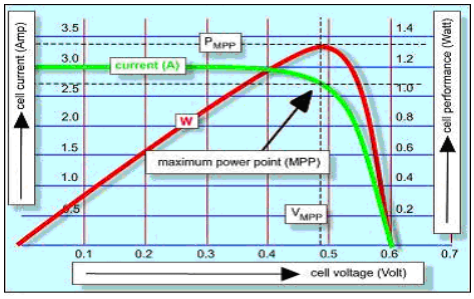

Fig.1. PV and load characteristics [2]

In order to increase this efficiency, MPPT controllers are used. Such controllers are becoming an essential element in PV systems.

A significant number of MPPT control schemes have been elaborated since the seventies. The most famous techniques are: a) Current feedback based methods b) Voltage feedback based methods c) perturbation and observation (P&O) [3].

In this paper a new developed method based Artificial Immunity system (AIS) is used to determine MPPT point. Perturbation and observation (P&O) controllers used to provide experimental results. The results are used in building and testing the proposed model. The proposed model provides very powerful results and proves to be a reliable

II. PERTURBATION AND OBSERVATION CONTROLLER

The controller main function is to manipulate pulse width modulation PWM duty cycle. According to the output PV curve the controller take the decision whether to increase or decrease PWM. Figure 2 explain the classical operation of perturbation and observation controller. It operates by perturbing the voltage of PV array. If the instant power P (k) is greater than the previous perturbation cycle P (k − 1), then the direction of perturbation is maintained otherwise it is reversed. This algorithm has two major disadvantages. First in case of small increment between two measurement points, the system will have very slow reaction. Second a larger increment will make the algorithm more reactive but inaccurate [4].

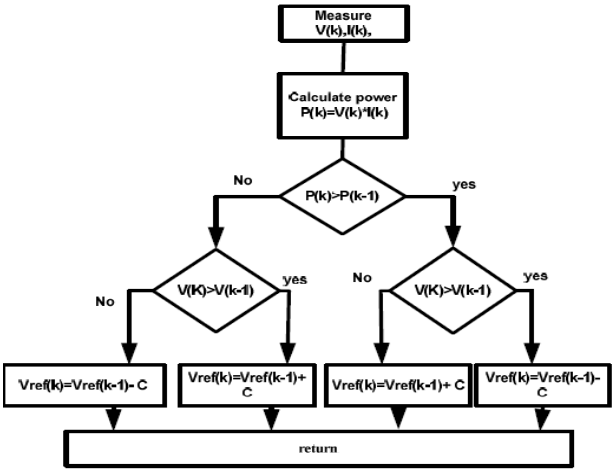

Fig.2 Flow chart of perturbation and observation (P&O) [3]

978-1-5090-1893-2/15 $31.00 © 2015 IEEE
DOI 10.1109/SmartCity.2015.133

v (k) Instant Voltage

I (k) Instant Current

P (k) Instant power

The results obtained from the controller are going to provide reference to test proposed model.

III. DEVELOPED MPPT CONTROLLER

The proposed model is build using Artificial Immunity System (AIS). Through the years many researchers have been developed in Expert System field.

Artificial Neural Networks, fuzzy logic, genetic algorithms and immunity system are being widely used in industrial applications [5]-[9]. Artificial Immune Systems (AIS) are adaptive systems, inspired by theoretical immunology and observed immune function. It can be used in various applications such as: pattern recognition, self organization and anomaly detection [10].

The immunity system composed of a range of cells and molecules that work together with other systems .The idea based on when antigen enter body (it infect the cell, activation T lymphocytes this cause activation of B cell) it try to bind with B cell (antibody) through receptors with affinity (the strong affinity will be taken) then it form plasma cell that made colonel expansion and convert into memory cell, when the same antigen enter the body again memory cell will identify it , shown in Fig. 3).

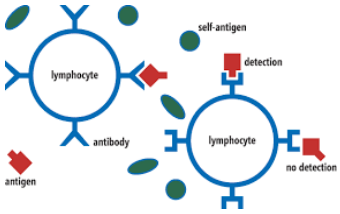

Fig.3 Immunity System [11]

Maximum power Point results obtained from Perturbation and observation controller is used to form a database structure for AIS. All calculated value is stored an array to form antibody. When the program received new values it compared it with the stored cases. Figure.4 illustrated the algorithm in form of flowchart.

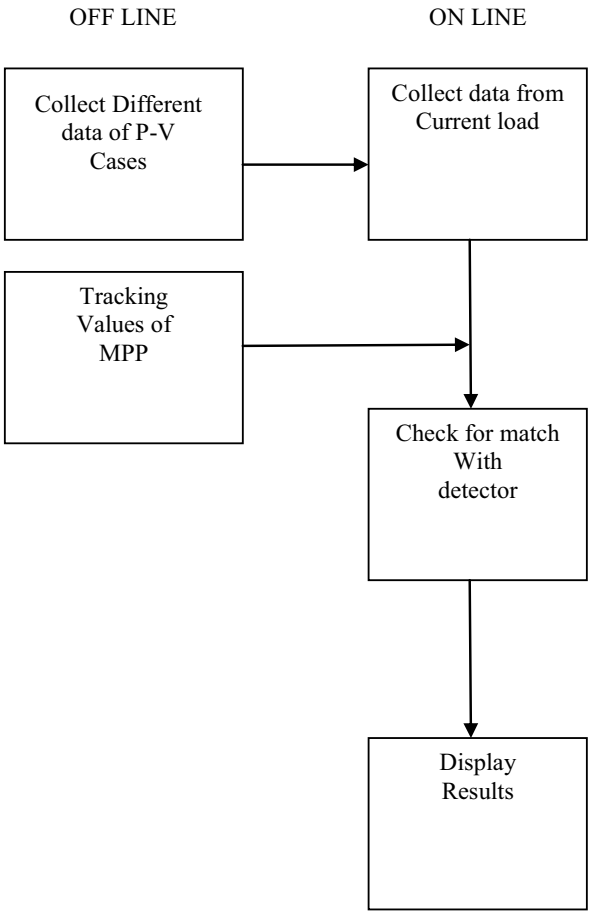

Fig.4 Flow chart of Artificial Immunity System

IV. SIMULATION AND RESULTS

The research work is progressed and implemented in a PC. The proposed system is realized in form of three main stages. The stages are described in the following block diagram of Fig.5.

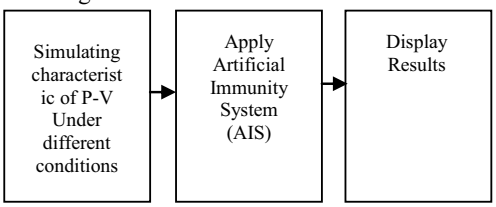

Fig.5 The main stages of developed technique

Stage1 Apply different conditions to the load and implement PV characteristics

Stage 2 A new developed AIS technique is developed to predict Maximum Power Point MPP

Stage 3 Display Result and take discussion whether to change the direction of PV cell or not to achieve maximum output.

The AIS technique is being tested under these conditions as follows:

[1] Variation of panel under standard conditions: insulation 1000 W/m2 and temperature of 25 °C

[2] Apply a rapid change in insulations conditions from 1000 to 800 W/m2 at 25 °C

Figure 6and 7 shows the results obtained by AIS. Each figure illustrate: a) Power signal in watt b) Battery signal c) Control Signal

Obviously, it can be deduced that the AIS controller is faster than the P&O controller in the transitional state

Case1

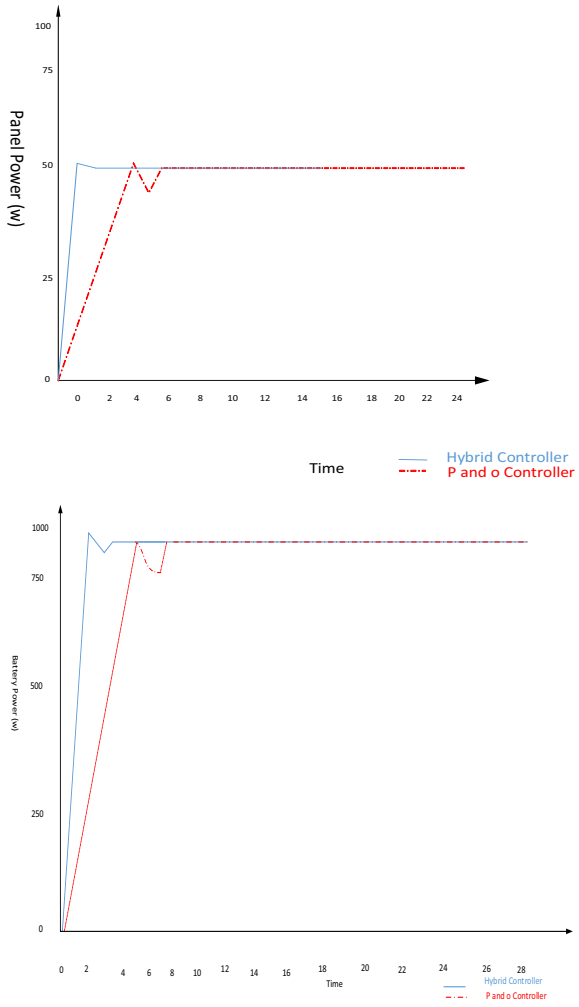

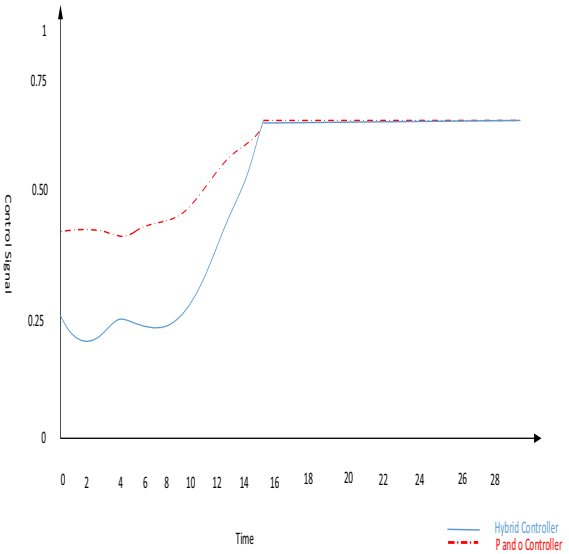

Fig. 6 Variation of the panel power, battery power under standard conditions: temperature (25 °C) and solar insulation (1000 W/m2)

Case 2:

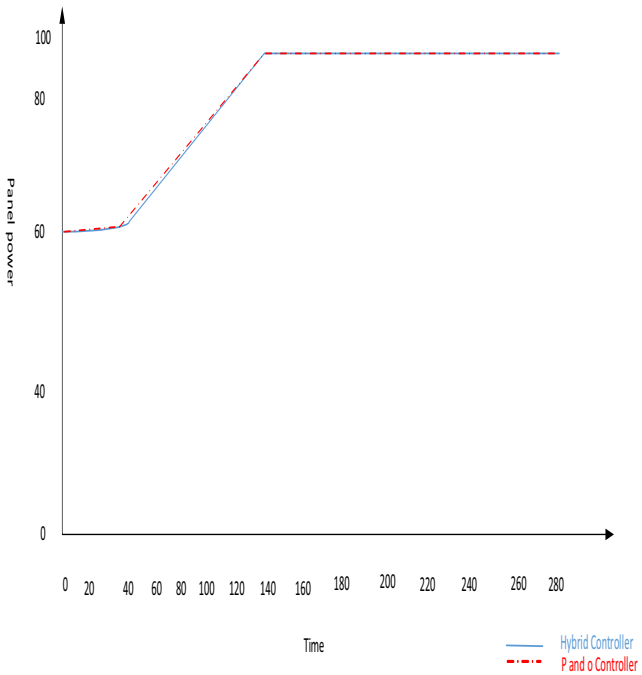

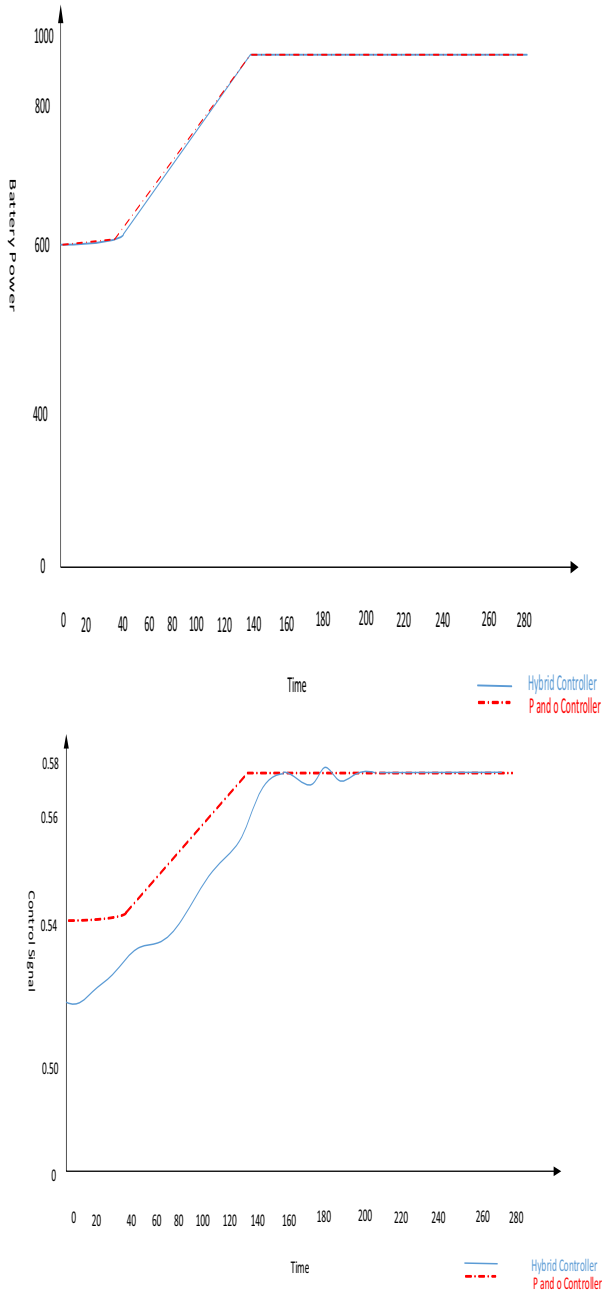

Fig. 7 MPPT controller responses: for a slow (120 s) solar insulations increase (800 W/m2 to 1000 W/m2 at 25 °C)

V. CONCLUSION

There is no doubt that the need for a new source of clean and reliable of energy is required. Through the years a quite number of researches have been developed in solar energy field. The researched aimed to improve the efficiency of Photovoltaic System panel by generating maximum power.

In this paper artificial immunity system is developed. The system AIS technique determine with advanced information encoding and adjustable rules Maximum Power Point MPP.

Artificial Immunity System succeeded to prove high flexibility and accuracy. The work is processed using Mat Lab. The execution time in micro seconds which form a great advantage. A small execution time allows the MPPT controller to be implemented in real sites.

The perturbation and observation (P&O) MPPT controller is used to provide results in order to train and test proposed model. Photovoltaic panels are being tested under different conditions by varying temperature and insulations.

The newly approach succeeded in providing reliable results and provide better results in some cases. The results obtained in this work can be used for tracking Maximum Power Point.

References

[1] Miro Zeman, Solar sell . 2rd ed, vol 2. Delft University of Technology: Photo voltic system2011, pp9.1-9.17

[2] Internet Website:
http://www.engineering.com/SustainableEngineering/RenewableEnergyEngineering/SolarEnergyEngineering/Photovoltaics/tabid/3890/Default.aspx

[3] H. Knopf, 'Analysis, Simulation and Evaluation of Maximum Power Point Tracking (MPPT) Methods fora Solar Powered Vehicle', Master Thesis, Portland State University,2012.

[4] H. Radwan, O. Abdel-Rahim, M. Ahmed," Two Stages Maximum Power Point Tracking Algorithm for PV Systems Operating under Partially Shaded Conditions",research gate , Vol.10,2009, pp 683-688.

[5] M. ursino, C. Cuppini, E.Magasso , "Neurocompetinonal approach to modeling multisens ory integration in the plane", Elsevier, Volume 60, December 2014, PP 141-165.

[6] R. Gessing, "Whether the opinion about superiority of fuzzy Controllers is justified", Bull. Pol. Ac.: Tech. Vol.1, 2010, PP59–65.

[7] S.A. Kalogirou, "Artificial intelligence for the modeling and control of combustion processes: a review", Progress in Energy and Combustion Science 29, 2003, PP 515–566.

[8] Simon,". Evolutionary Optimization Algorithms: Biologically-Inspired and Population-Based Approaches to Computer Intelligence", Hoboken: Wiley, 2013.

[9] Kephart, J. O., "A biologically inspired immune system for computers", Proceedings of Artificial Life IV: The Fourth International Workshop on the Synthesis and Simulation of Living Systems, MIT Press, pp. 130–139.

[10] Andrew Watkins and Jon Timmis, "Artificial Immune Recognition System AIRS: An Immune-inspired Supervised Learning Algorithm", Journal, Genetic Programming and Evolvable Machines, Vol. 5, issue 3, September, 2004.

[11] J. Maccfary, " Artificial Immune System for Intrusion Detection", MSDN magazine, January 2013.

Available online at www.sciencedirect.com

ScienceDirect

Procedia Computer Science 95 (2016) 507 – 515

Procedia Computer Science

Complex Adaptive Systems, Publication 6
Cihan H. Dagli, Editor in Chief
Conference Organized by Missouri University of Science and Technology
2016 - Los Angeles, CA

Permanent Magnet Synchronous Generator Stability Analysis and Control

Marwa A. Abd El Hamied [1*], Noha H.El.Amary[2]

[a]*Sapienza University ,Rome,Italy*
[b]*Arab Academy,Cairo,Egypt*

Abstract

In this paper a theoretical approach has been developed to address the stability problem of permanent magnet synchronous generator (PMSG). It is used because of great advantages such as reliability and effectiveness. The proposed technique is obtained through three stages. First stage is to apply linear approximation to the original system. The second stage is to obtain the transfer function in Laplace domain. The last stage is to separate the unstable zero from the original system. Once it's separated a suitable feedback will be designed to treat the instability phenomena. The proposed technique is simulated and tested using Mat Lab program. The results show that the developed approach proof to be a powerful tool for controlling the permanent magnet synchronous generator

Keywords: Permanent Magnet Synchronous Generator (PMSG); Stability Analysis ; Nyquist plot; PID control; Micro turbine; Multi input, Multi output system.

1. Introduction

Due to the great cost of power generation in economical and environmental sides, it became necessary to benefit from all accessible resources. Micro turbine introduces a very powerful solution for remote sites located far from the utility. It used variable speed wind turbine to create an autonomous system. Micro turbine system help avoid the

*Corresponding author. *Email: marwaahmed404@gmail.com*

doi:10.1016/j.procs.2016.09.328

high costs of having utility power lines extended to a remote location add to that it has zero emission and pollution in the environment. It also helps uninterruptible power supplies ride through extended utility outages [1]-[3]. Permanent Magnet Synchronous Generator (PMSG) forms an important role as a main component of wind turbine. The wind is fed as an input to the generator at variable speeds. According to the input varies the output electricity. Permanent magnet synchronous generator offers a variety of advantages such as: reliability, compact size, loss reduction, higher power density and finally optimal efficiency [4]-[6]. In the last decades a lot of researches have been introduced in the control area of Permanent magnet synchronous generator. In 2006 Kenji Amei and his colleagues introduces a quite interesting solution to generate electricity at maximum point. The paper suggested using a boost chopper for generation control of Permanent magnet synchronous generator [7]. The technique is useful but it still doesn't solve the problem of transient stability. Another example is novel where, direct torque control (DTC) scheme for an interior permanent magnet synchronous machine is introduced. The proposed technique has great advantage as its simple control structure. On the other hand it only uses a controller for torque and I have no say on the flux and this might be quite not useful [8]. Finally one of the updated papers demonstrates a multiplatform hardwarein-the-loop (HIL) approach to observe the operation of a high speed permanent-magnet synchronous generator coupled with a microturbine in an all-electric-ship power system [9]. Even though there are a lot of promising and powerful solution discussed in the past few years but not much of them deal with stability occurrence. Because of the nature of wind it's so hard to obtain a constant production of electricity at all times.

In this paper a new approach regarding permanent magnet synchronous generator stability is proposed. The strategy is build on the base of dealing with the transient stability occurs as a result of variable speed and nature of wind. The proposed technique is obtained through three stages. First stage is to apply linear approximation to the original system. The second stage is to obtain the transfer function in Laplace domain. The last stage is to separate the unstable zero from the original system. Once it's separated a suitable feedback will be designed to treat the effect of unstable zero. The paper is organized as follows. In section 2 permanent magnet synchronous generator modeling is recalled. The proposed control approach is introduced in section 3. Following that is the simulation and tested results. The results show that the approach proved to be a very powerful tool in treating and enhancing permanent magnet synchronous generator stability.

2. Permanent Magnet Synchronous Generator (PMSG) Modelling

The permanent magnet synchronous generator is represented in two phase synchronous rotor reference frame q-axis and d-axis. The electrical and mechanical model is going to be used to represent proposed model

The electrical equations [10]:

$$\frac{di_d}{dt} = \frac{v_d}{l_d} - Rs\frac{i_d}{l_d} + \frac{l_q}{l_d}pwi_q \tag{1}$$

$$\frac{di_q}{dt} = \frac{v_q}{l_q} - Rs\frac{i_d}{l_q} - \frac{l_d}{l_q}pwi_d - \frac{pw\tau}{l_d} \tag{2}$$

$$T_e = p(\tau i_q + (l_d - l_q)i_d i_q \tag{3}$$

The mechanical equation [10]:

(4)

$$\frac{dw}{dt} = \frac{1}{j}(T_e - fw - T_{m)} \tag{5}$$

$$\frac{dw}{dt} = \frac{1}{j}(pl_d i_d i_q - pl_q i_d i_q + p\tau i_q - f i_q - T_{m)} \tag{6}$$

Where,

i_d, i_q	Current of d&q axis
l_d, l_q	Inductance of d&q axis
v_d, v_q	D,q axis voltage
Rs	Stator winding resistance
p	Number of pole pairs
w	Angular velocity
τ	Induced flux by stator
j	Inertia
f	friction
T_m	Shaft mechanical torque

The previous equations are going to be used to put system in the standard form:

$$\dot{x} = f(x) + \sum_{i=1}^{m} g(x)_i u_i \tag{7}$$

State vector is chosen as follows:

$$X(t)=\begin{bmatrix} x_1 \\ x_2 \\ x_3 \end{bmatrix}=\begin{bmatrix} i_d \\ i_q \\ w \end{bmatrix},\ U(t)=\begin{bmatrix} v_d \\ v_q \end{bmatrix} \tag{8}$$

$$f(x) = \begin{bmatrix} -\frac{Rs}{l_d}x_1 + \frac{l_q}{l_d}px_2x_3 \\ -\frac{Rs}{l_q}x_2 - \frac{l_d}{l_q}px_1x_3 - x_3\frac{p\tau}{l_d} \\ \frac{pl_d}{j}x_1x_2 - \frac{pl_q}{j}x_1x_2 + \frac{p\tau}{j}x_2 - \frac{f}{j}x_2 - \frac{T_m}{j} \end{bmatrix} \tag{9}$$

$$g(x) = \begin{bmatrix} \frac{1}{l_d} & 0 \\ 0 & \frac{1}{l_q} \\ 0 & 0 \end{bmatrix} \tag{10}$$

3. Control Approach

In this section the control approach will be illustrated. Fist consider a class of multi input multi output non linear system

$$\dot{x} = f(x) + \sum_{i=1}^{m} g(x)_i u_i \quad (11)$$

$$y_1 = h_1(x) \quad (12)$$

$$y_{1m} = h_m(x) \quad (13)$$

In which $f(x), g_1, \cdots, g_m$ are smooth vector field and $h_1(x), \ldots, h_m(x)$ smooth function defined on an open set of R^n . For more simplicity the above equation will be rewritten in the more condensed form

$$\dot{x} = f(x) + u \quad (14)$$

$$y = h(x) \quad (15)$$

Where $x \in IR_n$ is the state, $u \in IR_m$ is the input, and $y \in IR_l$ is the output. The system assumed to have equilibrium point at the origin $X = 0, f(Xe) = 0$ .The system relative degree r<n Euler system [11] is applied to obtain linear approximation around equilibrium point, the result obtained as follows:

$$f(x) = f(Xe) + (x - xo)\frac{\partial f}{\partial x}\Big|_{x = xo} \quad (16)$$

$$g(x) = g(Xe) + (x - xo)\frac{\partial g}{\partial x}\Big|_{x = xo} \quad (17)$$

$$h(x) = h(Xe) + (x - xo)\frac{\partial h}{\partial x}\Big|_{x = xo} \quad (18)$$

Consider:

$\partial = (x - xo)$

$\triangle$= h(x)-h(Xe) , the new system is:

$$\dot{\partial} = A\partial + Bu \quad (19)$$

$$\triangle y = c\partial \quad (20)$$

Where A= $\frac{\partial f}{\partial x}$, B=g(0), C=$\frac{\partial h}{\partial x}$

After the system converted into linear form it became easier to obtain transfer function.

$$T.F = \frac{Y(s)}{R(S)} = C(SI - A)^{-1} B = \frac{G(s)}{1 + G(S)H(s)} \text{ [12]} \quad (21)$$

The next step is to separate the unstable part as follows:

T.F= $\frac{G\prime(s)}{D(S)} * w(s)$

Where,

W(s) is the unstable part of the system

$\frac{G\prime(s)}{D(S)} = G''$ is the stable part of the system

Subsequent is designing a suitable feedback E(s) to amend stabilization of the system. From the definition of closed loop system it is known that:

$$T' = \frac{w(s)}{1+w(S)E(s)} \quad (22)$$

Assume $w'(s)$ to be the desired stable function

$$w'(s) = \frac{w(s)}{1 + w(S)E(s)} \quad (23)$$

$$\frac{w'(s)}{w(s)} = \frac{1}{1 + w(S)E(s)} \quad (24)$$

$$w'(s)\big(1 + w(S)E(s)\big) = w(s) \quad (25)$$

$$\frac{w(s)}{w'(s)} - 1 = w(s)E(s) \quad (26)$$

$$E(s) = (\frac{w(s)}{w'(s)} - 1) * \frac{1}{w(s)} \quad (27)$$

$$E(s) = \frac{1}{w'(s)} - \frac{1}{w(s)} \quad (28)$$

$$E(s) = \frac{w - w'}{ww'} \quad (29)$$

From the general case a more specific concept can be extended regarding the improvement of zero stability. Figure 1 illustrate the steps for developed approach

$w' = (s + c)$

$w = (s - x)$

c is the desired zero, x is the unstable system zero

$$s + c = \frac{s - x}{1 + (s - x)E(s)} \tag{30}$$

$$s - x = (s + c)(1 + (s - x)E(s)) \tag{31}$$

$$\frac{s - x}{s + c} - 1 = (s - x)E(s) \tag{32}$$

$$E(s) = \left(\frac{s - x}{s + c} - 1\right) * \frac{1}{s - x} \tag{33}$$

$$E(s) = \frac{1}{(s + c)} - \frac{1}{(s - x)} \tag{34}$$

$$E(s) = \frac{-x - c}{(s + c)(s - x)} \tag{35}$$

According to stability definition the new zero "c" will vary between these bands

$$0 < c < \frac{1}{x}$$

3.1 Permanent Magnet Synchronous generator model after applying the approach

First step is to apply the linear approximation. Assume that the initial condition is at the origin and without loss of generality $f(Xe) = 0$. Followed by the system form is:

$$A = \begin{bmatrix} -\frac{Rs}{l_d} & \frac{l_q}{l_d} p x_3 & \frac{l_q}{l_d} p x_2 \\ -\frac{l_d}{l_q} p & -\frac{Rs}{l_q} & -\frac{p\tau}{l_d} \\ \frac{p l_d}{j} - \frac{p l_q}{j} & \frac{p\tau}{j} - \frac{f}{j} & 0 \end{bmatrix}, B = \begin{bmatrix} \frac{1}{l_d} & 0 \\ 0 & \frac{1}{l_q} \\ 0 & 0 \end{bmatrix}, c = \begin{bmatrix} 1 & 0 & 0 \\ 0 & 1 & 0 \end{bmatrix}$$

$$\text{T.F} = \frac{b_0 S^{N-1} + b_1 S^{N-1} + \cdots + b_n}{a_0 S^N + a_1 S^{N-1} + \cdots . + a_n} = \frac{(s+z1)(s-x)..(s+zn)}{a_0 S^N + a_1 S^{N-1} + \cdots . + a_n} = \frac{G''(s)}{a_0 S^N + a_1 S^{N-1} + \cdots . + a_n} * (s - x) \tag{36}$$

The following step is to design a suitable feedback $E(s)$. The main idea is manipulating the zero in order to enhance the system stability.

$$E(s) = \frac{-x - c}{(s + c)(s - x)}$$

Finally the new system can be represented as

$$GH(S)=\frac{(s+z1)(s+zn)}{a_0S^N+a_1S^{N-1}+\cdots.+a_n}*\frac{S^3+QS^2+mS+V}{S^2-2xS+T} \quad (37)$$

Where
$Q=c-2x, m$=- x c, V= cx^2 , $T=x$ c

4. Simulation and Results

In this paper, the stability of permanent magnet synchronous generator has been investigated. An approach has been introduced to refinement stability bandwidth and deal with transient stability problem. The permanent magnet synchronous generator has been modeled using Math Lab program .The values chosen for PMSG model is listed in Table.1.The work is progressed through three steps (shown in Fig.1):

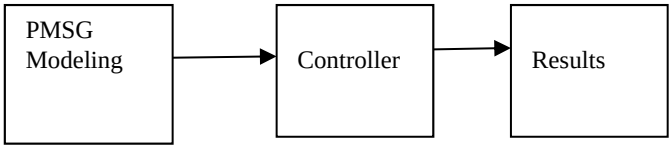

Fig.1 Work Progressed Diagram

PMSG	
No of Poles	8
Rated Current	10A
Rated Speed	600 rad/sec
Armature Resistance	0.32ohm
Stator inductance	8.3mH
Rated Torque	60Nm
Rated power	50 kW
Magnetic flux linkage	0.42 wb

Table.1 PMSG Paramete

The first step is divided into two parts. The first part is to represent system in the non linear standard form:

$$f(x)=\begin{bmatrix} -38x_1+0.2px_2x_3 \\ -20x_2-0.2x_1x_3-2x_3 \\ 6x_1x_2-4x_1x_2+2x_2-T_m \end{bmatrix} \quad g(x)=\begin{bmatrix} 3.12 & 0 \\ 0 & 12 \\ 0 & 0 \end{bmatrix}$$

Second part is to implement the PMSG parameters into Mat Lab and run the program. Figure 2 show the rotor speed generated from Mat Lab simulink. It is clear that system response will suffer from some instability problem as the system goes beyond the required reference. Nyquist plot was chosen to analysis the whole system stability behaviour. Figure 3 shows the nyquist plot of the PMSG transfer function extracted from non linear form. The system will go beyond the limits of unity circle -1<G(S)H(S)<1, which coincides with result generated from simulink model.

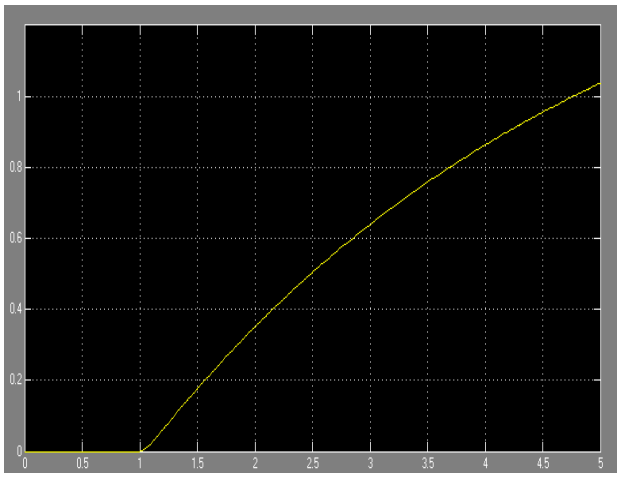

Fig.2 Rotor speed of PMSG

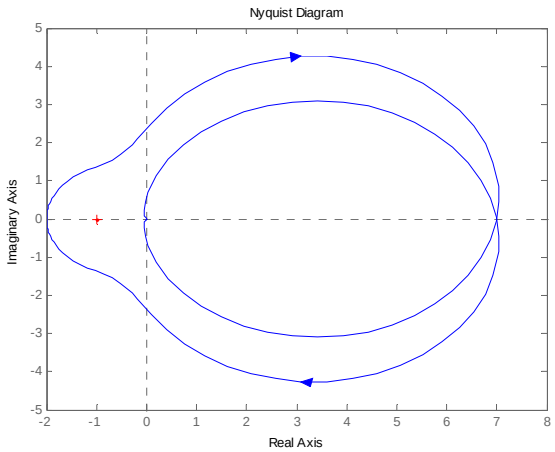

Fig.3 Nyquist polt PMSG

The second step is to execute the proposed control approach. The aim is to improve system stability whether to enlarge the range if it is too small or to reduce it if the situation verses. In this case the target is to enhance the stability by drove the system back in to the unity circle.

$$A = \begin{bmatrix} -38 & 0.1 & 0.4 \\ -20 & -0.2 & -2 \\ 4 & 2 & 0 \end{bmatrix}, B = \begin{bmatrix} 3.12 & 0 \\ 0 & 12 \\ 0 & 0 \end{bmatrix}, c = \begin{bmatrix} 1 & 0 & 0 \\ 0 & 1 & 0 \end{bmatrix}$$

The following steps is to designing a suitable feedback E(s). In order to determine the feedback, the value of zero "c' will be assigned. According to Routh stability definition the value of new zero will be chosen to be c=0.5.

Final step is to feed the new parameter to the simulink to see the affect in the rotor speed. The Nyquist plot will be plotted with respect to new transfer function. Figure 4 and 5 show the rotor speed and nyquist plot respectively. It is clarified that the system stability is improved by the developed approach.

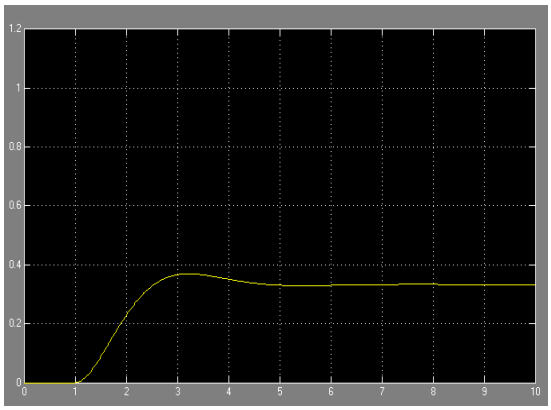

Fig.4 new Rotor speed of PMSG

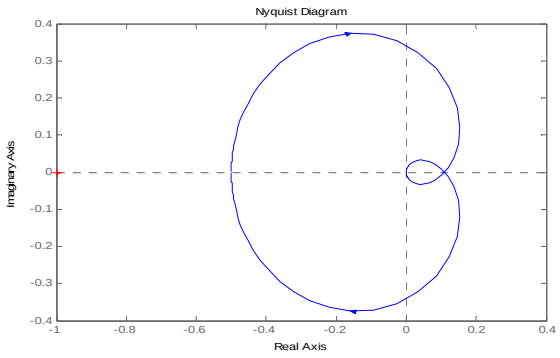

Fig.5 Nyquist polt of new PMSG system

5. Conclusion

This paper is dedicated to investigate the instability of permanent magnet synchronous generator (PMSG). A developed approach is introduced to enhance system performance in the occurrences of instability. The work is progresses through three stages. First stage is to build the PMSG model. The second main stage is to execute the control approach. The technique is based on transforming system into Laplace domain by means of linear approximation and transfer function methods. After obtaining transfer function a suitable feedback will be designed. The value of the feedback varies according to the situations. Finally the last stage is to implement the new system in the MAT LAB and invstigate the new system rliability. Nyquist and bode plot is used to rule the effictivness of the proposed approach. The results show that the introduced control strategy proove to provide good results.

References

1.Keith Sunderland and Michael Conlon," The Role of Micro Wind Generation in Ireland's Energy Future",proceeding of 43rd International Power Engineering Conference, pp.1-5. 1-4 Sept, 2008.

2.F. Blaabjerg, Z. Chen, R. Teodorescu, F. Iov," Power Electronics in Wind Turbine Systems", proceeding of power electronics and motion control conference,pp 23-34,2006.

3.C. Carrillo, M. Silva-Ucha, E. Diaz-Dorado and F. Perez-Sabín," Performance of a small wind energy generator under different configurations and settings", proceeding of EPE Wind Energy Seminar, pp 1-10,2010.

4.M. Dali, J. Belhadj and X. Roboam, Design of a stand-alone hybrid Photovoltaic-Wind generating system, Journal of Electrical Systems, 2008.

5.Md. Enamul Haque , Michael Negnevitsky and Kashem M. Muttaqi, A Novel Control Strategy for a Variable-Speed Wind Turbine With a Permanent-Magnet Synchronous Generator, IEEE Transaction on Industry Applications, VOL. 46, NO. 1,pp 331- 339, February 2010.

6.Ancan .D. Hansen and Gabrielle Michalke. Modeling and Controlling of Variable Speed- Multi –pole Permanent Magnet Synchronous Generator wind turbine, Wind Energy, Vol 11, pp 537-554, October 2008.

7.Kenji Amei ,Yukichi Takahisa and Ohji M. Sakui," A Maximum Power Control of Wmd Generator System Using a Permanent Magnet Synchronous Generator and a Boost Chopper Circuit", proceeding of IEEE power conversion conference,pp1447-1452,2002.

8.Lixin Tang and Yuwen Hu, A Novel Direct Torque Control for Interior Permanent-Magnet Synchronous Machine Drive With Low Ripple in Torque and Flux—A Speed-Sensorless Approach, IEEE Transaction on Industry Applications, VOL. 39, NO. 6,pp 1748- 1756, December 2003.

9.Amin Hasanzadeh, Chris S. Edrington, Nicholas Stroupe, and Troy Bevis. Real-Time Emulation of a High-Speed Microturbine Permanent-Magnet Synchronous Generator Using Multiplatform Hardware-in-the-Loop Realization, IEEE TRANSACTIONS ON INDUSTRIAL ELECTRONICS, VOL. 61, NO. 6, pp3109-3118, JUNE 2014

10.Mahmoud S. Kandil ,Magdi M. El-Saadawi ,Ahmed E. Hassan Khaled and M. Abo-Al-Ez,"Dynamic Modeling and Control of Microturbine DG System for Autonomous Operation", proceeding of IEEE 14th International Middle East Power Systems Conference, pp 311-315, 2008

11.Sydney Ludvigson and Christina H. Paxson," Approximation Bias In linearized Euler Equations", proceeding of Economics and Statistic conference, pp 242-256,2001

12.Katsuhiko Ogata. Modern Control Engineering.5 th edition: Prentice Hall press, 2007.

Asymptotic Output Tracking in Control of a Grid Connected Wind Turbine Based on Doubly Fed Induction Generator

Marwa Hassan
Department of Computer, Control and Management
Sapienza University of Rome
Rome, Italy
marwa.hassan@uniroma1.it

Noha El-Amary
Department of Electrical and Control Engineering
Arab Academy for Science and Technology
Cairo, Egypt
noha_helamary@hotmail.com

***Abstract*—This work presents a non-linear control technique for a grid-connected wind turbine based on Doubly Fed Induction Generator (DFIG) targeting improved adapted power efficiency with high voltage performance. The control approach is realized in the rotor reference frame and is based on Asymptotic output tracking technique. Thus, assigning specific zeros through a feedback process ensure the reproduction of an output that converges asymptotically to the required reference rotor current. As a consequence, active and reactive powers can be controlled. The mathematical models of the doubly-fed induction generator and the grid side converter command models are presented. Based on the mathematical model of the DFIG and the grid side converter, a nonlinear representation of them are developed. In this paper, two cases are studied. The Matlab program is applied to simulate and test the proposed control technique. The results are featured to show the effectiveness of the proposed control design.**

***Keywords*—Non Linear Control,Renewable Energy,Doubly Fed Induction Generator (DFIG),rotor side converter and Asymptotic Output Tracking.**

I. Introduction

Due to the growing integration of wind energy into power grids, the impact of wind generators on power system able to meet the growing energy demand is of increasing concern.In the latest years, the Doubly Fed Induction Generator (DFIG) became the dominant type of Wind Turbine system used in wind farms.This type of generators has numerous advantages over its counterparts as it provide better results in terms of weight, cost, and size.It also presents greater benefits such as power quality and efficiency[1-3].

In general, the standard structure of Wind turbines consists of a doubly-fed induction generator (DFIG) consist of a wound rotor induction generator and an AC/DC/AC converter. The stator winding is connected directly to the grid while the rotor is fed at variable frequency through the AC/DC/AC converter. The DFIG technology allows extracting maximum energy from the wind for low wind speeds by optimizing the turbine speed while minimizing mechanical stresses on the turbine during gusts of wind [4].

Even though the DFIG is considered as a stable symmetric induction machine but there might exist regions of instability due to the natural variation of the wind.The eigenvalue prediction for mapping the boundary of the stability region for DFIG machines was investigated by Banakar in[5]. The analysis shows that the stability region of DFIG machine can be defined by the variation of the d, the q rotor current angle in Idr-Iqr plane for sensorless rotor position estimation that based on model reference adaptive system [6].Though the aforementioned papers [5-7] explain the stability criterion for the DFIG machines, yet the control scheme for stable operation remains unaddressed by the authors.The nonlinear nature of the DFIG model motivated the researchers to develop a nonlinear control designed techniques that ensure a smooth and stable operation for the DFIG. There has been a lot of progress in the nonlinear control designing context in the past years.Most of these control techniques (for example back stepping, regulation, robust and tracking) have been used to control the DFIG[8-20].Some of the latest researches will be recalled.A nonlinear control strategy to stabilize the DFIG based on back stepping algorithm was proposed in[8]. The proposed controller was successful in tracking the reference rotor speed, stabilizing the stator power.While this control approach provides sufficient results but it still suffers from a lot of constraints with respect to the designing procedure. In[9] a robust nonlinear feedback control approach of a residential Savonuis Vertical Axis Wind Turbine (VAWT) based on Double Fed Induction Generator (DFIG) and connected to a power grid was introduced. The aim of this work was to control the Rotor Side Converter (RSC) using a robust non-linear feedback control scheme, in which, a robust control law based on Lyapunov theory associated with a sliding mode controller is used to handle the issue of parameters uncertainty and to guarantee a global asymptotic stability of the system. The results of this approach were proved to be acceptable.The work was considered incomplete because of the obtained results didn't show robust a good robustness against the parameters uncertainty.Another example of the nonlinear design technique was investigated in[13]. An input-state feedback linearization controller was proposed in this paper.The authors designed a system of eight ordinary differential equations is used to model

the wind energy conversion system.The generator has a wound rotor type with back-to-back three-phase power converter bridges between its rotor and the grid; it is modelled using the direct-quadrature rotating reference frame with aligned stator flux.The mathematical model developed in this paper is, in fact, an approximated model which made the result of this controller not an applicable in actual situations. Even though there have been several attempts to design the most powerful nonlinear control technique but it is still a wide-open area of research.In this paper, a control technique for a grid-connected doubly fed induction generator (DFIG)-based on wind energy conversion system was presented. Control strategy for the grid side and rotor side converters placed in the rotor circuit of the DFIG is introduced. The control approach is based on the asymptotic output tracking technique.Simply by applying a feedback with certainly assigned zeros, the system will reproduce an output rotor current that will converge to a specific reference signal. The paper is structured as follow: section II recalls the definition of asymptotic output tracking control technique.Section III illustrates the modelling considerations of the Doubly Fed Induction Generator and grid side converter command models.The control approach is discussed in section Iv. Finally, Section V presents the obtained results while Section VI concludes the paper and formulates further research directions.

II. RECALLS

Consider the class of SISO nonlinear systems

$$\begin{aligned} \dot{x} =& f(x) + g(x)u, \quad x \in \mathbb{R}^n, u \in \mathbb{R}, y \in \mathbb{R} \\ y =& h(x). \end{aligned} \tag{1}$$

where $x, f(x), g(x)$ represents the state, function of the whole system states and the input function respectively.Assume $x = 0$ is the equilibrium point (i.e., $f(0) = 0$). The system has a well define relative degree $r \leq n$ at the origin; namely, $L_g L_f^i h(x) = \frac{\partial L_f^i h(x)}{\partial x} g(x) = 0$ i.e.$L_f h(x) = \frac{\partial h}{\partial x} f(x)$ for $k < r-1$ and $L_g L_f^{r-1} h(x) \neq 0$ in a neighbourhood of $x = 0$.

Asymptotic output tracking,[21]
Since the system has a well define relative degree one can locally define a mapping $\Gamma(x)$ that introduce the system in the normal form.

$$\begin{pmatrix} \zeta \\ \eta \end{pmatrix} = \Gamma(x) = \begin{pmatrix} h(x) \\ \vdots \\ L_f^{r-1} h(x) \\ \Gamma_2(x) \end{pmatrix}. \tag{2}$$

where $\Gamma_2(x)$ is such that $L_g \Gamma_2(x)) = 0$ locally puts the system into the normal form; i.e., it gets the form

$$\begin{cases} \dot{\zeta} = \hat{A}\zeta + \hat{B}(b(\zeta, \eta) + a(\zeta, \eta)u) \\ \dot{\eta} = q(\zeta, \eta) \\ y = \zeta_1 \end{cases} \tag{3}$$

with

$$\hat{A} = \begin{pmatrix} \mathbf{0} & I_{r-1} \\ \mathbf{0} & \mathbf{0} \end{pmatrix}, \quad \hat{B} = \begin{pmatrix} \mathbf{0} \\ 1 \end{pmatrix}.$$

In order to guarantee the exact reproduction of specific reference output function $y_R(t)$ the input is chosen in the form of $u = \frac{1}{a(\zeta,\eta)}(-b(\zeta, \eta) + y_R^r - \sum_{i=1}^{r} c_{i-1}(z_i - y_R^{i-1}))$for $1 \leq i \leq r$ and $c_0, \ldots, c_{r-1}$are real numbers .

Remark 1 Imposing the input in the normal form implies $\dot{z}_r = y^r = y_R^r - c_{r-1}e^{r-1} - \cdots - c_0 e$, i.e $e^r + c_{r-1}e^{r-1} + \cdots + c_0 e = 0$.The roots of the characteristic equation can be arbitrarily assigned.

III. MODELLING

This section address the modelling of Doubly Fed Induction Generator (DFIG) and grid side converter command model respectively.These equations will later be used to form the non linear models.

A. Doubly Fed Induction Generator model

In order to simplify the Doubly Fed Induction Generator (DFIG) model ,the following assumption is assumed [22]

1 The flow distribution is sinusoidal.
2 The air-gap is constant.
3 The influences of the heating and the skin effect are not taken into account.
4 The saturation of the magnetic circuit is negligible.

The DFIG modelling with respect to a rotor flux oriented reference frame will be expressed as:

1-Stator Equations

$$V_{sd} = R_s i_{sd} + \frac{d}{dt}\phi_{sd} - \phi_{sq} W_s \tag{4}$$

$$V_{sq} = R_s i_{sq} + \frac{d}{dt}\phi_{sq} + \phi_{sd} W_s \tag{5}$$

$$\phi_{sd} = L_s i_{sd} + M i_{rd} \tag{6}$$

$$\phi_{sq} = L_s i_{sq} + M i_{rq} \tag{7}$$

2-Rotor Equations

$$V_{rd} = R_r i_{rd} + \frac{d}{dt}\phi_{rd} - \phi_{rq} W_r \tag{8}$$

$$V_{rq} = R_r i_{rq} + \frac{d}{dt}\phi_{rq} + \phi_{rd} W_r \tag{9}$$

$$\phi_{rd} = L_r i_{rd} + M i_{sd} \tag{10}$$

$$\phi_{rq} = L_r i_{rq} + M i_{sq} \tag{11}$$

$$W_r = g.W_s \tag{12}$$

with

$$i_{sd} = \frac{\phi_{sd} - M i_r d}{L_s} \tag{13}$$

$$i_{sq} = \frac{-M i_{rq}}{L_s} \tag{14}$$

Where, R_s and R_r are, respectively, the stator and rotor phase resistances, Ls, Lr, MStator and rotor per phase winding and magnetizing inductances and $W_s, W_r$are the stator and rotor speed pair pole number.The direct and quadratic stator and

rotor currents are respectively represented asi_{sd}, i_{sq}, i_{rd} and i_{rq}.The voltage of the stator side for both direct and quadratic defined as V_{sd}, V_{sq} while the voltage of the rotor direct and quadratic represented as V_{rd}, V_{rd}.The stator-flux linkage for direct and quadratic frame are given byϕ_{sd}, ϕ_{sd}.The ϕ_{rd}, ϕ_{rq} referred to the rotor flux for both the direct and quadratic respectively. The Electromagnetic torque is presented by the following equation

$$J\frac{dW_r}{dt} + f_r W_r = c_{em} - c_r \tag{15}$$

$$C_{em} = p(\phi_{rq} i_r d - \phi_{rd} i_{rq}) \tag{16}$$

with J is the moment of inertia.c_{em}, c_r are the magnetic torque and rationale torque while p is the numbers of pairs per pole. The system now will be modelled with respect to the rotor side direct and quadratic (d,q) synchronous reference frame.The input in such case are i_{rd}andi_{rq}.
First the system expression with respect to d axis frame

$$v_{rd} = R_r i_{rd} + \frac{d}{dt}(L_r i_{rd} + M i_{sd}) - (L_r i_{rq} + M i_{sq}) W_r \tag{17}$$

$$= R_r i_{rd} + \frac{d}{dt} i_{rd}(L_r - \frac{M^2}{L_s}) - L_r i_{rq} W_r - M W_r(\frac{-M i_{rq}}{L_s}) \tag{18}$$

$$= R_r i_{rd} + L_r \frac{d}{dt} i_{rd}(1 - \frac{M^2}{L_s L_r}) - L_r i_{rq} W_r + \frac{M^2}{L_s} W_r i_{rq} \tag{19}$$

$$= R_r i_{rd} + L_r \Lambda \dot{i}_{rd} - L_r \Lambda W_r i_{rq} \tag{20}$$

$$\dot{i_{rd}} = \frac{1}{L_r \Lambda} v_{rd} - \frac{R_r}{L_r \Lambda} i_{rd} + w_r i_{rq} \tag{21}$$

$$\dot{i_{rd}} = \frac{1}{L_r \Lambda} v_{rd} - \frac{1}{\mathcal{T}\Lambda} i_{rd} + w_r i_{rq} \tag{22}$$

with $\Lambda = (1 - \frac{M^2}{L_s L_r}), \mathcal{T} = \frac{R_r}{L_r}$.
Now consider q axis frame

$$V_{rq} = R_r i_{rq} + \frac{d}{dt}\phi_{rq} + \phi_{rd} W_r \tag{23}$$

$$= R_r i_{rq} + L_r \Lambda \dot{i}_{rq} - L_r \Lambda W_r i_{rd} \tag{24}$$

$$\dot{i}_{rq} = \frac{1}{L_r \Lambda} v_{rq} - \frac{1}{\mathcal{T}\Lambda} i_{rq} - w_r i_{rd} \tag{25}$$

Finally we obtain the speed from the torque equation as: $\dot{W}_r = -\frac{f_r}{J} W_r + \frac{p}{J}\phi_{rq} i_{rd} - \frac{p}{J}\phi_{rd} i_{rq}$.

B. Grid Side Converter command model

In order to eliminate the harmonics from the converter operation an RL filter is installed[24-25].

$$v_{fd} = R_f i_{fd} + L_f \frac{d}{dt} i_{fd} - W_r L_f i_{fq} - V_{Gd} \tag{26}$$

$$v_{fq} = R_f i_{fq} + L_f \frac{d}{dt} i_{fq} + W_r L_f i_{fd} - V_{Gq} \tag{27}$$

$$\dot{i}_{fd} = \frac{1}{L_f}(-R_f i_{fd} + v_{fd} + W_r L_f i_{fq} + V_{Gd}) \tag{28}$$

$$\dot{i}_{fq} = \frac{1}{L_f}(-R_f i_{fq} + v_{fq} - W_r L_f i_{fd} + V_{Gq}) \tag{29}$$

with V_{Gd}, V_{Gq} indicated the input voltage of AC-DC converter in the direct and quadrature frame.The electric network components of voltage and current on the AC side for both the direct and quadrature frame are given by v_{fd}, v_{fq}, i_{fd} and i_{fq} respectively, while the L_f referred to the inductance of the system. The active and reactive power are expressed as:

$$P = V_{Gd} i_{fd} + V_{Gq} i_{fq} \tag{30}$$

$$Q = V_{Gq} i_{fq} - V_{Gd} i_{fd}. \tag{31}$$

Remark 2 Through setting the power factor to be 1 and neglecting the filter losses one can get the following expression $V_{Gd} = V_{fd} = V_G, \quad V_{Gq} = V_{fq} = 0$, leading the active and reactive power to be $P_f = V_G i_{fd} and Q_f = -V_G i_{fq}$.

IV. CONTROL STRATEGY

In this section, the asymptotic output tracking technique will be applied in the Doubly-Fed Induction Generator and the grid side converter command models.The control will be realized in the rotor reference frame so the d axis regulate the reactive power and the q axis regulate the active power.In general, the system will produce an output that, regardless of the initial state of the system will converge asymptotically to the rotor reference current.

A. Non linear model of DIFG

Recalling from the modelling section ,the system is introduced in the condensed nonlinear form

$$\Sigma_C : \begin{cases} \dot{x} = f(x) + g_1(x)u_1 + g_2(x)u_2, \quad x \in \mathbb{R}^n, u \in \mathbb{R}^n \\ y = h(x). \end{cases} \tag{32}$$

where, $X = [x_1 \quad x_2 \quad x_3]^T = [i_{rd} \quad i_{rq} \quad W_r]^T$,$U = [u_1 \quad u_2]^T = [v_{rd} \quad v_{rq}]^T$.The function$f(x), g(x)$ are smooth vector fields and the output function$h(x)$ is a smooth scalar function.

$$f(x) = \begin{pmatrix} -\frac{1}{\mathcal{T}\Lambda} x_1 + x_2 x_3 \\ -\frac{1}{\mathcal{T}\Lambda} x_2 - x_2 x_3 \\ -\frac{f_r}{J} x_3 + \frac{p}{J}\phi_{rq} x_1 - \frac{p}{J}\phi_{rd} x_2 \end{pmatrix} \tag{33}$$

$$g_1(x) = \begin{pmatrix} \frac{1}{\mathcal{T}\Lambda} \\ 0 \\ 0 \end{pmatrix}, \quad g_2(x) = \begin{pmatrix} 0 \\ \frac{1}{\mathcal{T}\Lambda} \\ 0 \end{pmatrix}. \tag{34}$$

Note that $\Lambda = (1 - \frac{M^2}{L_s L_r}), \mathcal{T} = \frac{R_r}{L_r}$. Since the purpose of this study is to control the rotor side converter current, the output was chosen as $h(x) = [i_{rd}, i_{rq}]^T$.

Remark 3 According to the previous results obtained by isidori, A multi variable nonlinear system in the form of (32) has a relative degree$r_1, \ldots, r_m$at point x^0 if $L_{g_j} L_f^k h_i(x) = 0$ for all$1 \leqslant j \leqslant m$, for all $1 \leqslant i \leqslant m$,for all $k \leqslant r_i - 1$, and for all neighbour ofx^0.

Following the same definition it can be easily verified that the system relative degree with respect to the outputs $r = 2$

Control of d-axis rotor current

In order to track rotor currenti_rq we assume that the system is only affected by u_1 and $u_2 = 0$

$$\dot{x} = f(x) + g_1(x) \tag{35}$$
$$y = h_1(x) = i_{rd} \tag{36}$$

The system relative degree w.r.to the output $r = 1$.Now we apply a coordinate transformation and introduce the system in to the normal form.

$$\Gamma(x) = \begin{pmatrix} z_1 = x_1 \\ \eta_1 = x_2 \\ \eta_2 = x_3, L_g.\eta = 0. \end{pmatrix} \tag{37}$$

$$\begin{cases} \dot{z}_1 = -\frac{1}{\mathcal{T}\Lambda} z_1 + \eta_1\eta_2 + \frac{1}{\mathcal{T}\Lambda} u_1 \\ \dot{\eta}_1 = -\frac{1}{\mathcal{T}\Lambda}\eta_1 - z_1\eta_2 \\ \dot{\eta}_2 = p\phi_{rd} z_1 - p\phi_{rd}\eta_1 - \frac{f_r}{J} eta_2 \end{cases} \tag{38}$$

After applying the proper control law in the form of$u = \mathcal{T}\Lambda(-\frac{1}{\mathcal{T}\Lambda}x_1 + x_2x_3 + x_1^r - c_0x_1)$where x_1^r, c_0 represents the rotor current desired value and the chosen zero,we obtain the desired output .

Control of q-axis rotor current

In this case the effect ofu_2 is studied

$$f(x) = \begin{pmatrix} -\frac{1}{\mathcal{T}\Lambda}x_1 + x_2x_3 \\ -\frac{1}{\mathcal{T}\Lambda}x_2 - x_2x_3 \\ -\frac{f_r}{J}x_3 + \frac{p}{J}\phi_{rq}x_1 - \frac{p}{J}\phi_{rd}x_2 \end{pmatrix}, g_2(x) = \begin{pmatrix} 0 \\ \frac{1}{\mathcal{T}\Lambda} \\ 0 \end{pmatrix} \tag{39}$$

$$y = h_2(x) = i_rq. \tag{40}$$

The system relative degree $r_q = 1$.The coordinate transformation and the normal take the form of

$$\Gamma(x) = \begin{pmatrix} z_1 = x_2 \\ \eta_1 = x_3 \\ \eta_2 = x_1 \end{pmatrix} \tag{41}$$

$$\begin{cases} \dot{z}_1 = -\frac{1}{\mathcal{T}\Lambda} z_1 - \eta_1\eta_2 + \frac{1}{\mathcal{T}\Lambda} u_2 \\ \dot{\eta}_1 = p\phi_{rd}\eta_2 - p\phi_{rd} z_1 - \frac{f_r}{J}\eta_1 \\ \dot{\eta}_2 = -\frac{1}{\mathcal{T}\Lambda}\eta_2 + z_1\eta_2. \end{cases} \tag{42}$$

The input$u = \mathcal{T}\Lambda(-\frac{1}{\mathcal{T}\Lambda}x_2 - x_1x_3 + x_2^r - c_0x_2)$.

B. Non linear grid side converter model

Referring to remark 2 we know that through setting the power factor to unity we get $V_{Gd} = V_{fd} = V_G$, $V_{Gq} = V_{fq} = 0$.In such a case the system is converted into single input-single output system in the form:

$$f(x) = \begin{pmatrix} -\frac{R_f}{L_f}x_1 + x_3x_2 \\ -\frac{R_f}{L_f}x_2 - x_3x_1 \\ -\frac{f_r}{J}x_3 - \frac{p}{J}\phi_{rd}x_2 \end{pmatrix}, \quad g(x) = \begin{pmatrix} \frac{2}{L_f} \\ 0 \\ 0 \end{pmatrix} \tag{43}$$

$$y = x_1. \tag{44}$$

where, x:state vector=$[i_{fd} \quad i_{fq} \quad W_r]^T$,$U = [u_1 \quad u_2]^T$.

d-axis control

In this part the focus will be in tracking the d-axis reference filtered current.Since the system obtained a well define relative degree $r = 1$ then we apply a coordinate transformation in the form $\Gamma(x) = \begin{pmatrix} x_1 \\ x_3 \\ x_2 \end{pmatrix}$.

The state space description in the new coordinates

$$\begin{cases} \dot{z}_1 = a(z,\eta) + b(z,\eta) \\ \dot{\eta}_1 = \frac{f_r}{J}\eta_1 - \frac{p}{J}\phi_{rd}\eta_2 \\ \dot{\eta}_2 = -\frac{R_f}{L_f}\eta_1 - \eta_2 z_1. \end{cases} \tag{45}$$

Through setting the input u to be $u = \frac{L_f}{2}(-\frac{R_f}{L_f}x_1 + x_3x_2 + x_2^r - c_0x_1)$, one can regulate the rotor current in order to meet a specific active and reactive power.

V. SIMULATION AND RESULTS

This section is dedicated for the evaluation of the performance of the proposed technique.Two cases were developed.The first case investigated the performance of controller when it's directly connected to the DFIG while in the second case the focus was in investigating the behaviour of the DFIG when it's connected to the network and under the operating condition of setting power factor to one.The DFIG and grid side models referred to in the third section are used to test the proposed design.Table 1 presents the values of the DIFG parameters used to build the models.The block diagram of figure 1 illustrated the design process of the DFIG model while the block diagram shown in figures 2 illustrated the second case scenario. In order to evaluate the ability of the proposed designed technique for tracking the d and$q$ axis rotor currents reference signal generated at maximum efficiency an input in the form$u = \mathcal{T}\Lambda(-\frac{1}{\mathcal{T}\Lambda}x_1 + x_2x_3 + x_1^r - 1000x_1), u = \mathcal{T}\Lambda(-\frac{1}{\mathcal{T}\Lambda}x_2 - x_1x_3 + x_2^r - 1200x_2)$ were applied respectively.Figure $3, 4$ illustrated the rotor side reference signal and the generated current signals verses time in seconds in the direct and quadratic frames respectively.It can be noticed from Figure $3, 4$ that the proposed control technique succeeded in reproducing a current signal that coincides with the required reference signal in both cases. Figure5 presents the continuous bus voltage of the DFIG regulated to the standard reference voltage fixed at 1000 V.It is clear that in spite of fluctuation of the wind the voltage remain stationary.In fact the proposed design succeeded in reducing the voltage disturbance in comparison to sliding mode design introduced in[25].In the second case the the stator of the DFIG was directly connected to the grid while its rotor was connected to it via a cascade (Rectifier, Inverter and Filter).In order to evaluate the grid side model the power factor was set to one (shown in Figure 6), thus only the direct rotor current will be produced.The voltage on the output of the inverter will suffer from disturbance signals formed by the original of frequency$f = 50$Hz and other signals.A passive R-L filter was used to eliminate harmonics.The input in the form $u = \frac{L_f}{2}(-\frac{R_f}{L_f}x_1 + x_3x_2 + x_2^r - 900x_1)$ ensures the reproduction of an output i_{rd} that will track the required

reference signal(shown in Figure7).Finally, the analysis of this technique has shown that the system hasn't just succeeded in reproducing an output that will converge asymptotically to the required reference signals but it also minimizes the effect of disturbance.

Table.1 The DFIG data sheet

The DFIG data of a typical 3.6 MW generator	
Frame / power	7 kW
Efficiency at rated speed	appr. 97...97.5
Voltage	690 V
Locked rotor voltage	approx. 1000 V
Operation speed range	1000...2000 rpm
Power factor	p.f. 0.90 cap ...1.0
Rotor Resistance	1 K Ω
Rotor Inductance	.2 mH
Stator Resistance	0.5 K Ω
Stator Inductance	.001 mH
Mutual inductance	Msr= 0.078 H
Number of poles	4
Inertia moment	j=0.3125 Nms2

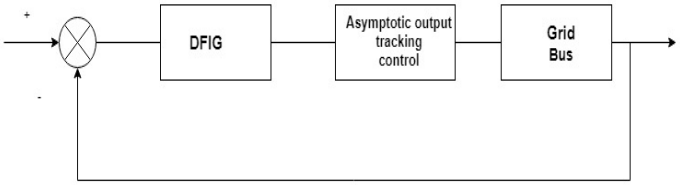

Fig. 1: Simplified Block diagram of the Asymptotic output tracking technique for the DFIG model

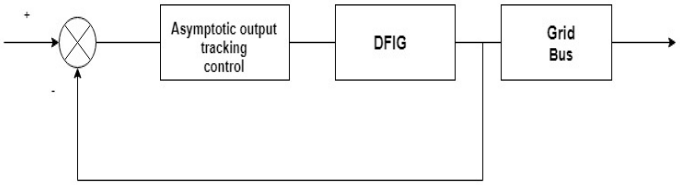

Fig. 2: Block diagram of the Asymptotic output tracking for the Grid side model

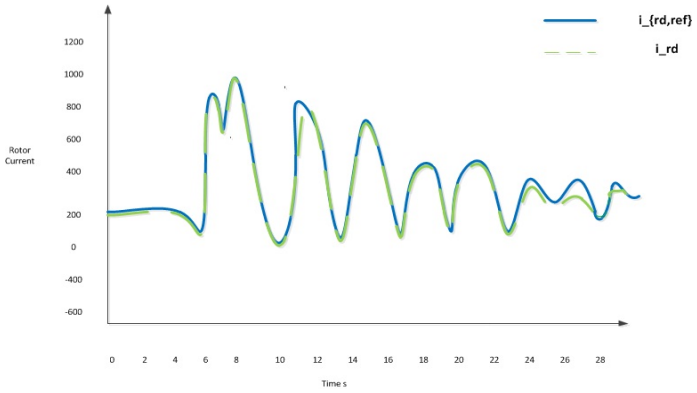

Fig. 3: Doubly Fed Induction Generator i_{rd}rotor current

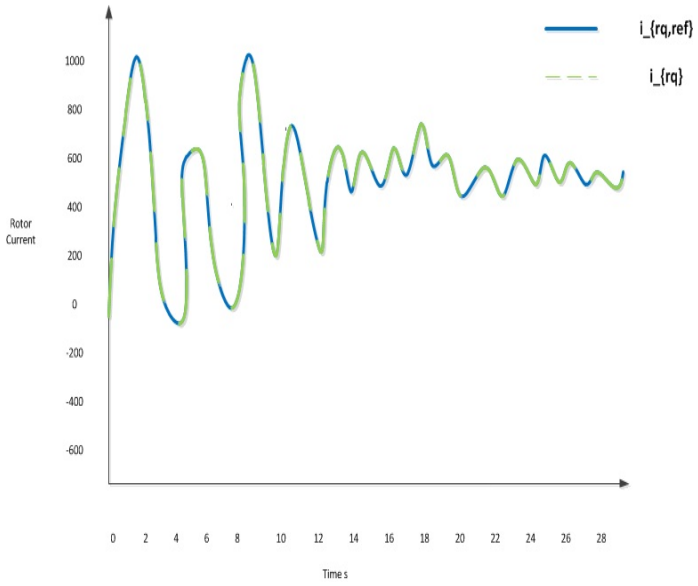

Fig. 4: Doubly Fed Induction Generator i_{rq}rotor current

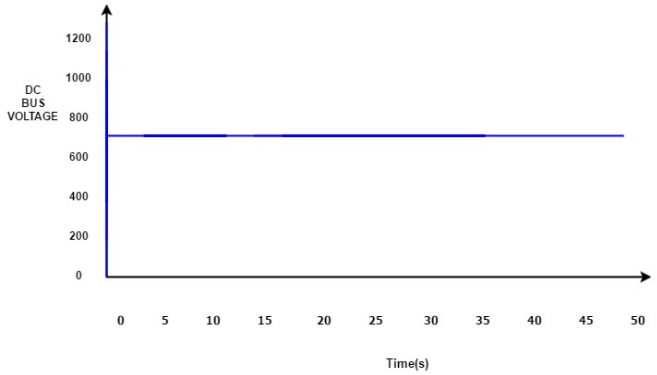

Fig. 5: Doubly Fed Induction Generator continuous bus voltage

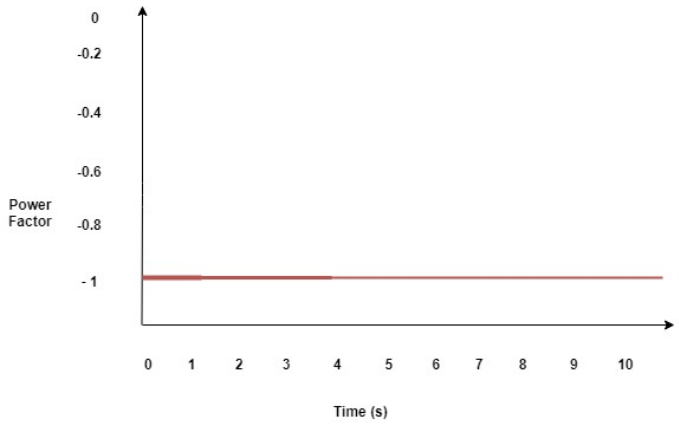

Fig. 6: Power factor of DFIG connected to Grid

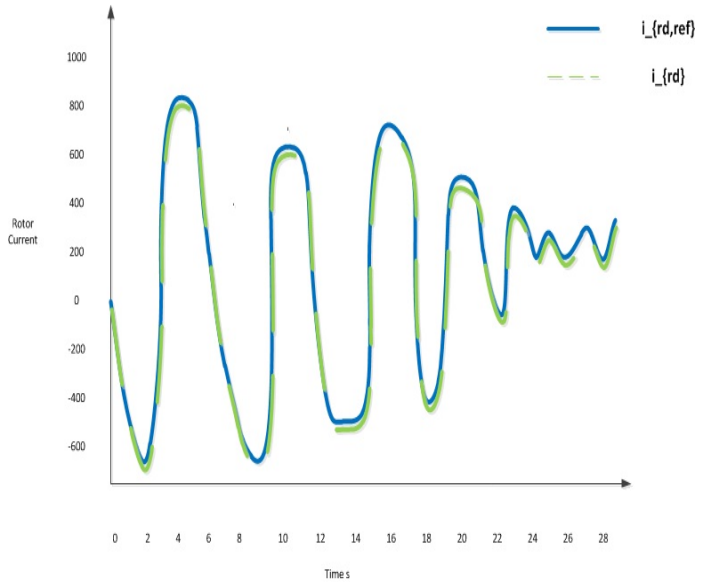

Fig. 7: The rotor direct current of DFIG connected to grid

VI. Conclusion

The aim of this work is to introduce a non-linear control technique that asymptotically tracks the rotor current of the grid-connected wind turbine based on Double Fed Induction Generator (DIFG). In general, the idea is to produce a certain rotor current in order to meet a specific requirement of active and reactive power production.The modelling of DFIG and the grid side converter command models have been studied. The control of the grid side converter command model was studied under the assumption of the system obtaining a unity power factor.Maximum power point strategy makes it possible to provide totally of the active power produced by the grid with a unity power factor. Two cases have been developed based on the DIFG model and the grid side converter command model. The performance of the DFIG when it's connected to the proposed design controller was investigated in the first case .In the second case the stator of the DFIG was directly connected to the grid while its rotor was connected to it via a cascade (Rectifier, Inverter and Filter) ,finally the filter was connected to the suggested controller.The results in both cases shown that the control approach succeeded in reproducing an output signal that coincides with the required reference signal. It was also shown in that the system has a very powerful performance under disturbance such as the wind variation. Finally, further investigation will be carried out regarding practical cases.

References

[1] A. Tiwari, A. Shewale, and N. Lokhande(2011). Comparison of various Wind Turbine Generators. Multidisciplinary Journal of Research in Engineering and Technology, Volume 1, Issue 2, pp.129-135.

[2] R. Pena, J. C. Clare, and G. M. Asher, Doubly fed induction generator using back-to-back PWM converters and its application to variablespeed wind-energy generation, Proc. Inst. Elect. Eng., Elect. Power, vol. 143, no. 3, pp. 231241, May 1996.

[3] J. B. Ekanayake, L. Holdsworth, X. G. Wu, and N. Jenkins, Dynamic modeling of doubly fed induction generator wind turbine, IEEE Trans. Power Syst., vol. 18, no. 2, pp. 803809, May 2003.

[4] A. Kumar, A. Satwase, and R.Mishra(2015). Transient Behavior of Doubly Fed Induction Generator Using Simulink Model in Wind Energy Conversion System. International Journal of Innovative Research in Science, Engineering and Technology Vol. 4, Issue 2, pp. 2319 - 8753.

[5] H. Banakar, C. Luo and B.T. Ooi, " Steady-state stability analysis of doubly-fed induction generators under decoupled PQ control," IEE Proceedings - Electric Power Applications, 2006, Vol. 153, pp. 300 306.

[6] G. D. Marques, Duarte M. Sousa, New Sensorless Rotor Position Estimator of a DFIG Based on Torque CalculationsStability Study, IEEE Trans. on Energy Conversion, Vol. 27, Mar 2012, pp. 196-202.

[7] R. H. Nelson, T. A. Lipo, P.C. Krause, Stability analysis of a symmetrical induction machine, IEEE Transactions on Power Apparatus and Systems , vol. PAS-88, Nov. 1969, pp. 1710-1717.

[8] I.K.Amin and M. N. Uddin,Nonlinear Control Operation of DFIG based WECS with Stability Analysis,Procd. of. IEEE Industry Applications Society Annual Meeting,Cincinnati, OH, USA, 2017.

[9] R. Cheikh and H. Belmili,Nonlinear Control of a Grid-Connected Double Fed Induction Generator Based Vertical Axis Wind Turbine: A Residential Application,International Journal of Electrical Energy, Vol. 4, No. 4, December 2016.

[10] Z. Boudjema, A. Meroufel and Y. Djerriri,Nonlinear control of a doubly fed induction generator for wind energy conversion , Carpathian Journal of Electronic and Computer Engineering 6/1 (2013) 28-35 .

[11] G. Abad, et al., Doubly Fed Induction Machine: Modeling and Control for Wind Energy Generation, 1st ed., IEEE-John Wiley and Sons, Inc., 2011.

[12] A.D. Hansen, P. Srensen, F. Iov, F. Blaabjerg(2004), Control of variable speed wind turbines with doubly-fed induction generators, Wind Eng. 28 (4) 411434.

[13] M. T. AlrifaiMohamed, Z. M. RayanMohamed and M Rayan,Feedback Linearization Controller for a Wind Energy Power System,proc. of 24th Mediterranean Conference on Control and Automation,Athens, Greece,2016.

[14] J.; Jiang, L.; Yao, W.; Wu, Q.H. Perturbation estimation based non-linear adaptive control of a full-rated converter wind turbine for fault ride-through capability enhancement. IEEE Trans. Power Syst. 2014, 29,27332743.

[15] Xiang, D.; Ran, L.; Tavner, P.J.; Yang, S. Control of a doubly fed induction generator in a wind turbine during grid fault ride-through. IEEE Trans. Energy Convers. 2006, 21, 652662.

[16] Z. Boudjema, A. Meroufel and Y. Djerriri,Nonlinear control of a doubly fed induction generator for wind energy conversion , Carpathian Journal of Electronic and Computer Engineering 6/1 (2013) 28-35 .

[17] J. Lopez, P. Sanchis, X. Roboam, L. Marroyo, Dynamic behavior of the doubly fed induction generator during three-phase voltage dips, In: IEEE Transaction on Energy Conversion, 22 September, 2007, 709717.

[18] N. Khemiri, A. Khedher and M. F. Mimouni, Wind Energy Conversion System using DFIG Controlled by Backstepping and Sliding Mode,INTERNATIONAL JOURNAL of RENEWABLE ENERGY RESEARCH Nihel Khemiri et al., Vol.2, No.3, 2012 Strategies.

[19] Ouari K., Rekioua T. and Ouhrouche M. A, Non Linear Predictive Controller for Wind Energy Conversion System, International Renewable Energy Congress IREC, pp. 220-226, November 2010.

[20] Trabelsi R., Khedher A., Mimouni M.F., MSahli F. and Masmoudi A. Rotor flux estimation based on nonlinear feedback integrator for backstepping-controlled induction motor drives, Electromotion Journal 17, 2010, pp:163-172.

[21] Isidori A. Nonlinear Control Systems (3rd edn). Springer: New York, 1995.

[22] A. LTIFI, M. GHARIANI, R. NEJI, "Comparison of Two Techniques for Control Nonlinear Systems :The PI Regulator and Sliding Mode Control", international Conference on Control, Engineering Technology,Sousse, Tunisia ,2014.

[23] Yougui Guo , Ping Zeng , and Deng Wenlang ,"Modeling and simulation of grid side converter based wind power generation system",Proc. Information Science and Engineering,Hangzhou, China 2011.

[24] E. Tremblay, A. Chandra, P. J. Lagace. Grid-side converter control of DFIG wind turbines to enhance power quality of distribution network. IEEE Power Engineering Society General Meeting. Montreal: IEEE, 2006: pp 22332238.

[25] W.AMOR,M.GHARIANI,"Nonlinear Control for a Grid Connected Wind Turbine Based on Double Fed Induction Generator",International Renewable Energy Congress (IREC),Hammamet, Tunisia,2016.

Chapter 7
Conclusion and Future work

7.1 Conclusion

This thesis is divided into two parts .In the first part of the thesis, we addressed the Input-Output feedback linearization and Disturbance Decoupling Problem with stability for a class of nonminimum SISO nonlinear systems that are controllable in the first approximation through exploring the idea of partial dynamic cancellation.In fact the classical techniques failed in solving the problem due to the existence of unstable zero dynamics.More in details, we propose a two step design approach:First we consider the linear tangent model of the original system, a dummy output is constructed via a suitable factorization of the numerator of its transfer function so that the corresponding linearized system is minimum phase;then, classical input output linearization of the locally minimum phase nonlinear system is performed with respect to the after mentioned dummy output.Finally it was proved that, when applying the result feedback to the original systems the problems is solved.

The extended results in both cases were extended to the sampled-data context through multirate sampling design to overcome the well-known pathologies induced by the sampling zero dynamics where the minimum phase property are lost.The results obtained in the Disturbance Decoupling consider the first step towards this direction as the results shows that the problem is more complicated under sampling as sampling induces more conservative design which require the disturbance to be measurable and piecewise constant over the sampling interval.

Finally a power system application based on the Wind turbine system driven by the Doubly Fed Induction Generator (DFIG) was studied.

In the second part we collect part of the individual research conducted during the Phd period in the power system machines where the main contribution was based on the mixing between the Artificial Intelligent technique and the nonlinear based control.

7.2 Future Work

Future work concerns deeper analysis of control strategy for the sampled data design , new proposals to try different methods, or simply curiosity can be obtained .This thesis has been mainly focused on the Single Input Single Output System , the investigation towards the extension of these argument to the Multi Input- Multi Output case and to a global characterization of the results possibly combined with input -output stability and related results could be carried out.

As for the application side tests, and experiments could be executing based on the sampled data model in practical the renewable energy field.As we have seen in

chapter five the Multi rate sampled data design can preserve the continuous time behaviour and provide better performances than the direct implementation of the continuous time design which could be useful from a theoretical point of view during transient behaviour.

Bibliography

[1] Jeffrey Ahrens and Hassan Khalil. Closed-loop behavior of a class of nonlinear systems under ekf-based control. *IEEE Transactions on Automatic Control*, 52(3):536–540, 2007. (Cited on page 19).

[2] Alma Alanis, Edgar Sanchez, and Alexander Loukianov. Discrete-time backstepping synchronous generator stabilization using a neural observer. *IFAC Proceedings Volumes*, 41(2):15897–15902, 2008. (Cited on page 4).

[3] Frank Allgower. Approximate input-output linearization of nonminimum phase nonlinear systems. In *Control Conference (ECC), 1997 European*, pages 2359–2364. IEEE, 1997. (Cited on page 17).

[4] Bader Aloliwi and Hassan Khalil. Adaptive output feedback regulation of a class of nonlinear systems: Convergence and robustness. *IEEE Transactions on Automatic Control*, 42(12):1714–1716, 1997. (Cited on page 19).

[5] Mohamed Jemli Asma Chihi, Hechmi Ben AzzaA and Anis sellami. Nonlinear discrete-time integral sliding mode control of an induction motor: Real-time implementation. *Informatics and Control*, 26:23 – 32, 2017. (Cited on page 4).

[6] Karl Astrom, Per Hagander, and Jan Sternby. Zeros of sampled systems. In *Decision and Control including the Symposium on Adaptive Processes, 1980 19th IEEE Conference on*, volume 19, pages 1077–1081. IEEE, 1980. (Cited on pages 4 and 26).

[7] Karl Åström, Per Hagander, and Jan Sternby. Zeros of sampled systems. *Automatica*, 20(1):31–38, 1984. (Cited on page 54).

[8] Ayokunle Awelewa. *Development of nonlinear control scheme for electric power system stabilizion,pro cess.* PhD thesis, Univ. imperial College London, 2010. (Cited on page 3).

[9] Corneliu Barbu, Rodolphe Sepulchre, Wei Lin, and Petar Kokotovic. Global asymptotic stabilization of the ball-and-beam system. In *Decision and Control, 1997., Proceedings of the 36th IEEE Conference on*, volume 3, pages 2351–2355. IEEE, 1997. (Cited on page 18).

[10] Giuseppe Basile and Giovanni Marro. Controlled and conditioned invariant subspaces in linear system theory. *Journal of Optimization Theory and Applications*, 3(5):306–315, 1969. (Cited on page 17).

[11] Stefano Battilotti. *Noninteracting control with stability for nonlinear systems.* Springer-Verlag London, 1994. (Cited on page 17).

[12] Brahim Behar, Françoise Lamnabhi-Lagarrigue, and Tarek Ahmed-Ali. Robust nonlinear control of transient stability of power systems. In *Decision and Control, 2003. Proceedings. 42nd IEEE Conference on*, volume 1, pages 294–299. IEEE, 2003. (Cited on page 18).

[13] Boubekeur Boukhezzar and Houria Siguerdidjane. Nonlinear control of variable speed wind turbines for power regulation. In *Control Applications, 2005. CCA 2005. Proceedings of 2005 IEEE Conference on*, pages 114–119. IEEE, 2005. (Cited on page 3).

[14] Roger Brockett. System theory on group manifolds and coset spaces. *SIAM Journal on control*, 10(2):265–284, 1972. (Cited on page 14).

[15] Christopher Byrnes and Alberto Isidori. Asymptotic stabilization of minimum phase nonlinear systems. *IEEE Transactions on Automatic Control*, 36(10):1122–1137, 1991. (Cited on page 19).

[16] Christopher Byrnes, Francesco Delli Priscoli, and Alberto Isidori. *Output regulation of uncertain nonlinear systems*. Springer Science & Business Media, 2012. (Cited on page 18).

[17] Claudia Califano, Salvatore Monaco, and Dorothé Normand-Cyrot. On the discrete-time normal form. *IEEE transactions on automatic control*, 43(11):1654–1658, 1998. (Cited on page 20).

[18] Diego Carrasco, Graham Goodwin, and Juan Yuz. Modified euler-frobenius polynomials with application to sampled data modelling. *IEEE Transactions on Automatic Control*, 62(8):3972–3985, 2017. (Cited on page 30).

[19] Ryan Caverly and James Forbes. Zero shaping of nonminimum phase aircraft dynamics. In *2018 AIAA Guidance, Navigation, and Control Conference*, page 0601, 2018. (Cited on page 17).

[20] Masood Cheema, John Edward Fletcher, Mohammad Farshadnia, Dan Xiao, and Faz Rahman. Combined speed and direct thrust force control of linear permanent-magnet synchronous motors with sensorless speed estimation using a sliding-mode control with integral action. *IEEE Transactions on Industrial Electronics*, 64(5):3489–3501, 2017. (Cited on page 3).

[21] Zhiyong Chen and Jie Huang. A general formulation and solvability of the global robust output regulation problem. In *Decision and Control, 2003. Proceedings. 42nd IEEE Conference on*, volume 1, pages 1071–1079. IEEE, 2003. (Cited on page 18).

[22] Zhiyong Chen and Jie Huang. Global robust output regulation for output feedback systems. *IEEE Transactions on Automatic Control*, 50(1):117–121, 2005. (Cited on page 18).

[23] Edward Colgate and Gerd Schenkel. Passivity of a class of sampled-data systems: Application to haptic interfaces. *Journal of robotic systems*, 14(1):37–47, 1997. (Cited on page 3).

[24] Raymond Comeau and Noriyuki Hori. State-space forms for higher-order discrete-time models. *Systems & Control Letters*, 34(1-2):23–31, 1998. (Cited on page 3).

[25] Giuseppe Conte, Anna Perdon, and Bostwick Wyman. *New Trends in Systems Theory: Proceedings of the Università di Genova-The Ohio State University Joint Conference, July 9–11, 1990*, volume 7. Springer Science & Business Media, 2013. (Cited on page 17).

[26] Jesuse De Leon-Morales, Krishna Busawon, Goshqe Acosta-Villarreal, and Enrique Acha-Daza. Nonlinear control for small synchronous generator. *International Journal of Electrical Power & Energy Systems*, 23(1):1–11, 2001. (Cited on page 3).

[27] Claude Moog Descusse. Decoupling with dynamic for strong invertible affine nonlinear systems. *International Journal of Control*, 42:1387–1398, 1985. (Cited on page 16).

[28] Joseph Descusse, Lafay, and Malabre. Solution to morgan's problem. *IEEE Transactions on Automatic Control*, 33(8):732–739, 1988. (Cited on page 17).

[29] André J Fossard and Dorothée Normand-Cyrot. *Nonlinear Systems: Control 3*. Springer Science & Business Media, 2012. (Cited on pages 28 and 32).

[30] Elmer Gilbert. The decoupling of multivariable systems by state feedback. *SIAM Journal on Control*, 7(1):50–63, 1969. (Cited on page 17).

[31] Tomomichi Hagiwara and Mituhiko Araki. Fr-operator approach to the h/sub 2/analysis and synthesis of sampled-data systems. *IEEE Transactions on Automatic Control*, 40(8):1411–1421, 1995. (Cited on page 3).

[32] Marwa Hassan. Tracking and controlling maximum power point utilizing artificial intelligent system,. In *Proc. ISC2 ,Chengdu*, pages 586–589, 2015. (Cited on page 4).

[33] Marwa Hassan and Noha El-Amary. Voltage instability prediction using artificial immunity technique. *International Journal of Scientific and Engineering Research*, 4:559–593, 2013. (Cited on page 4).

[34] Marwa Hassan and Noha El-Amary. Permanent magnet synchronous generator stability analysis and control,. In *Proc. Complex Adaptive System ,Los Angeles*, pages 507–515, 2016. (Cited on page 4).

[35] John Hauser, Shankar Sastry, and George Meyer. Nonlinear control design for slightly non-minimum phase systems: Application to v/stol aircraft. *Automatica*, 28(4):665–679, 1992. (Cited on page 17).

[36] George Haynes and Henery Hermes. Nonlinear controllability via lie theory. *SIAM Journal on Control*, 8(4):450–460, 1970. (Cited on page 14).

[37] Robert Hermann. On the accessibility problem in control theory. In *International Symposium on Nonlinear Differential Equations and Nonlinear Mechanics*, pages 325–332. Elsevier, 1963. (Cited on page 14).

[38] Robert Hermann and Arthur Krener. Nonlinear controllability and observability. *IEEE Transactions on automatic control*, 22(5):728–740, 1977. (Cited on page 14).

[39] Tohru Ieko, Yoshimasa Ochi, and Kimio Kanai. New design method for pulse-width modulation control systems via digital redesign. *Journal of guidance, control, and dynamics*, 22(1):123–128, 1999. (Cited on page 3).

[40] Tohru Ieko, Yoshimasa Ochi, and Kimio Kanai. New design method for pulse-width modulation control systems via digital redesign. *Journal of guidance, control, and dynamics*, 22(1):123–128, 1999. (Cited on page 34).

[41] Alberto Isidori. *Nonlinear control systems*. Springer Science & Business Media, 1999. (Cited on page 18).

[42] Alberto Isidori. *Nonlinear control systems*. Springer Science & Business Media, 2013. (Cited on pages 16 and 17).

[43] Alberto Isidori. The zero dynamics of a nonlinear system: From the origin to the latest progresses of a long successful story. *European Journal of Control*, 19(5):369–378, 2013. (Cited on page 19).

[44] Alberto Isidori and Christopher Byrnes. Output regulation of nonlinear systems. *IEEE transactions on Automatic Control*, 35(2):131–140, 1990. (Cited on page 18).

[45] Alberto Isidori and Jessy Grizzle. Fixed modes and nonlinear noninteracting control with stability. *IEEE transactions on automatic control*, 33(10):907–914, 1988. (Cited on page 17).

[46] Alberto Isidori, Arthur Krener, Claudio Gori-Giorgi, and Salvatore Monaco. Nonlinear decoupling via feedback: a differential geometric approach. *IEEE transactions on automatic control*, 26(2):331–345, 1981. (Cited on page 14).

[47] Alberto Isidori and Claude Moog. On the nonlinear equivalent of the notion of transmission zeros. In *Modelling and Adaptive Control*, pages 146–158. Springer, 1988. (Cited on page 16).

[48] Pierre Kabamba. Control of linear systems using generalized sampled-data hold functions. *IEEE transactions on Automatic Control*, 32(9):772–783, 1987. (Cited on page 30).

[49] Hassan Khalil and Ali Saberi. Adaptive stabilization of a class of nonlinear systems using high-gain feedback. *IEEE Transactions on Automatic Control*, 32(11):1031–1035, 1987. (Cited on page 19).

[50] Mohamed Khanchoul, Mickaël Hilairet, and Dorothée Normand-Cyrot. A passivity-based controller under low sampling for speed control of pmsm. *Control Engineering Practice*, 26:20–27, 2014. (Cited on page 4).

[51] Geun Bum Koo, Jin Bae Park, and Young Hoon Joo. Decentralised sampled-data control for large-scale systems with nonlinear interconnections. *International Journal of Control*, 89(10):1951–1961, 2016. (Cited on page 4).

[52] Arthur Krener. A generalization of chows theorem and the bang-bang theorem to nonlinear control problems. *SIAM Journal on Control*, 12(1):43–52, 1974. (Cited on page 14).

[53] Weiyao Lan, Ben Chen, and Zhengtao Ding. Adaptive estimation and rejection of unknown sinusoidal disturbances through measurement feedback for a class of non-minimum phase non-linear mimo systems. *International Journal of Adaptive Control and Signal Processing*, 20(2):77–97, 2006. (Cited on page 18).

[54] Jing Lei. Performance recovery of regional input-to-state stabilization by sampled-data output feedback control for nonlinear systems in the presence of disturbance. *European Journal of Control*, 39:78–94, 2018. (Cited on page 3).

[55] Daniel Liberzon. Output–input stability implies feedback stabilization. *Systems & control letters*, 53(3-4):237–248, 2004. (Cited on page 16).

[56] Daniel Liberzon, Stephen Morse, and Eduardo Sontag. Output-input stability and minimum-phase nonlinear systems. *IEEE Transactions on Automatic Control*, 47(3):422–436, 2002. (Cited on page 19).

[57] Claude Lobry. controllability of nonlinear systems. *SIAM Journal on Control*, 8:573–605, 1970. (Cited on page 14).

[58] Riccardo Marino. High-gain feedback in non-linear control systems. *International Journal of Control*, 42(6):1369–1385, 1985. (Cited on page 19).

[59] Riccardo Marino and Giovanni Santosuosso. Global compensation of unknown sinusoidal disturbances for a class of nonlinear nonminimum phase systems. *IEEE Transactions on Automatic Control*, 50(11):1816–1822, 2005. (Cited on page 18).

[60] Riccardo Marino and Patrizio Tomei. Output regulation for linear systems via adaptive internal model. *IEEE Transactions on Automatic Control*, 48(12):2199–2202, 2003. (Cited on page 18).

[61] Noha El-Amary Marwa Hassan and Mohamed Mansour. Micro grid studies due to fault occurrence using immunity technique,. In *Proc. 11th IASTED,Napoly*, pages 20–25, 2012. (Cited on page 4).

[62] Mattia Mattioni, Salvatore Monaco, and Dorothée Normand-Cyrot. Immersion and invariance stabilization of strict-feedback dynamics under sampling. *Automatica*, 76:78–86, 2017. (Cited on page 53).

[63] Salvator Monaco and Dorothée Normand-Cyrot. Nonlinear systems in discrete time. In *Algebraic and geometric methods in nonlinear control theory*, pages 411–430. Springer, 1986. (Cited on page 20).

[64] Salvator Monaco and Dorothée Normand-Cyrot. On nonlinear digital control. In *Nonlinear systems*, pages 127–155. Springer, 1997. (Cited on page 53).

[65] Salvatore Monaco and Dorothée Normand-Cyrot. Minimum-phase nonlinear discrete-time systems and feedback stabilization. In *Decision and Control, 1987. 26th IEEE Conference on*, volume 26, pages 979–986. IEEE, 1987. (Cited on page 20).

[66] Salvatore Monaco and Dorothée Normand-Cyrot. Zero dynamics of sampled nonlinear systems. *Systems & control letters*, 11(3):229–234, 1988. (Cited on page 34).

[67] Salvatore Monaco and Dorothée Normand-Cyrot. Multirate sampling and zero dynamics: from linear to nonlinear. In *Nonlinear synthesis*, pages 200–213. Springer, 1991. (Cited on pages 27, 28, 33 and 53).

[68] Salvatore Monaco and Dorothée Normand-Cyrot. Advanced tools for nonlinear sampled-data systems analysis and control. *European Journal of Control*, 13:221–241, 2007. (Cited on page 4).

[69] Salvatore Monaco and S Normand-Cyrot, Dorothéeand Stornelli. On the linearizing feedback in nonlinear sampled data control schemes. In *Decision and Control, 1986 25th IEEE Conference on*, volume 25, pages 2056–2060. IEEE, 1986. (Cited on page 3).

[70] Stephen Morse and Walter Wonham. Decoupling and pole assignment by dynamic compensation. *SIAM Journal on Control*, 8(3):317–337, 1970. (Cited on page 17).

[71] Stephen Morse and Walter Wonham. Status of noninteracting control. *IEEE Transactions on Automatic Control*, 16(6):568–581, 1971. (Cited on page 17).

[72] Shahid Nazrulla and Hassan Khalil. Robust stabilization of non-minimum phase nonlinear systems using extended high-gain observers. *IEEE Transactions on Automatic Control*, 56(4):802–813, 2011. (Cited on page 17).

[73] Dragan Nesic, Efstratios Skafidas, Iven Mareels, and Robin J Evans. Minimum phase properties for input nonaffine nonlinear systems. *IEEE Transactions on automatic control*, 44(4):868–872, 1999. (Cited on page 18).

[74] Marwa Hassan Noha El-Amary and Mohamed Mansour. Immunity technique in determine micro grid studies due to fault occurrence. *Advanced Science Letters Journal*, 20:1286–1291, 2012. (Cited on page 4).

[75] James Pearson. Linear multivariable control, a geometric approach. *IEEE Transactions on Automatic Control*, 22(6):1000–1001, 1977. (Cited on page 17).

[76] Witold Pedrycz. Robust control design an optimal control approach, 2007. (Cited on page 18).

[77] William Porter. Diagonalization and inverses for non-linear systems. *International Journal of Control*, 11(1):67–76, 1970. (Cited on page 17).

[78] Fransesco Delli Priscoli, Lorenzo Marconi, and Alberto Isidori. Adaptive observers as nonlinear internal models. *Systems & Control Letters*, 55(8):640–649, 2006. (Cited on page 18).

[79] Mohsen Rahimi and Mostafa Parniani. Transient performance improvement of wind turbines with doubly fed induction generators using nonlinear control strategy. *IEEE Transactions on Energy Conversion*, 25(2):514–525, 2010. (Cited on page 3).

[80] Ramakrishna and Bhatti. Sampled-data automatic load frequency control of a single area power system with multi-source power generation. *Electric Power Components and Systems*, 35(8):955–980, 2007. (Cited on page 4).

[81] Sanchez-Orta, Jorge De Leon Morales, and Lopez-Toledo. Discrete-time nonlinear control for small synchronous generator. In *Control Applications, 2001.(CCA'01). Proceedings of the 2001 IEEE International Conference on*, pages 277–282. IEEE, 2001. (Cited on pages 4 and 18).

[82] Murat Şeker, Erkan Zergeroğlu, and Enver Tatlicioğlu. Non-linear control of variable-speed wind turbines with permanent magnet synchronous generators: a robust backstepping approach. *International Journal of Systems Science*, 47(2):420–432, 2016. (Cited on page 3).

[83] Sahjendra Narain Singh and Wilson Rugh. Decoupling in a class of nonlinear systems by state variable feedback. *Journal of Dynamic Systems, Measurement, and Control*, 94(4):323–329, 1972. (Cited on page 17).

[84] Sudarshan Singh. A modified algorithm for invertibility in nonlinear systems. *IEEE Transactions on Automatic Control*, 26(2):595–598, 1981. (Cited on page 16).

[85] Eduardo Sontag. Smooth stabilization implies coprime factorization. *IEEE transactions on automatic control*, 34(4):435–443, 1989. (Cited on page 19).

[86] Gilbert Strang. *Computational science and engineering*, volume 791. Wellesley-Cambridge Press Wellesley, 2007. (Cited on page 18).

[87] Hector Sussmann. Transactions of the american mathematical society. *SIAM Journal on Control*, 11:171–188, 1973. (Cited on page 14).

[88] Hector Sussmann and Velimir Jurdjevic. Controllability of nonlinear systems. *Journal of Differential Equations*, 12:95–116, 1972. (Cited on page 14).

[89] Hossein Tohidi, Koksal Erenturk, and Sajjad Shoja-Majidabad. Passive fault tolerant control of induction motors using nonlinear block control. *Control Eng. Appl. Inform*, 19(1):49–58, 2017. (Cited on page 3).

[90] Antonio Tornambè. Output feedback stabilization of a class of non-minimum phase nonlinear systems. *Systems & Control Letters*, 19(3):193–204, 1992. (Cited on page 17).

[91] Rudolf Wagner. Nonlinear noninteraction with stability by dynamic state feedback. *SIAM journal on control and optimization*, 29(3):609–622, 1991. (Cited on page 17).

[92] Shenshen Wang. Design of precompensator for decoupling problem. *Electronics letters*, 6(23):739–741, 1970. (Cited on page 17).

[93] Yueying Wang, Hao Shen, and Dengping Duan. On stabilization of quantized sampled-data neural-network-based control systems. *IEEE transactions on cybernetics*, 47(10):3124–3135, 2017. (Cited on page 3).

[94] Emertius Murray Wonham. Disturbance decoupling and output stabilization. In *Linear Multivariable Control*, pages 86–102. Springer, 1985. (Cited on page 61).

[95] Mehdi Karbalaye Zadeh, Roghayeh Gavagsaz-Ghoachani, Jean-Philippe Martin, Serge Pierfederici, Babak Nahid-Mobarakeh, and Marta Molinas. Discrete-time tool for stability analysis of dc power electronics-based cascaded systems. *IEEE Transactions on Power Electronics*, 32(1):652–667, 2017. (Cited on page 4).

[96] Jianzhong Zhang, Ming Cheng, and Zhe Chen. Nonlinear control for variable-speed wind turbines with permanent magnet generators. In *Electrical Machines and Systems, 2007. ICEMS. International Conference on*, pages 324–329. IEEE, 2007. (Cited on page 3).

[97] Alex Zheng and Manfred Morari. Stability of model predictive control with mixed constraints. *IEEE Transactions on Automatic Control*, 40(10):1818–1823, 1995. (Cited on page 18).

Abstract: Sampled data systems have come into practical importance for a variety of reasons. The earliest of these had primarily to do with economy of design. A more recent surge of interest was due to increase utilization of digital computers as controllers in feedback systems. This thesis contributes some control design for a class of nonlinear system exhibition linear output. The solution of several nonlinear control problems required the cancellation of some intrinsic dynamics (so-called zero dynamics) of the plant under feedback. It results that the so-defined control will ensure stability in closed-loop if and only if the dynamics to cancel are stable. What if those dynamics are unstable? Classical control strategies through inversion might solve the problem while making the closed loop system unstable. This thesis aims to introduce a solution for such a problem. The main idea behind our work is to stabilize the nonminimum phase system in continuous- time and undersampling using zero dynamics concept. The overall work in this thesis is divided into two parts. In Part I, we introduce a feedback control designs for the input-output stabilization and the Disturbance Decoupling problems of Single Input Single Output nonlinear systems. A case study is presented, to illustrate an engineering application of results. Part II illustrates the results obtained based on the Artificial Intelligent Systems in power system machines. We note that even though the use of some of the AI techniques such as Fuzzy Logic and Neural Network does not require the computation of the model of the application, but it will still suffer from some drawbacks especially regarding the implementation in practical applications. An alternative used approach is to use control techniques such as PID in the approximated linear model. This design is very well known to be used, but it does not take into account the non-linearity of the model. In fact, it seems that control design that is based on nonlinear control provide better performances.